Basic Studies on Radiation-Induced Luminescence from Natural Quartz and Its Application to Retrospective Dosimetry

Hiroki FUJITA

Doctoral Program in Fundamental Science and Energy Technology
Graduate School of Science and Technology
Niigata University

Abstract

It is very important to have a method of estimating radiation-dose received by people or irradiated in environmental space, without having or setting conventional dosemeters. However, dose evaluation method is not always established in the case of emergency situation. The purpose of this study was to confirm whether thermoluminescence (TL) and optically stimulated luminescence (OSL) from naturally occurring quartz could be used to estimate such accidental radiation doses or not.

When ionizing radiation is interacted with a dielectric material, some parts of concerned radiation energies will be converted into luminescence such as TL, OSL and so on. Luminescence intensity contains information of total radiation-dose received in the past. Therefore, TL- and OSL-phenomena from natural minerals have been utilized for dating in the geological and archaeological fields, and for retrospective dosimetry. However, details of such luminescence mechanisms have not yet been clear, including difference of dose response in each sample and sensitivity change after annealing treatment.

First of all, the existence of atomic hydrogens besides intense Al-hole centers was ascertained in electron spin resonance (ESR) spectrum measurements of various natural quartz grains after irradiation at -196 °C. Remarkable decrease of Al-hole center signals, coincident with the complete disappearance of ESR-signal due to atomic hydrogens, was

observed during heating up to room temperature. A positive correlation was established between the atomic hydrogen signals and the reduced proportion of the Al-hole centers. Additionally, the thermal annealing treatments of the quartz samples beyond 800 °C before irradiation induced the significant decrease of H^0 as well as the removal of OH absorbance in IR-spectra around 3500 cm^{-1}. On the basis of these experiments, it was presumed that atomic hydrogens derived from radiolysis of OH-related impurities could operate as "killers" of radiation-induced Al-hole centers. This quenching mechanism due to atomic hydrogen was also found in RTL quartz. The existence of atomic hydrogen plays an important role in the phase-transition temperature of β-quartz / tridymite on the TL-property changes.

The ESR spectra of Ti-centers and Al-hole centers were measured in RTL quartz irradiated at -196 °C, before and after warming up to room temperature. Only three kinds of Ti-centers were observed as electron-trapping centers in the samples: $[TiO_4/H^+]^0$, $[TiO_4/Li^+]^0$ and $[TiO_4/Na^+]^0$ centers. They were affected by annealing treatments. The $[TiO_4/H^+]^0$ center behaved just like atomic hydrogens. Tendency of the $[TiO_4/Na^+]^0$ center resembled to the RTL-intensity change associated with increasing annealing temperature. The phenomena were supported by both results of RTL glowcurves broadened and kinetic parameters, which were influenced by the annealing temperatures.

Secondary, mechanism of the different OSL sensitivities for quartz aliquots from different origins was investigated in terms of

radioluminescence (RL) during artificial irradiation. RL spectra of RTL-quartz consisted of two broad RL emission peaks, assignable to a violet region (V-RL, 400 nm) and a red one (R-RL, 630 nm). OSL sensitivity changed with the total amounts of V-RL emissions during irradiation of 20 Gy at different dose rates. Additionally, bleaching effects of RL with shorter wavelength light than OSL-illuminating light (470nm) were assured from another experiment with a combination of quartz slices and optical filter. Conclusively, it was confirmed that V-RL emissions appreciably affect the residual or naturally accumulated doses when the OSL / SAR protocol was applied.

To develop retrospective dosimetry of unexpected radiation accident, the basic studies on VTL phenomena were conducted using natural quartz grains extracted from surface soils. All VTL glowcurves of as-received samples exhibited no peaks below 250 °C, although there remain VTL peaks with their intrinsic mean lives in the temperature region below 250 °C for artificially irradiated quartz samples. Therefore, accident doses would be estimated without interference of naturally accumulated doses if VTL measurement was applied to soil samples collected from ancient site. The mean lives of VTL were evaluated by the various heating rates method and then the range of values was between some days and ten thousands of years depending on each peak. Especially, the mean life of VTL peak at 200 °C was years order, supporting the results of natural VTL glowcurve measurements. Furthermore, since the VTL intensity was proportional to the irradiation doses, the lower detection limit were calculated to be tens of

mGy from the response curve. This value was lower than that of other methods such as ESR dosimetry. From these results, VTL dosimetry would be preferable for accidental evaluation.

Finally, nine kinds of luminescence, including TL, OSL and infrared stimulated luminescence (IRSL) measurements were applied to determination of residual doses in atomic bomb-explosion suffered roof-tiles collected near epicenter areas in Hiroshima and Nagasaki, Japan. RTL-measurements of quartz extracts showed the highest residual doses in both tiles, which were consistent with the previous dose-evaluations. However, in addition to dose estimation with BTL and OSL for the same quartz fractions, all of the estimations for, including five kinds of TL and IRSL for feldspar extracts showed lower values than the RTL-dose value in quartz extracts. The lower residual-doses in the quartz and feldspar extracts would reflect unstability of their luminescence-centers and/or well-known anomalous fading effects. Conclusively, the highest residual doses of RTL from atomic bomb-suffered roof tiles are considered to be an evidence of the most stable property of RTL-centers in quartz.

Contents

1. Introduction

Since the radioactivity was discovered by Becquerel, A. H. in 1896 and the nuclear fission was found by Hahn, O. in 1938, nuclear energy has been used in wide fields such as the generation of electricity, the application for medical treatment, agriculture, science and engineering. However, some nuclear accidents were happened in the world. Besides, nuclear proliferation and aging nuclear power industry pose ever-present risks of nuclear accidents.

In the southern Urals, a radiation accident occurred in September 1957. This accident at the Mayak nuclear materials production complex, east of the town of Kyshtym in Chelyabinsk Region, resulted from a thermal explosion of a concrete tank containing liquid radioactive wastes (Kryshev et al., 1997). In April 1986, the Chernobyl nuclear reactor disaster resulted in a large amount of radioactivity spread over tens of thousands of square kilometers (UNSCEAR 2000). A large population was exposed, and people who lived in Belarus and Ukraine within about 30 km of the reactor were evacuated. Populations in more distant than 30 km were generally not evacuated, and depending upon rainfall and wind direction, radioactive materials was deposited on the ground, exposing these people continuously for many years (Chumak et al., 1998; Edwards et al., 2004).

In Japan in March 1997, there was a fire and explosion at a reprocessing plant of the Power Reactor and Nuclear Fuel Development Corporation (subsequently reestablished the Japan Atomic Energy Agency), and trace quantities of plutonium and cesium were released at Tokai-mura

(STA, 1997; Igarashi et al., 1999). A critical accident occurred in September 1999 at the uranium conversion facility of the JCO Company Ltd. in Tokai-mura, Japan and released fission neutrons for about 20 hr (Fujimoto, 2001). Radionuclides induced by neutrons in environment have been detected using a low-level counting system (Komura et al., 2000).

Currently, in an event of a radiation accident the dose evaluation method of the general public, without having conventional dosemeters, is not necessarily established where the dosimetry is not beforehand set up. In the event of the radiation accident accurate radiation dosimetry is necessary to address vital immediate and long term personal and public concerns. Several methods of physical and biological analysis have been available for estimating the absorbed dose in an accidental irradiation. These methods are becoming increasing available, such as electron spin resonance (ESR) dosimetry of organic and inorganic substances (Ikeya et al., 1984; Kamenopoulou et al., 1986; Kai et al., 1990; Wu et al, 1998), chemiluminescence dosimetry (Hammermaier et al., 1986; Heide et al., 1987; Nickel et al., 1991) and chromosome aberration techniques (Fatôme et al., 1997). For neutron dose measurements, activated blood sodium and the activity of ^{32}P in hair were used and the specific activity of induced ^{51}Cr was determined (Hankins, 1980; Fatôme et al., 1997; Endo et al., 2000). However, in all these cases a lengthy amount of trial and error was necessary to find a material sensitive to radiation and to investigate its dose sensitivity. Furthermore, these methods only have the detection limit over 0.1 Gy for gamma radiation. Given sufficient speed, accuracy and the

lower detection limit, the utility of another method would be developed.

Recent studies of thermoluminescence (TL) and optically stimulated luminescence (OSL) to determine the accidental doses indicate that these methods have the capability to detect the doses in dielectric materials such as natural minerals and artificial ceramics (Bøtter-Jensen et al., 1996; Hashimoto et al., 2002a). OSL is a well-established tool for measuring radiation doses in unfired sediments (Huntley et al., 1985). It has features in common with TL which has long been used in measuring radiation doses (Mckeever et al., 1985). Both TL and OSL need a natural dosimeter such as white mineral, which does not need to be specially installed in advance, prior to dose estimation. Quartz is an excellent material for use in dosimetry, because of its almost ubiquitous availability including an accidental place. Feldspar is an extensive ternary family of minerals appropriate for TL dosimetry as they display a strong luminescence and are quite common in the Earth's formation. However, it is known that most feldspars are handicapped by 'anomalous fading' in TL: that is, loss of TL from all traps during long storage (Wintle, 1977), leading to underestimation in dosimetry.

Conventional TL and OSL dosimetry of the dose component due to natural background sources can be an involved and time-consuming process made more difficult in contaminated areas with residual exposure from a nuclear accident. In addition, the detail emission mechanisms of TL and OSL are not clear yet. Although the bulk structure of quartz used is normally the same regardless of its origin (usually α-quartz), the detailed

dosimetric properties of the materials depend upon the point defects contained within the crystal matrix. However, the defect type, structure and population can vary markedly from sample to sample.

In this paper, the basic studies on radiation-induced luminescence from natural quartz were conducted and new dosimetry with violet-TL (VTL) was developed. In chapter 2, the emission mechanism of both blue-TL (BTL) and red-TL (RTL) was investigated in conjunction with some radiation-induced phenomena after annealing treatments of natural quartz samples. In chapter 3, the OSL sensitivities were studied from an aspect of influence of the dose rate changes during irradiation, followed to radioluminescence (RL) intensity changes. The VTL dosimetry method was developed in chapter 4. The effects of changing the size of the irradiation dose, the preheat temperature, kinetic parameters and sun-bleaching were investigated. In chapter5, the residual doses using several luminescence-methods were compared in quartz and feldspar extracts from atomic bomb-suffered roof tiles.

2. Effects of annealing treatments on radiation-induced phenomena from natural quartz samples

2. 1. Introduction

It is well known that there are lots of radiation-induced luminescence phenomena in white minerals, such as radioluminescence (RL), thermoluminescence (TL), optically stimulated luminescence (OSL), and so on. The luminescence phenomenon arises from the recombination of luminescent holes with electrons which are released from metastable energy levels within dielectric materials (natural materials and ceramics). In the TL-measurements, the blue-TL (BTL) has been utilized for both quartz and feldspar grains till 1980s, although anomalous fading effects have been noticed especially for feldspars. In 1986, the red-TL (RTL) phenomenon from quartz grains has been initially discovered from beach sands (Hashimoto et al., 1986) and subsequently from volcanic tephra layers and burnt archeological porcelain pieces (Hashimoto et al., 1987, 1999a, 2000a). The estimation of equivalent dose using RTL from natural quartz and artificial sample has been verified to be efficient for the reliable dating of tephra layer as well as retrospective dosimetry (Hashimoto et al., 1993, 1996a, 1999b; Takano et al., 2003).

Quartz from volcanic ash layers always indicates RTL, whereas quartz from plutonic rock such as pegmatite origin and granite strata gives a typical BTL. BTL has been considered to be attributable to the contribution of aluminum (Al) impurities by substituting silicon atoms. However, the non- or negative correlation between Al impurity concentrations and BTL

intensities has been often observed when the correlations were researched in natural quartz samples collected from different origins (Hashimoto et al., 1994, 1997a). They also suggested that atomic hydrogens derived from radiolysis of OH-related impurities could operate as killers of radiation-induced Al-hole centers corresponding to typical BTL-centers (Hashimoto et al., 1998). The non- or negative correlation was also occurred within single rock crystal slices (Hashimoto et al., 2003a). However, the understanding of defect production in natural BTL quartz is still insufficient. Furthermore, the reason for the emission mechanism of RTL has not yet to be well explained.

In this study, the emission mechanism of both BTL and RTL was investigated in conjunction with some radiation-induced phenomena after annealing treatments of quartz samples. For the BTL, the quenching model concerning atomic hydrogen and Al-hole centers based on electron spin resonance (ESR) spectra was examined for quartz by applying various annealing treatments. The RTL-related centers were also investigated using ESR techniques. Furthermore, kinetic parameters such as activation energies were evaluated by applying both the isothermal decay and various heating rates methods in order to make clear emission mechanism on RTL.

2. 2. Experimental

2. 2. 1. Sample preparation

Madagascar quartz sample has a hydrothermal origin and exhibits BTL (Hashimoto et al., 2003a). Medeshima quartz grains are volcanically originated and show RTL phenomena (Nakagawa et al., 2003). Both quartz samples were extracted by a usual treatment of 6M hydrochloric acid (HCl) and 6M sodium hydroxide (NaOH) followed by 20 min of concentrated hydrofluoric acid (HF). The etching condition applied by HF was at room temperature under continuous ultrasonic agitation to remove surface layer with effects of α-ray in quartz. Further purification of the quartz grains was performed by hand selection for the sake of elimination of feldspar grains as low as possible under a microscope. The purified quartz samples were sieved to adjust the grain sizes ranging from 150 μm to 250 μm in a diameter for ESR spectrometry, BTL and RTL measurements. Prior to irradiation, the grains were annealed at 450 °C for 5 min in an electric furnace to eliminate the effects of irradiation.

A portion of each quartz sample was annealed for 24 hr at 100 °C temperature intervals ranging from 400 to 1000 °C. The heating and cooling rates were 1000 °C/hr and 300 °C/hr, respectively.

A Z-cut slice (2 mm in thickness) of Madagascar crystalline quartz was also subjected to infrared (IR) spectrometry after the annealing treatments.

The quartz grains were irradiated with a ^{60}Co source (20kGy at a dose rate of approximately 15 kGy/h, which was subsequently evaluated for the absorbed dose of quartz from water-absorbed dose) at room temperature

and -196 °C in Kyoto University Research Reactor Institute.

2. 2. 2 ESR measurements

All samples examined were 100 ± 10 mg in weight. Upon γ-ray irradiation, the sample annealed was stored in –196 °C. The ESR measurements were carried out at -196 °C and at room temperature, even after the annealing experiment at room temperature using an ESR spectrometer (Jeol Ltd. JES-TE 200). The g-values used in this experiment were derived with a determining Mn^{2+} marker equipped in the spectrometer. Prior to these ESR measurements, saturation curves were also measured by the application of variety of microwave power levels as far as four centers were concerned. As results, the condition for hydrogen radicals was curried out under the following conditions: microwave power, 0.03 mW (for BTL-quartz) or 0.64 μW (for RTL-quartz); magnetic field modulation, 0.5 mT at 100 kHz; sweep time, 15 min; time constant, 0.3 sec; magnetic field, 294.4 ± 10 mT. The conditions for Al-hole centers, Ti-centers and an unidentified centers were as follows: microwave power, 1 mW; magnetic field modulation, 0.5 mT at 100 kHz; sweep time, 8 min; time constant, 0.3 sec; magnetic field, 326 ± 25 mT. Each of the signal intensities was normalized to 100 mg.

The ESR signals produced by γ-ray irradiation of the quartz grains were measured at -196 °C. The first ESR results hereafter are called initial Al-hole center. Subsequently, the samples were warmed up to room temperature and the ESR signals were measured at the room temperature. Finally, the ESR measurements were again performed at -196 °C. The results measured are called second Al-hole center, henceforth.

2. 2. 3. Measurements of BTL and RTL

An on-line spectrometric system for extremely weak photo-emission derived from TL has been assembled (Hashimoto et al., 1997b). The system consists of two main parts, a heater controlling unit and a spectrometric one. The sample temperature was controlled to be heated at a linear heating rate of 1 °C/sec. Each intensity/wavelength was scanned by a photo-diode array (PDA, 512 channels, Hamamatsu Photonics) and saved in the controller memory as 16 bit digital values. The scanning interval was 35 msec. Each of 512 channel data in wavelength width, consisting of 8 bits per channel, was summed up to 28 cycles to form one spectrum per sec in a spectrometric controller.

The BTL and RTL glowcurves were obtained by a conventional photon-counting TL-measuring system (Hashimoto et al., 1986). The BTL measurement was performed using a photomultiplier tube (PMT) with a bi-alkali surface (Hamamatsu, R585S). For the detection of BTL, a blue filter (Hoya, B-480) was installed between the PMT and the heater site. On the other hand, the RTL glowcurves were measured using a PMT with a multi-alkali surface (Hamamatsu, R649S) sensitive to the red region. To detect the RTL, two infra-red (IR) cut filters (Kenko, IRC-65L and Kureha, UCF-02) and a red filter (Toshiba, R-60) were set in the front of the PMT.

In both measurements of TL spectrum and TL glowcurve, a ceramic heater was entirely covered with biotite plate to avoid the effect of black body radiation and the heating rate was used 1 °C/sec. About 5mg of quartz samples were employed for these experiments.

2. 2. 4. Measurements of IR-absorption spectra

IR spectrometry of the z-cut slice of Madagascar quartz was carried out at room temperature before and after applying the annealing treatments (400-1000 °C) using a conventional apparatus (HITACHI, 270-30). Before spectrometry, the measuring area of the quartz slice was checked for the aspects of homogeneity of color center patterns caused by X-ray irradiation. IR-transmittance measurements were used to investigate the hydroxyl impurity groups by measuring their OH stretching mode absorption in the 3600-3200 cm^{-1} region.

2. 2. 5. Measurements of kinetic parameters

There are many methods available for the analysis of TL glow peaks to obtain values of the trapping parameters, the activation energy E, the frequency factor s and the order of kinetics b in thermal stimulation of trapped electrons.

Two different methods (Prokein and Wagner, 1993) were applied in this study, which are presented briefly below. The apparatus was adjusted to RTL measurements as described in section 2.2.3.

On the basis of the fundamental TL kinetics equation, the mean life τ, which is the average residence time of electrons in trapping centers, is inversely proportional to the probability (λ) of the electron escaping from the capture center within unit time (Marfunin, 1979):

$$\tau = \frac{1}{\lambda} = s^{-1} \exp\left(\frac{E}{kT}\right), \qquad (2\text{-}1)$$

where k is the Boltzmann constant. For a given trap depth the mean life of electrons in a trapping state depends strongly on the storage temperature T. E typically ranges between 0.8-2 eV, giving mean lives at an ambient temperature of 283 K (15 °C) or 298 K (25 °C) ranging from seconds up to millions of years for very shallow traps to very deep traps, respectively (Prokein and Wagner, 1993; Hashimoto et al., 1999b).

2. 2. 5. 1. Isothermal decay method (ITD)

The trap parameters E, s and b are determined with ITD method. The method makes use of the decay of TL peaks as a function of heating duration t when the sample is held isothermally at an elevated temperature

$T_{n\,(n=1,\,2,\,3,\,\ldots)}$. The quartz grain sample was heated from 40 °C up to the target temperature T_1 at a constant heating rate of 1 °C/sec, which contained the position of a glow peak. Thereafter, the temperature was retained at the T_1 for 300 sec. The measurements were performed using different target temperatures (250-350 °C).

For general-order kinetics the decay curve of TL intensity I at an elevated temperature T_n with retaining time t is given by:

$$\left(\frac{I_0}{I}\right)^{1-1/b} = 1 + I_0 n_0 t(b-1), \qquad (2\text{-}2)$$

where n_0 is the initial number of traps filled with electrons (Chen, 1984).

The $(I_0/I)^{1-1/b}$ vs t plots are in a straight line only when the correct value of b is substituted (May and Partridge, 1964). Thus, the kinetic order b of the decay can be determined by trial and error (Azorin, 1986). Preheating (200 °C, 5min) was done in order to achieve a single glow peak above 250 °C before RTL measurements.

2. 2. 5. 2. Various heating rates method (VHR)

The trap parameters E and s are obtained with this technique (Hoogenstraaten, 1958). The temperature T_m at the glowcurve maximum depends on the heating rate β:

$$\ln\left(\frac{\beta}{T_m^2}\right) = \ln\left(\frac{sk}{E}\right) - \left(\frac{E}{kT_m}\right). \qquad (2\text{-}3)$$

Consequently T_m shifts to higher glowcurve temperatures with increasing heating rate β. In an Arrhenius diagram in which ln (T_m^2/β) was plotted

against $1/T_m$ for various β, a straight line with the slope E/k is obtained, from which E is calculated. The frequency factor s is obtained from the intercept ln (ks/E). The method is strictly applicable only to peaks obeying first-order kinetics (b=1). However, Chen and Kirsh (1981) showed that the method practically yielded a very good approximation of E for any kinetic order even if the frequency factors were temperature-dependent (Gartia et al., 1992). The method is available for the estimation of the activation energy within 1% overestimation in the case of non-first-order kinetics (Singh et al., 1990).

The sample was heated up to 450 °C at various heating rates to obtain the heating rate dependence of RTL glowcurves. The heating rates used were 0.1, 0.2, 0.5, 1.0 and 2.0 °C/sec. The preheating was done under the same condition to that in the ITD method (see section 2.2.5.1.).

2. 3. Results and discussion

2. 3. 1. Changes of some radiation-induced phenomena in BTL-quartz associated with annealing treatments

Six ESR spectra from the natural Madagascar quartz grains are illustrated in Figure 2.1. Figure 2.1 (a)-(c) shows the spectra of initial Al-hole centers, atomic hydrogen and second Al-hole centers in the quartz annealed at 800 °C, while Figure 2.1 (d)-(f) indicates each spectrum of these centers in the quartz annealed at 1000 °C.

The atomic hydrogen signal almost disappeared in the ESR-spectrum (e) of quartz grains annealed at 1000 °C, although the atomic hydrogen signal existed until 800 °C in annealing temperature in Figure 2.1 (b). Once the quartz grains were heated up to room temperature after irradiation, the atomic hydrogen signal completely disappeared in all samples used. Similar results in synthetic quartz and glasses were found by Weeks and Abraham (1965) and Person and Weil (1974). On the other hand, the Al-hole centers show the similar characteristic pattern between initial {(a) and (d)} and second spectra {(c) and (f)}, although the intensities of Al-hole centers were significantly decreased by warming up to room temperature. The decreasing proportion of Al-hole center in quartz annealed at 800 °C is greater than that at 1000 °C. These decreasing rates are in good agreement with the intensities of the atomic hydrogen {(b) and (e)} at -196 °C, supporting a role of the atomic hydrogen as a killer of Al-hole center (Hashimoto et al., 1997, 2000b) with the previous results for the synthetic quartz by Halliburton et al. (1981).

Figure 2.2 shows the intensity changes of the initial Al-hole centers, the atomic hydrogen and the second Al-hole centers with annealing temperatures, respectively. The intensities of the initial Al-hole center in Figure 2.2 (a) tended to increase linearly in the entire regions of the annealing temperature from 400 °C to 1000 °C. This enhancement in the intensity might be attributed to the gradual remove of the disturbing barrier which causes ionization in the vicinity of the substituted Al sites, such as relaxation of lattice distortion or crystal stress by thermal treatments, and some replacement of interstitial Al into substitutional Al (Cohen, 1960).

The ESR signal intensities of atomic hydrogen also increased linearly up to 800 °C (Figure 2.2 (b)) similar to the initial Al-hole centers. It is probably owing to release from rigid binding. However, the intensities dropped down close to zero above 800 °C. This tendency was significantly different from that in the initial Al-hole centers. The different behavior suggests the existence of a different mechanism above 800 °C between the initial Al-hole centers and the atomic hydrogen. From this result, it is clear that the sudden steep elimination of atomic hydrogens is intimately associated with the phase-transition temperature of β-quartz / tridymite around 870 °C, probably associated with OH impurities, as described below.

Contrary to the intensity changes of atomic hydrogens, it should be emphasized that the apparent steep increase of the second Al-hole centers occurred after the annealing treatment beyond 800 °C as seen in Figure 2.2 (c). This sudden change is in good agreement with the steep disappearance

of atomic hydrogen in Figure 2.2 (b). The second Al-hole center curve in Figure 2.2 (c) agreed excellently with the difference between the initial Al-hole center in Figure 2.2 (a) and the atomic hydrogen curves in Figure 2.2 (b).

These results allow us to make the reasonable assumption that the atomic hydrogen can operate as a killer or quencher of Al-hole center during irradiation; Al-hole center is decreased by interaction with atomic hydrogen, as observed earlier in synthetic quartz by Halliburton et al. (1981) and Campone et al. (1995).

The IR-results could also offer information regarding origin of the atomic hydrogens. It was revealed that the IR-absorbance at ~3492 cm^{-1}, which was assigned to Li-dependent OH bonds (Kats, 1962), showed a negative correlation with the second Al-hole centers as shown in Figures 2.2 (c) and 2.3. In the IR-spectra, almost similar shapes of IR-absorption spectra are shown up to 700 °C in annealing temperature. However, it is obvious that the OH-stretch absorption bands start to decrease at 800-900 °C. This decreasing tendency in the wide region of 3000-3600 cm^{-1}, which has been assigned to hydroxyl groups, probably corresponds to elimination of ionizable OH impurities by annealing treatments. Thermal reactions of dangling bonds should produce H_2O molecules. The individually isolated H_2O could not be mobile within quartz crystal. However, since the annealing treatment of the quartz slice beyond 800 °C is certainly related to the phase transition temperature of β-quartz / tridymite around 870 °C, the phase transition could cause relatively large

clusters of H_2O molecules. As a result, the vaporization of molecular H_2O from quartz brings great changes in radiation-induced phenomena. This mechanism could explain the reason why the broad absorption around 3100-3500 cm^{-1} gradually vanished from the IR spectra with annealing temperatures. However, some main peaks still appeared in this region beyond 800 °C.

The TL-spectrometric analysis was applied to the Madagascar quartz grains which showed stronger BTL. Figures 2.4 and 2.5 show the BTL glowcurves and the integrated BTL intensities dependent on the annealing temperature, respectively. The integrated BTL intensity is the total photon counts through the heating range. It was found that there was little sensitivity change of BTL in the annealing temperatures ranging between 400 °C and 700 °C, whereas the sensitivity increased suddenly beyond 800 °C. This BTL-response resembles closely the annealing behavior of second Al-hole center in ESR spectrum as illustrated in Figure 2.2 (c). These results strongly support a widely believed mechanism that BTL of quartz irradiated with ionizing radiation is attributed to recombination of Al-hole centers $[AlO_4/h^+]^0$ and electrons released from the trapped sites (Marfunin, 1979; McKeever, 1991; Martini et al., 1995).

On the basis of these annealing experiments, it was ascertained that the atomic hydrogen derived from radiolysis of OH impurities could eventually operate as a killer or quencher of radiation-induced Al-hole centers, resulting in a decrease of BTL in quartz up to 800 °C of annealing temperature, whereas a lack of ionizable OH causes a sharp enhancement

of BTL together with second Al-hole centers beyond 800 °C in annealing treatment.

Natural quartz includes substitutional Al as an impurity (Iwasaki and Iwasaki, 1993). Al ions exist in the 3+ valence state in quartz and easily substitute for silicon (4+), thus requiring charge compensation. The Al^{3+} is mainly charge-compensated in two different ways: (1) Al-Li^{+}; the interstitial Li^{+} exists adjacent to Al^{3+}. (2) Al-OH; the hydrogen is located on a non-bonding p-orbital of an oxygen that is adjacent to the Al. The Al-OH center gives a strong IR absorption at 3367 cm^{-1} as seen in Figure 2.3. According to Halliburton et al. (1981), irradiation at the liquid nitrogen-temperature does not affect to the Al-Li^{+} related OH bond, while the Al-OH brings on the Al-hole center and interstitial atomic hydrogen as follows:

$$[AlO_4/H]^0 \rightarrow [AlO_4/h^+]^0 \text{ (Al-hole center)}$$

$$+H^0 \text{ (interstitial atomic hydrogen).} \qquad (4)$$

The ESR-centers of Al-hole center and atomic hydrogen are stable up to about 120-130 K as indicated in Hashimoto et al. (2003a). Above this temperature region, some parts of both Al-hole center and atomic hydrogen become mobile and recombine to Al-OH center $[AlO_4/H]^0$ as mentioned above. However, the irradiation at room temperature (300 K) converts the Al-Li into a mixture of Al-hole center, Al-OH center and Li^{+} by the reaction of atomic hydrogen, which comes from the H-related defect centers. It is noteworthy that these H-related centers induce many satellite bands as shown in Figure 2.3. In fact, a main peak of Al-OH at 3367 cm^{-1}

band does not seem to change with annealing treatment, although the other satellite OH defect bands do clearly change. Among these OH bands, Li dependent OH at 3492 cm^{-1} band in a lot of natural quartz is most influenced by annealing treatment. The weaker bands also disappear with the annealing procedure. Their OH-defect bands identified at 3581, 3437, 3400 and 3350 cm^{-1} seem somewhat different from those in the natural quartz. Additionally, they also found that as-grown cultured quartz dose not change any Al-OH absorption bands at 3367 and 3306 cm^{-1} with annealing treatment. These results are generally consistent with the present experimental results.

2. 3. 2. Changes of some radiation-induced phenomena in RTL-quartz associated with annealing treatments

Figure 2.6 shows a TL spectrum in contour map form of unannealed quartz grains exposed to 1.2 kGy of X-ray at room temperature. The TL spectrum has a TL emission peak around 330 °C at 630 nm (red-region).

Figure 2.7 shows RTL glowcurves of Medeshima quartz after annealing at various temperatures (three aliquots each). Figure 2.8 shows the changes of RTL intensities, which were integrated in the whole region as a result of annealing temperatures, with standard deviation of the multi-aliquot measurement. The changes of RTL intensities with annealing temperatures were qualitatively described as followed: The intensities of RTL increased sharply up to 800 °C. After reaching the maximum peak, the RTL suddenly decreased with increasing annealing temperatures. The emission changes of RTL seem to be closely related to the phase-transition temperature of β-quartz / tridymite around 867 °C as also suggested in BTL described in section 2.3.1., from BTL intensity changes.

Figure 2.9 represents typical ESR spectra of Medeshima quartz grains. In Figure 2.9 (a), two signals with equal intensity due to atomic hydrogens appear at an interval of approximately 53 mT. Al-hole center signals emerge at the middle of the two atomic hydrogen signals. The separation of atomic hydrogen resonance was due to the hyperfine (hf) splitting caused from proton spin (I = 1/2). On the other hand, the Al-hole center resonance gave sixlet signals due to the hf structure of ^{27}Al (I = 5/2). Figures 2.9 (b) and (c) show ESR spectra of samples without annealing treatment (or

unannealed) and with annealing treatment at 900 °C, respectively. Both figures include the ESR signals before and after warming up to room temperature, corresponding to the initial and second Al-hole centers, respectively. By comparing two Al-hole centers between the initial and second, it is noticeable that the appearance of Ti-centers could certainly be observed only after the warming up in both samples. These results imply that atomic hydrogens and alkaline ions can be created and stored at -196 °C after irradiation. Several researchers have already suggested that the Ti-center has been attributed to a substitutional Ti associated with an extra electron. In addition to the hf structure due to major Ti isotopes, the center exhibits a super-hyperfine (shf) structure owing to adjacent alkaline ions (McMorris et al., 1971; Falgueres et al., 1991; Toyoda, 1998). Mainly, Ti-centers have been assigned from the derivation of hydrogen, lithium and sodium ions. Furthermore, it was noteworthy that the signal of atomic hydrogens completely disappeared after warming up to room temperature. This phenomenon concurs with a previous result obtained in BTL-quartzes (Hashimoto et al., 1997a). In Figure 2.9 (d), ESR spectra of atomic hydrogens in unannealed (or as-received) and annealed samples are demonstrated. The intensity of the unannealed quartz is higher than that of the annealed quartz, although both line widths were assigned to be approximately 1 mT.

Figure 2.10 (a) represents the ESR intensity of the initial Al-hole center as a function of annealing temperature. The intensity decreased with increasing the annealing temperature. Particularly, there is a large

difference in intensity between 900 °C and 1000 °C. This tendency is clearly different from the result of BTL-quartz as shown in section 2.3.1. The intensities of initial Al-hole center from BTL-quartz linearly grew over the entire range of annealing temperature. Figure 2.10 (b) and (c) show the intensities of atomic hydrogen and second Al-hole center from annealed quartz, respectively. The intensity of atomic hydrogens became smaller and smaller associated with increment of the annealing temperatures. The decreasing tendency of atomic hydrogen was especially remarkable between 600 °C and 700 °C. On the other hand, the changes of second Al-hole center showed a rapid increase between 600 °C and 700 °C. The intensity difference of Al-hole centers between 700 °C and 900 °C annealing temperatures was indistinguishable. The decrease of Al-hole center intensity was affected by the annealing treatments above 900 °C. The above changes obviously show different behavior between RTL- and BTL-quartz grains. In the case of BTL-quartz, steep increment of the second Al-hole centers was confirmed after annealing treatments beyond 800 °C. The reasons would be due to their origins, the different impurity contents, the different structures of crystals and so on. The degrees of disorder in crystal might be responsible for these results.

The power saturation curves were measured for atomic hydrogens to confirm such evidence. Figure 2.11 shows the result for Medeshima quartz as a representative RTL-quartz. The RTL-related atomic hydrogens were clearly delayed to saturate in comparison with BTL-related atomic hydrogens (0.03 μW). In general, the application of higher microwave

power is required to reach saturation in ESR signal intensity if atomic hydrogens exist at narrow spaces and cause large interaction with adjacent lattice or other materials. The saturation will be quickly progressed if the atomic hydrogens exist in isolated sites (Hase, 1985). On the basis of this result, RTL-related atomic hydrogens are considered to exist in narrower space, whereas BTL-related atomic hydrogens were captured in wide space sites as isolated states. The hf splitting (53mT) of the atomic hydrogen signal in RTL-quartz was larger than that in BTL-quartz (52mT). The value of free hydrogen is 50.8mT. This also means that the atomic hydrogen in RTL-quartz should locate in narrower space, comparing to that in BTL-quartz as described in the above.

A relationship between the intensity of atomic hydrogens and the reduced amount of Al-hole centers was investigated to confirm whether or not atomic hydrogens operate as killers of Al-hole centers in RTL quartz, as illustrated in Figure 2.12. The reduced amount of Al-hole centers corresponds to difference between the initial Al-hole center intensity (Figure 2.10 (a)) and the second Al-hole center intensity (Figure 2.10 (c)). In Figure 12, the intensities of atomic hydrogens, equivalent to values in Figure 2.10 (b), are plotted against the reduced amounts of Al-hole centers. It can be confirmed certainly that the positive correlation between the atomic hydrogens and the reduced amounts of Al-hole centers. This was verified with a good correlation factor of 0.96. This result will also be a strong evidence of the following process: A part of the initial Al-hole centers produced by the irradiation at -196 °C disappears as a result of

interaction or recombination with atomic hydrogens or similar radiation-induced radicals. This process agrees with the previous suggestion, in which hydrogen radicals were reasonably considered to behave as killers of Al-hole centers in BTL-quartz (Hashimoto et al., 2000b).

Any clear correlation was not induced between the Al-hole center intensities and the RTL intensities. In order to search RTL-related holes, ESR measurements at room temperature were conducted as a function of annealing at various temperatures. An ESR signal having the g-value of 2.00_3 was detected as shown in Figure 2.13 (a). The intensity of this signal is plotted against the annealing temperatures in Figure 2.13 (b). An annealing temperature dependency appeared for the intensity of this ESR-signal, which is similar to that of RTL. Therefore, it can tentatively be proposed that RTL-hole centers are responsible for this ESR signal detected at room temperature. Contrary to the case of BTL, the role of atomic hydrogen is still unclear in the RTL-concerned quartz, although its noticeable connection was proved with Al-hole centers.

2. 3. 3. Changes of RTL property by annealing treatments

From the change of RTL glowcurves, it was confirmed that trapped sites or electrons were affected by annealing treatments (Figure 2.7). The glow peak was broadened and shifted to lower temperature after the annealing treatments. As a result, the redistribution of original trapping sites occurs in more flexible as well as non-rigid sites when the thermal treatment was applied. When quartz samples were irradiated by γ-ray under liquid nitrogen temperature, no signals from Ti-centers were present. However, ESR signals of the Ti-centers were measured together with Al-centers at -196 °C after once warming up to room temperature. The Ti-centers were experimentally confirmed as electron-trapping centers in this ESR-spectrum only. These Ti-centers changed as a function of the annealing temperature. The grain sample was stored for 1 hr at room temperature after irradiation at -196 °C. The storage was required to be sufficient for all diffusion process to be completed and all Ti centers to be formed, as suggested by Isoya (1988).

Figure 2.14 shows three Ti-centers in unannealed Medeshima quartz which was irradiated at -196 °C or room temperature. The Ti-centers as electron trapping centers in three configurations: $[TiO_4/H^+]^0$, $[TiO_4/Li^+]^0$ and $[TiO_4/Na^+]^0$. The effect of irradiation temperature was observed. The intensity of Ti-centers irradiated at room temperature was higher than that of Ti-centers irradiated at -196 °C. In the case of irradiation at -196 °C, the intensity of $[TiO_4/H^+]^0$ was apparently higher than the intensities of $[TiO_4/Li^+]^0$ and of $[TiO_4/Na^+]^0$ as shown in Figure 2.14. In the case of

irradiation at room temperature, the intensity of $[TiO_4/H^+]^0$ was similar to the intensities of $[TiO_4/Li^+]^0$ and of $[TiO_4/Na^+]^0$. On the basis of these results, it was ascertained in unannealed quartz that alkaline ions would easily move to Ti sites during irradiation at room temperature as compared with the case of irradiation at -196 °C.

The maximum amount of $[TiO_4/H^+]^0$ centers in the unannealed quartz gradually decreased with increasing annealing temperature as shown in Figure 2.15. This behavior of $[TiO_4/H^+]^0$ centers is quite similar to that of atomic hydrogens themselves as described in Figure 2.16. This result can be explained by the following approach. The more atomic hydrogens are produced by the irradiation at -196 °C, the more atomic hydorgens can be trapped in the Ti-centers after warming up to room temperature. In Medeshima quartz annealed at different temperatures, it is confirmed that a probable correlation between the intensities of atomic hydrogens and of $[TiO_4/H^+]^0$ centers (Figure 2.17) with the correlation factor of 0.96. Therefore, it is suggested that a part of the atomic hydrogens in an irradiated state at -196 °C is recombined with those of the Al-hole centers when emitting luminescence is accompanied with the elevation of temperatures as suggested by Hashimoto et al. (2000b). Alternatively, the remained part of atomic hydrogens can be combined with the Ti-centers at room temperature. The same model that the $[TiO_4]^0$ center acts as a trap for the atomic hydrogen, was suggested also by Rinneberg (1972). That is, the atomic hydrogens are captured in Ti-centers as the electron trap or operate as killers of Al-hole centers in Medeshima quartz.

The $[TiO_4/Li^+]^0$ centers increased with elevating annealing temperatures as seen in Figure 2.15. This tendency is a completely opposite to the $[TiO_4/H^+]^0$ centers (Figure 2.15). Furthermore, the behavior of $[TiO_4/Na^+]^0$ represents a similar tendency regarding RTL intensities (Figure 2.8). These $[TiO_4/Li^+]^0$ and $[TiO_4/Na^+]^0$ centers were created after performing a -196 °C irradiation and warming up to the room temperature. Irradiation at sufficiently low temperature (-196 °C) with γ-rays, ultimately causes creation of holes (removal of an electrons) on oxygen ions nearest to Al. The cation M^+ (H^+, Li^+, Na^+) does not have sufficient thermal energy to diffuse away under liquid nitrogen temperature. During warming, the ions M^+ diffuse away, resulting in $[AlO_4/h^+]^0$ and $[TiO_4/M^+]^0$. A general scheme for the formation of the impurity related paramagnetic centers in quartz was suggested by Weil (1984). From this scheme, the formation of Ti-centers need the existence of potential electron donors (e.g. $[AlO_4/Li^+]^0$) and potential electron accepters (e.g. $[TiO_4]^0$). The changes of Ti-center intensities suggest that the electron-trapping centers are affected by thermal annealing treatments.

It was noteworthy that similar annealing temperature dependency appeared in the intensities of $[TiO_4/Na^+]^0$ in ESR measurements and RTL as shown in Figures 2.15 and 2.8. Moreover, it was tentatively proposed that the electron trapping centers related to RTL emission were responsible for the $[TiO_4/Na^+]^0$ signals. This is similar result of Schilles (2001), who have obtained a simultaneous increase of the RTL and the ESR intensity of $[TiO_4/Na^+]^0$ center in the quartz sample.

RTL glowcurves were affected by annealing treatments as seen in Figure 2.7. A glow peak position around 330 °C shifted to a lower temperature region and the shapes of the peaks broadened, when the thermal annealing treatment was applied. Since the peak position and shape relate to electron traps, and then electron traps was apparently influenced by annealing treatments. On the basis of these experimental results, both the isothermal decay (ITD) and various heating rates (VHR) methods were applied in order to determine the kinetic parameters of trapped electrons.

The results are summarized in Table 2.1. The activation energy is well known as the trap depth energy level below the conduction band. Unannealed (or as-received) quartz gives the highest activation energy value determined by ITD method. With increasing annealing temperature, the activation energy decreases to 0.92 eV. On the other hand, the activation energy in the VHR method no longer shows a systematic decrease with elevating annealing temperature. The difference between the results in the ITD and VHR methods indicates that the electron traps responsible for the RTL peak are influenced by the higher temperature annealing treatment. If it was completely unaffected, the similar results would be obtained in both the ITD and VHR methods. The sites of electrons trapped are found again to be influenced by the annealing treatment. The frequency factor also takes an analogous tendency to the activation energy. In addition, the kinetic order was greater as the annealing temperature was higher in the ITD method. According to the

Halperin-Braner equations (Horowitz et al., 1995), TL glow peaks become broader with increasing order of kinetics, i.e., reflecting an increase of retrapping. The RTL glowcurves became broader with increasing annealing temperature as seen in Figure 2.7, in which the similar tendency was confirmed from aspects of change in kinetic orders. Otherwise, the reason why RTL peak was broadened with annealing treatment is the overlapping of several peaks.

As McKeever (1985) pointed out, fitting of a general order isothermal decay curve with an irresolvable sum of first-order decay curves can deliver wrong results. However, Singh et al. (1990) showed that, based on a theoretical and experimental studies, the VHR method could be considered independent of the order of kinetics of the TL process. Thus this method can deliver reliable results and can be safely applied for all types of TL peaks regardless of their order of kinetics.

Thermodynamic or kinetic parameters obtained in the ITD and VHR methods were used for estimating of the mean lives of trapped electrons at ambient temperature. The results are summarized in the last column of the Table 2.1. The mean lives obtained by both methods are longer than million years in quartz samples with annealing treatments until 700 °C. However, the difference of the mean lives between the ITD and VHR methods is appeared over 800 °C in the annealing temperature. This tendency relates to the activation energy.

2. 4. Conclusion

These experiments allow us to conclude that there are some correspondences between ESR signals and TL peaks. In BTL, the quenching model concerning atomic hydrogens and Al-hole centers was confirmed. In the annealing experiments, the increasing trends in both the atomic hydrogens and initial Al-hole centers up to 800 ^{O}C were proved. However, atomic hydrogen signals suddenly disappeared when the samples were annealed above 800 °C, in good coincident with a significant decrease in the IR-absorption due to OH stretching around 3500 cm^{-1} region. This sharp change should be related to the phase-transition temperature of β-quartz / tridymite. As a result, it is possible that atomic hydrogens from OH-related impurities could also operate as the main "killer" of all radiation-induced phenomena, such as Al-hole centers, color centers and BTL in natural quartz.

The RTL-related centers in ESR spectra were searched in combination with the annealing experiments. A positive correlation was found between the hydrogen radicals and the reduced amounts of Al-hole center in RTL-quartz. This behavior of hydrogen radicals agrees with the result that hydrogen radicals behave as killers of Al-hole centers in BTL-quartz. A positive hole center having the g-value of 2.00_3 tends to increase with the RTL intensity up to 800 °C of annealing temperature, but from 900 °C, remarkably, decrease to the level of an unannealed sample.

The ESR for Ti-centers was measured together with Al-hole centers at -196 °C after warming up to room temperature. It should be emphasized

that only three kinds of Ti-centers were experimentally recognized as electron-trapping centers except for Al-hole centers in the ESR measurement. The intensities of $[TiO_4/H^+]^0$, $[TiO_4/Li^+]^0$ and $[TiO_4/Na^+]^0$ centers were affected by the annealing treatment.

Additionally, the amount of $[TiO_4/H^+]^0$ was proportional to the amount of atomic hydrogens created by irradiation in Medeshima quartz. This could be explained that atomic hydrogens created are captured in Ti-centers or operate as killers of Al-hole centers.

Trapping sites of electrons were found again to be certainly influenced by the annealing treatments, according to differences of the kinetic parameters evaluated from between the ITD and VHR methods.

3. Influence of radioluminescence on optically stimulated luminescence from natural quartz grains

3.1. Introduction

An important application of the OSL, which is light emission during illumination to naturally or artificially irradiated materials, is dating of ancient archeological samples as well as geological ones. Additionally, OSL measurements have been utilized for retrospective dosimetry using quartz extracted from fired bricks and unfired mortars (Banerjee, et al., 2000; Bøtter-Jensen et al., 2000). In a pioneering work on OSL, Huntley and his workers started OSL dating of sediments using an argon ion laser (1985). Recent OSL readers are able to illuminate irradiated samples with blue light-emitting diodes (LEDs) or a blue laser (Bøtter-Jensen et al., 1999a, b). On OSL-dosimetry and dating, OSL-responses against some known doses can be obtained in laboratory. However, artificial doses are generally administered to higher dose rates in comparison with natural ones. Therefore, much attention must be paid whether OSL signals are dependent or independent of the dose rate.

In the OSL / SAR (single-aliquot regenerative-dose) protocol, the repeating cycle of heating, illuminating and irradiating procedures will give rise to systematic changes on luminescence sensitivity (Wintle et al., 1999). According to Spooner (1994), the OSL-decaying (or shine-down) rates at about 400 nm became 10 times faster than that at 514.5 nm argon-ion laser line as a stimulation source. In addition, bleaching effects were found to be effective at shorter wavelengths more than at longer ones

(Bøtter-Jensen et al., 2003).

Radioluminescence (RL) phenomenon, light emission during irradiation procedure, has been investigated using natural and artificial materials (Marazuev et al., 1995; Pető et al., 1996; Krbetschek et al., 2000). Some RL emission bands have been reported in various quartz samples (Pető et al., 1996; Krbetschek et al., 2000). If RL emission wavelength could be observed during artificial irradiation in shorter than wavelength of OSL-stimulation source, RL may be a cause of bleaching or diminishing effects of OSL of quartz sample just like during the OSL-stimulation.

In this section, OSL sensitivities are studied based on an aspect of influence of the dose rate changes during irradiation. Then, RL spectra are measured using an RL spectrometric system. Subsequently, influence of 400 nm RL (V-RL) intensity on OSL intensity is examined at various irradiation dose rates. OSL-bleaching phenomena will be discussed in conjunction with the effects of V-RL emission.

3. 2. Experimental

3. 2. 1. Sample preparation

Extraction of quartz grains (150–250 μm) from two surface soil samples around JAEA (Japan Atomic Energy Agency) was carried out by the following sequential procedures; acid-base treatments with 6M HCl and 6M NaOH solutions for a few hours each, etching treatment with 46% HF for 20 min, and heavy liquid density separation (2.63–2.67 g cm^{-3}) using a sodium polytungstate solution. Further purification of the quartz grains was done by hand selection under microscope for the sake of elimination of feldspar grains. Single Japanese twin crystal from a museum collection was also employed in the present experiment after crushing and sieving to adjust the grains sizes ranging from 150 μm to 250 μm in diameter. Prior to irradiation, each sample was annealed at 450 °C for 5 min in an electric furnace to remove natural irradiation doses.

The quartz samples were then exposed to γ-ray of a ^{137}Cs source (111 TBq, 365 mm distance). The fixed dose of 20 Gy was irradiated at the dose rate of approximately 1Gy min^{-1} at room temperature in the Radioisotopes Center of Niigata University.

3. 2. 2. RL spectrometry

On-line RL spectrometric system was developed to measure RL emission spectra of quartz samples as demonstrated in Figure 3.1. The system possesses sensitivity to wavelength between 350 and 750 nm (Hashimoto et al., 1991, 1995). For RL-measurements, an X-ray irradiation system (Varian, VF-50J tube with W-target, 50kV, 0.3 mA) surrounded by shielding lead blocks was set above quartz samples. RL observation was carried out twice for each sample, the first data being acquired for a quartz sample and the second one without the sample as background. These raw data were reconstructed into two dimensional relationship draws consisting of RL wavelengths and intensities.

3. 2. 3. OSL / RL measurements

Both OSL and RL measurements were carried out by an automated TL / OSL–reader system, improved for the OSL / SAR protocol (Hashimoto et al., 2002a, b). OSL of quartz grains previously irradiated to 20 Gy was evaluated using the OSL / SAR protocol as described by Wintle and Murray (2000). This protocol compensates for any sensitivity changes of the OSL signals by interpolating a test dose of 5 Gy for every regenerative dose (Murray and Mejdahl, 1999).

The OSL-reader equipped sixteen blue-LEDs (Nichia Chemical Industries Ltd., NSPB-500S) that had an emission peak at 470 nm with 20 nm FWHM. A GG420 filter (Schott) of 2mm thick was placed in front of each LED in order to remove the troublesome tail of blue light (<400 nm), which can cause cross-talk between the blue-ultraviolet OSL and the stimulating light. The OSL signals were detected with a photomultiplier tube (PMT, Hamamatsu, R585S) by inserting a UG-11 (Schott) and an IRC-65L (Kenko) optical filters. After 5 min preheating procedure at 220 ^{o}C, OSL-decay curves were recorded every 0.2 sec under blue light-illumination for 200 sec.

For RL-measurements, a small X-ray tube (Varian, VF-50J) installed in the luminescence leader was conveniently utilized. RL during X-ray irradiation was introduced to the PMT through an optical bundle fiber as illustrated in Figure 3.2. The V-RL signals were detected using the combination of PMT and optical filters analogous to the OSL measurements. The R-RL signals were detected using the combination of

PMT and optical filters analogous to the RTL measurements. This system allowed RL measurement in the temperature range 50 – 450 °C under continuous radiation exposure. Measurements were fully automated, allowing up to 16 samples to be measured in any one experimental run. To check reproducibility of V-RL measurements, the V-RL intensities were repeatedly measured. The integrated V-RL intensities of each measurement were compared and indicated very good reproducibility with <5 % of relative standard deviation.

3. 3. Results and discussion

3. 3. 1. RL property

An RL spectrum of the investigated natural quartz sample is shown in Figure 3.3. Two broad RL emission bands were recognized at 400 nm (violet) and 630 nm (red), although the present quartz grains fraction showed only the intrinsic RTL-property at higher heating temperature above 250 °C as illustrated in Figure 2.6. There existed clear difference between RL (two peaks) and TL emissions (single peak). V-RL emission centers were expected to be unstable above room temperature, because intense violet TL (V-TL) was not observed or was bleached from the natural quartz grains.

The V-RL intensity variations as a function of the X-ray irradiation duration for natural quartz samples are illustrated in Figure 3.4. All of V-RL curves show constant intensity with irradiation, although V-RL intensity increases with the increment of the dose rate. The V-RL curve decreases slowly at higher dose rates. Figure 3.4 shows the behavior of the V-RL signal, taken as the luminescence integrated over the 0.2 sec period, as a function of irradiation time. All of V-RL curves indicate constant intensity with irradiation, although the V-RL intensity increases with the increment of the dose rate. It is considered that these tendencies are caused by the equilibrium state of electron traps filling.

Figure 3.5 shows the R-RL intensity changes as a function of irradiation period. The R-RL curve of the same quartz sample gradually increases with irradiation. In a general model (Polf et al., 2004), an

increase in the RL is expected with the filling of all electron traps, including shallow and deep electron traps, as the trapping probability decreases and more electrons become available for recombination.

Figure 3.6 shows the R-RL intensity changes with heating temperatures for a natural quartz sample. The curve is obtained by the repeated R-RL measurements after each annealing treatment at 450 °C, 5 min in order to eliminate former irradiation. The R-RL intensity was the count at the start of irradiation. The temperature dependence of the derived R-RL signal reveals the thermal quenching. A similar temperature dependence of RL was observed by Wintle (1975) in natural quartz. The trap parameters for TL peaks in a number of TL glow curves have been determined using the initial rise method or the fractional glow technique. The obtained value has been corrected with the temperature dependence of RL intensity (Petrov and Bailiff, 1996; Hashimoto et al., 1999b).

3. 3. 2. Intensity variation of OSL and V-RL with irradiation dose rates

Variations of OSL intensities were practically examined for three kinds of natural quartz grains sampled at different places. Sample A was extracted from surface soil in Tokai, Ibaraki, Japan. Sample B was made from Japanese twin crystal. Sample C was extracted from surface soil in Hitachinaka, Ibaraki, Japan. Each aliquot was pre-irradiated to 20 Gy at 1.0 Gy min^{-1}. The OSL / SAR procedure was applied to confirm the fixed dose irradiation. Since the evaluated doses should agree to the fixed dose (20 Gy), they were compared among the samples at various dose rates. Figure 3.7 shows dependences of OSL intensities on several dose rates. It is confirmed that the estimated OSL-doses are meaningfully influenced on the irradiation dose rate beyond the experimental errors. Additionally, some different tendencies exist among the samples; samples A and C show overestimation, while sample B underestimation over 2 Gy min^{-1} dose rates. The former two samples show the reduction of OSL centers during artificial irradiation at the dose rates of more than 2 Gy min^{-1}. The reason why the phenomena occurred it was considered owing to effects of V-RL emission. This means that RL in the violet region brings on elimination (so-called self-bleaching effect) of OSL related electron centers in quartz.

The broad V-RL emission peak, as seen in Figure 3.3, is of photons whose wavelength is slightly shorter than that of the stimulating light (470nm). Spooner (1994) reported that the shorter wavelength for stimulation illumination cause the greater bleaching effects (Figure 3.8). There is negligible (<5 %) bleaching for wavelengths greater than 690 nm.

According to Figure 3.8, apparent decreases of OSL signals in quartz samples might be attributed to self-bleaching effects from the V-RL during ionizing irradiation.

This reduction of OSL intensity due to V-RL effects was studied further from V-RL intensity changes by varying the dose rate. In Figure 3.4, the dose rate dependence of V-RL signals is shown as a function of irradiating duration. The V-RL intensities are integrated during irradiation periods to accumulate the fixed dose (20 Gy), indicated as shadow areas in this figure. The resultant V-RL intensities are plotted as a function of the dose rate as shown in Figure 3.9. This figure exhibits that the total V-RL intensities are differently affected to variations of the irradiation dose rate. V-RL intensities of other two quartz samples are illustrated in Figures 3.10 and 3.11. These two V-RL intensities were also influenced by the changes of the dose rates.

Figure 3.12 shows the OSL intensity against the integrated V-RL intensity is at five different dose rates. The figure reveals that the OSL intensity possesses a negative relation to the V-RL intensity. The same tendency is also confirmed in other natural quartz grain samples as illustrated in Figures 3.13 and 3.14. These negative correlations should support the certain presence of self-bleaching effects during artificial irradiation. This means that V-RL emission release the electrons from trapped site in quartz even during artificial irradiation with regions at 1.0 - 10 Gy min^{-1} of the dose rate.

3. 3. 3. Another evidence of self-bleaching effects on OSL

The concept of self-bleaching effects on OSL signals, as described in 3.3.2., were supported from the following experimental evidence. As seen in Figure 3.15, three kinds of arrangements were conducted in this experiment. Arrangement (a) was used for the standard OSL intensity, which was compared with the OSL-results under other arrangements (b) and (c). Two kinds of X-ray irradiation arrangements (b) and (c) were utilized by inserting each quartz slice, which were able to bring on the different V-RL intensities derived from the slices irradiated. All of quartz slices were prepared from Madagascar quartz and were annealed at several temperatures. Several quartz slices were employed to obtain different V-RL intensities. In arrangement (c), a gelatin optical filter (Fuji SC42) was inserted between a quartz slice and a grain sample. Three aliquots from the sample C (Hitachinaka, Ibaraki) were followed to the three kinds of irradiation arrangements and OSL-measurements with a fixed dose of 20 Gy. The resultant OSL intensities are plotted against the integrated V-RL intensities of each slice. The V-RL intensities were measured dependent on each quartz slice in advance. The results are summarized in Figure 3.16. The remnant OSLs of an ordinate are the OSL intensity ratios from arrangements (b) and (c) against in (a), which are normalized to the lowest V-RL intensity obtained from a quartz slice. Figure 3.16 indicates that absence of bleaching effects is confirmed when the V-RL intensity of the slice is lower than 2.2×10^7 counts in every case. However, presence of bleaching effects is confirmed when the V-RL intensity of the quartz slices

is more than $2.2x10^7$ counts in arrangement (b). In the case of the highest V-RL intensity, the OSL intensity reduces by about 20 % (arrangement b) without filter insertion. However, the OSL intensity with a sharp cut filter insertion (arrangement c) shows almost no difference even in the case of high RL intensity region in comparison with the arrangement (b). The RL from the slice with the filter insertion contains violet region, whereas the other does not. These results reveal that V-RL could reduce OSL of the quartz grain aliquot.

3. 4. Conclusion

These experiments allow us to conclude that there exists apparent self-bleaching effect due to RL on OSL-phenomena of natural quartz grains. The RL emission bands of natural RTL-quartz grains had two broad peaks, V-RL (400 nm) and R-RL (630 nm). V-RL emission was found to be more effective for self-bleaching of quartz grains irradiated at different dose rates, together with covering the grain aliquot by quartz slices with different V-RL intensities coupled with an optical filter. Therefore, it should be noticed that such self-bleaching effects can influence to the OSL-accumulation with different degrees dependent on the V-RL from the neighboring quartz grains. The reduction of OSL intensity would be caused by the RL not only from the slice and neighboring quartz grains but also in the irradiated grains with higher efficiency. Therefore, much attention should be paid on the self-bleaching effects during artificial irradiation, particularly in accurate retrospective dosimetry and the OSL-dating. That is, when the dose response curve will be produced by artificial irradiation, the dose rate should be applied as low as possible. Otherwise, the equivalent dose obtained by OSL dosimetry could be corrected using the OSL-accumulation with dose rates.

4. A usability of on VTL from natural quartz grains for retrospective dosimetry

4. 1. Introduction

Small-scale nuclear power facilities or laboratories handling for radioactivity possess ever-represent risks of nuclear or radiation accidents as well as nuclear power plants. In the event of such accident, radiation dosimetry or retrospective dosimetry is necessary in order to evaluate any possible radiation effects on residents. However, the dose assessment method of general people is not necessarily established except for a place where the dosimetry is beforehand installed. In addition to this, when sufficient speed and accuracy is accomplished, the utilization of TL techniques applied to natural materials can extend to a variety of dosimetric fields.

In the TL-measurements, the BTL-emission has been utilized for both quartz and feldspar grains till 1980s, although anomalous fading effects have been noticed especially for feldspars. In 1986, the RTL phenomena from quartz grains, which have been initially discovered from volcanic ash layers and subsequently from burnt archeological porcelain pieces, have been verified to be efficient for the reliable dating of tephra layer as well as retrospective dosimetry (Hashimoto et al., 1986, 1997b; Takano et al., 2003). In addition to minerals, luminescent measurement technique also brought from ceramic materials, such as earthenware, pottery, porcelain pieces, burnt stones, kiln materials and blocks, have been employed to a reliable retrospective dosimetry on the basis of accumulated radiation

defects (Mckeever, 1985).

In addition to archeological dating, luminescence measurements of natural minerals are also useful for the retrospective dosimetry. RTL-measurements of ceramics and quartz extracts were successfully applied to two samples in the JCO (uranium fuel conversion company)-critical accident site in 1999 (Hashimoto et al., 2002a) and some atomic bomb-suffered samples in Hiroshima (Hashimoto et al., 2003b). Evaluated doses were in concordant with the calculated values.

RTL measurements are carried out under higher background counts by black-body radiation from heater source. The naturally accumulated component of dose may contribute to the largest source of error in the evaluation process for retrospective RTL measurements. Natural dosimetric materials must possess certain fundamental characteristics: (1) it must be sensitive to ionizing radiation at the dose levels of interest, (2) it must have the ability to retain a record of the accident exposure with known or negligible fading in dose over the time interval between exposure and measurement, (3) it must be capable of being prepared for measurement without the introduction of confounding signals and (4) the 'natural' component in measured dose must be accurately measurable, certainly estimative or negligible. In this chapter, for the sake of retrospective dosimetric use, the basic study of VTL dosimetry is carried out in conjunction with both background measurements of accumulated dose and black-body radiation, the kinetic parameters related to trapped electrons and sun-light bleaching effects. Finally, the detection limit in

VTL measurements is evaluated.

4. 2. Experimental

4. 2. 1. Sample preparation

The samples were extracted from surface soils which were collected from a certain depth to avoid direct sun-light effects, around JAEA (Japan Atomic Energy Agency). All procedure was carried out under faint red light to prevent fading of luminescence signals. Iron-related components were removed by magnetic separation after drying at 70 °C. Then, the samples were treated with 6 M HCl, 6 M NaOH and then 46 % HF in the ordinary way using an ultrasonic agitator. Density separation was done using sodium polytungstate solution to isolate and identify quartz. Final fraction settled in specific gravity range of 2.63-2.67 g cm^{-3} was used. Further purification of the quartz grains was performed by hand picking for the sake of elimination of feldspar grains as low as possible. The quartz was sieved to select the grain size from 150 μm to 250 μm in diameter. One part of each sample was annealed at 450 °C in air using electric furnace to eliminate natural irradiation doses, and the others were not.

The quartz samples were then exposed to γ-ray of ^{137}Cs source (111TBq, 365 mm distance). A fixed dose of 20 Gy was irradiated by a dose rate of approximately 1 Gy min^{-1} at room temperature in the Radioisotopes Center of Niigata University.

4. 2. 2. TL measurements

A TL spectrometry has been applied for the quartz grain samples using highly sensitive on-line spectrometric system equipped with an image-intensifier photo-diode array (IPDA) detector (Hashimoto et al., 1997b). The system was controlled at a linear heating rate of 1 ^{o}C / sec.

VTL glowcurves were measured by an automated TL / OSL-reader system installed with a small X-ray irradiator (Varian, VF-50J tube), which has been developed for a single aliquot regeneration (SAR) method (Hashimoto et al., 2002b, c; Nakagawa et al., 2003). For the detection of VTL, a violet (Schott, UG-11) and an infrared cut (IRC-65L) filters were installed between the photomultiplier tube (PMT, Hamamatsu, R585S) and the sample heating site.

The same apparatus was also used to determine kinetic parameters from VTL peaks in the glowcurves. Various heating rates (VHR) method was applied for determinations of kinetic parameters (Prokein et al., 1993). The details of VHR method were shown in section 2.2.5.2.

4. 3. Results and discussion

4. 3. 1. Luminescence measurements

Figure 4.1 shows a typical TL spectrum in contour expression from natural quartz grains irradiated to 1 kGy of X-ray. In addition to the existence of the RTL, the VTL peak ranging from 350-450 nm in wavelength and around 110 °C could be recognized in the contour map. Thus, VTL from the quartz was measured by adjusting the optical filters and PMT combinations to pass through violet emission of ~ 400 nm.

Changes of VTL-glowcurves by applying the SAR-method are shown in Figure 4.2, for quartz extracts from surface soils. There exist five peaks at 80, 110, 130, 200 and 270 °C. Four peaks below 250 °C were induced by artificial X-ray irradiation, because natural VTL-glowcurve does not present any peaks in this temperature region as illustrated in Figure 4.3. Alternatively, the natural VTL-glowcurve offered two broad peaks in the temperature region above 250 °C. It was noteworthy that the utility of the VTL peaks as the retrospective dosimetry below 250 °C could exclude the interference from naturally accumulated dose. Furthermore, since the background counts in the whole temperature regions were very low in some counts, the highly precise dose assessment using VTL measurements might be expected to give the lower detection limit than the other luminescence methods.

The VTL intensities were integrated between 20 °C intervals across each peak. The integrated VTL intensity as a function of the regenerative dose brought on the corresponding response curve as shown in Figure 4.4.

VTL dose response curve at 80 °C peak was not indicated in Figure 4.4 because the intensity was not proportional to irradiation dose. VTL dose response curves beyond 110 °C peak showed proportional property to the applied dose between 0 and 30 Gy, while VTL curve at 110 °C peak was saturated below 20 Gy of the applied dose. The dose response curves show no supra-linear tendency between 0 and 30 Gy of regenerative doses.

Table 4.1 shows the dose detection limit calculated at each range (110, 130, 200 and 270 °C peak area). The detection limit was estimated with three times of the standard deviation of background counts in the VTL measurements. All of the detection limits are under 2.0×10^2 mGy and the lower detection limit is acquired at range of 110 °C peak. These detection limits are lower than these of the other methods such as ESR dosimetry, chemiluminescence dosimetry and chromosome aberration techniques.

From these results, the peaks between 110 °C and 250 °C could be sensitive to ionizing radiation at the accidental dose levels without the consideration due to natural component.

4. 3. 2. Sensitivity changes to repeated cycles

In the reliable luminescence dosimetry, sensitivity change with repeat of measurement cycles (i.e., irradiation, preheat and then heating process) is a very important factor when the SAR-method is employed. VTL sensitivity variations were checked by adding repeatedly a test dose irradiation of 20 Gy followed by VTL measurement. The results are demonstrated in Figure 4.5, in which respective integrated VTL values at each peak region were utilized. There are sensitivity changes for three peaks of 80 (not indicated), 110, 130 °C, although other peaks appear no sensitivity changes. Therefore, both peaks at 200 and 270 °C may be favorable for determining accidental doses from viewpoint of sensitivity changes to repeated cycles.

4. 3. 3. Bleaching effects on VTL

Effects of sun-light bleaching (max. 28000 lux) on VTL were studied on a shiny day in September, 2005. Firstly, these quartz grains were simultaneously irradiated with 20 Gy of X-ray after annealing at 450 °C for 5 min to eliminate effects of natural irradiation. Thereafter portions of each sample were illuminated with sun-light. Others were stored in a dark room. After 8 hr, VTL glowcurves were measured. Both glowcurves are illustrated in Figure 4.6. VTL peaks below 300 °C were almost bleached by sun-light and the other peak at 380 °C remained, although four peaks still existed in the glowcurves from samples stored in dark. It found that all of VTL peaks are very sensitive to sun-light exposure.

On the other hand, blue-LEDs exposed the quartz samples for 10 - 30 sec. Only the VTL peak at 130 °C was reduced by no more than 10 % which occurred in the 30 sec of blue-LED exposure, however the other VTL peak on both conditions remained.

The above experiments showed that the preparation of quartz samples should be conducted in a dim room and the sample (cf. surface soil) could be collected from a certain soil depth without sun-light effects.

4. 3. 4. Kinetic parameters of VTL peak

The various heating rates (VHR) method has an advantage that the activation energy is relatively unaffected by thermal quenching effects (in this work, peak intensity was sufficient for thermal quenching not to affect the precision with which Tm could be identified). Therefore, this method was applied to VTL peaks in the whole temperature regions.

Plots of ln (T_m^2 / β) against 1 / T_m for the 110, 130, 200 and 270 °C VTL peaks are shown in Figure 4.7. The whole measurements were performed a day after the exposure of 20 Gy-γ doses. The derived kinetic parameters are shown in Table 4.2. The kinetic parameters of each peak at 130, 200 and 270 °C were estimated by the VHR method except for those of 110 °C peak.

The mean life of peak at 130 °C was extremely short and then the dose assessment has difficulty using this peak for dosimetry because of appreciable fading effect during pretreatment including both procedures of sample collection and extraction of quartz. In the case of the peak at 200 °C, the mean life was hopeful for the dose evaluation without background dose accumulated in an accidental field. The longest mean life was observed in the region around 270 °C. This result suggests that the utility of the peak was influenced by naturally residual doses as shown in Figure 4.3.

4. 4. Conclusion

The dose estimation method with VTL-measurement was investigated using quartz extracts from surface soil around JAEA. VTL dosimetry has (1) the absence of natural dose accumulated over geological period, (2) the ability to retain a record of accident exposure with negligible fading over the time interval within one day until measurement and (3) the detection limit to determine accidental doses of tens on mGy. This method should be conducted under condition of no sun-light bleaching effects during sample collection and pretreatments.

5. Comparison of residual doses in quartz and feldspar extracts from atomic bomb-suffered roof tiles using several luminescence-methods

5. 1. Introduction

Nowadays, a variety of radiation-induced luminescence phenomena have been employed to the dosimetry tools such as thermoluminescence (TL) and optically stimulated luminescence (OSL) using either quartz or feldspar samples (Aitken, 1985, 1998; Boetter-Jensen et al., 2003). Although both quartz and feldspar are commonly coexisted in a burnt archaeological and geological materials, there are a few reports on inter-comparisons of dose-evaluations from different luminescence-methods using mineral extracts from the same material. In the burnt archaeological materials, the authors have compared the naturally accumulated doses after pottery manufacture between RTL (red TL)-, BTL (blue TL)-, OSL-doses from quartz, and IRSL (infra-red stimulated luminescence)-ones from feldspar (Hashimoto et al., 2003b, 2005a). The highest naturally accumulated doses, which were obtained from RTL-measurements of quartz extracts, led to the determination of final ages concordant with the archeologically and stratigraphically predicted ages. Causes of different stability among luminescent sources have been considered to be attributed to relatively easy-to-bleaching effects of OSL and BTL in quartz and well-known anomalous fading effects in feldspar. It was concluded that the RTL-dating is a favorable dating-method when quartz grains were available in burnt archaeological materials from 3,500 to 6,000 years ago, which might be corresponding to about the ranges of

7-24 Gy (Hashimoto et al., 2005a).

In addition to archeological dating, luminescence measurements of natural minerals are also useful for retrospective dosimetry. The RTL-measurements of ceramics and quartz grains were successfully applied to two samples in the JCO (uranium fuel treatment company)-critical accident site in 1999 (Hashimoto et al., 2000c) and some atomic bomb-suffered samples in Hiroshima (Hashimoto et al., 2003b) . Evaluated doses were in concordant with the calculated values.

In the present paper, nine kinds of luminescence dosimetries were employed for two atomic bomb-suffered roof tile-pieces collected from close to epicenters in Hiroshima and Nagasaki. For quartz extracts, RTL-, BTL-, and OSL-measurements were applied while VTL (violet TL)-, BTL-, Green TL (GTL)-, RTL-, far-RTL-, and IRSL-ones were applied to feldspar grains extracted from the roof tiles using a SAR (single aliquot regenerative dose) protocol. Since various luminescent centers were assumed to form simultaneously on the atomic bomb-suffered roof tiles, the residual doses from a variety of luminescence measurements should reflect the stability tendency of the related luminescent centers. In this viewpoint, the luminescence dose-evaluations were carried out for two kinds of roof tile-pieces from Hiroshima and Nagasaki during storage period of 59 years after the nuclear explosions, which is relatively short storage duration in comparison with archaeological materials.

5. 2. Experimental

5. 2. 1. Preparation of measuring samples

Two pieces of the roof tiles suffered by atomic bombs are shown in Figure 5.1 (a) and (b) and sampling locations are illustrated in Figure 5.2. The samples recently have been excavated from the underground in the Hiroshima Peace Memorial Park and the Nagasaki Peace Park, where the atomic bombs were exploded on August 6, 1945 and the 9th, respectively. However, the accurate distances of both sampling locations from the epicenter are unknown. The surface of samples showed the distinctive bubbling pattern due to the heat ray of explosion.

Quartz and feldspar grains were isolated by almost similar procedure described in the preceding papers (Hashimoto et al., 2003b, 2005b). All procedures were done in dim room with red light to avoid light-bleaching effects. After removing the outer layer (about 2 mm thickness) damaged by heat-rays, samples were crushed using an agate mortar and a pestle. Subsequently, ferromagnetic components were removed by means of a magnet-method, following by soaked in 6M HCl for 1day and in 6M NaOH to get rid of metallic oxide contamination and of organic materials, respectively. Heavy liquid separation using three solutions of sodium polytungstate (2.55, 2.63 and 2.67 in specific gravity) was applied to isolate the quartz and the potassium-rich feldspar fractions. The "feldspar" fraction (i.e., 2.55-2.63 of specific gravity) contains predominantly potassium feldspar (e.g., microcline, albite etc.) and quartz fraction (specific gravity of 2.65), was collected from fraction ranging from

2.63-2.67 specific gravity. The resultant quartz fractions were furthermore etched with 46% HF to remove surface layer which may have been affected by α-ray from surrounding materials. This procedure is helpful for removal of concomitant feldspar grains by dissolution. Finally, all quartz and feldspar grains were adjusted to be 75-150 μm in diameter by sieving.

5. 2. 2. Luminescence measurements

An automated TL and OSL-reader system installed with a small X-ray irradiator (Varian, VF-50J tube), which has been developed for a SAR-method (Hashimoto et al., 2002b, Nakagawa et al., 2003), was used through the whole luminescence measurements. The SAR-sequence was slightly improved from the ordinal method (Wintle and Murray, 2000) as shown in Table 5.1. Ordinal exposure dose-rate of X-ray was 5.5 Gy/min when applying 100 μm Al-absorber, 50 kV tube potential, and 0.1 mA tube current. Luminescence sensitivity changes during the repeated procedures were corrected by the test dose irradiation, fixed to 5 Gy (cf. Figure 5.5 (b)). Three aliquots consisting of 5 mg were measured in both cases of TL and OSL (and IRSL) measurements.

TL properties of quartz and feldspars in emission wavelength-regions were checked using color photographic images, involving TLCIs (TL color images), and an on-line spectrometric system combined with image-intensifier photo-diode array (IPDA) (Hashimoto et al., 1989, 1997b). On the basis of these results, the far-RTL, RTL, GTL, BTL and VTL were measured with the detection windows of 700-750 nm, 600-700 nm, 500-600 nm, 400-500 nm and 300-400 nm, respectively. The transmission characteristics of the used filter combinations are shown in Figure 5.3.

Concerning OSL- and IRSL-measurements, sixteen blue or infrared light emitting diodes (blue-LED, Nichia or IR-LED, Hamamatu Photonics) were installed to the measuring system. The blue-LED has an emission

peak at 470 nm with 20 nm of FWHM and the stimulating power was estimated to be 12 mW/cm^2. OSL from quartz aliquot was counted in every 0.1 sec for 100 seconds under keeping sample temperature of 125 °C.

The IRSL measurements of feldspar were carried out in 350-600 nm detective regions (Hashimoto et al., 2002c). The IR-LED possesses an emission peak at 890 nm with 50 nm FWHM. Other conditions were similar to the case of OSL-detection.

5. 3. Results and discussion

5. 3.1 TL, OSL, and IRSL

Figure 5.4(a) show TL-contour maps of quartz extracts from the Nagasaki-roof tile. The quartz grain shows the mixture of bluish and reddish TL properties, consisting a peak of 450-500 nm and 620-630 nm in wavelength, respectively. Almost same TL-contour was also obtained from the quartz aliquot from Hiroshima-roof tile. It reveals again here that RTL intensities are stronger than BTL-ones in the quartz extract from burnt archaeological materials or old roof tiles (Hashimoto el al., 2005a, b).

Besides the effects of impurities, the different TL properties of quartz extracts might be greatly affected by their thermal history, involving cooling rate and atmospheric condition during burnt process of roof tiles (Hashimoto et al., 1996b). It is well known that the roof tiles have been dealt for relatively short period under the reductive condition at the end of manufacturing process, whereas almost all of firing process start and maintain under oxidative condition in high-temperature kiln. Tentatively, the author assumes that such oxidative firing condition might bring on RTL-property of quartz rather than BTL-one induced from reductive firing conditions. Thus, the quartz extracts from both Nagasaki- and Hiroshima-roof tiles were found to be applicable to both RTL and BTL measurements.

Concerning the feldspar extract, the strongest emission in violet regions appears around 200 °C, and secondary intense emission follows in far-red regions around 700 nm at lower temperature of 120 °C by interposing

broad emission in visible light regions as seen in Figure 5.4 (b). The feldspar aliquot of Hiroshima-roof tile showed the almost same TL-properties. These results imply that the feldspar extracts consist of the mixture from various kinds of feldspar minerals (Hashimoto et al., 2001). On the basis of these results, five kinds of TL measurements, involving far-RTL, RTL, GTL, BTL and VTL regions, were applied for the residual dosimetries in quartz or feldspar grains.

RTL-glowcurves of quartz fractions are presented in Figure 5.5 (a) for Nagasaki sample. In these glowcurves, there is no apparent signal below 170 °C from original and as-received quartz grains because of applying preheating treatment for 180 sec at 210 °C and decaying out short-lived components during 59-years storage periods, respectively.

In all TL-measurements, the repeated cycles caused, more or less, enhancement of sensitivity, which was corrected by variations of TL-intensity from the inserting test dose. An RTL dose-response curve is demonstrated in Figure 5.5 (b). Integrated temperature regions of respective TL-glowcurves are presented in Table 5.2.

Concerning the feldspar samples, the TL-intensities should be dependent not only on widths of detective wavelengths, but also on optical transmittance of filter assemblies. However, the most intense TL was GTL, while the weakest emission appeared on far-RTL glowcurves. In general, the longer wavelength give the weaker TL by interpolating remarkably weak RTL, concordant roughly with the contour mapping results as seen in Figure 5.4 (b). Almost similar tendency was found in the

Hiroshima-feldspar extract.

IRSL-decay curve and its dose-response of feldspar from Nagasaki-roof tile are indicated in Figure 5.6 (a) and (b), respectively. The IRSL-dose response curves were also corrected for sensitivity changes, amounted up to 30%. Finally, IRSL-intensities from as-received fraction were used for the residual dose-evaluations.

5. 3. 2. Comparison of residual doses among various luminescence measurements

All dose results from the quartz grains (a) and feldspar ones (b) are summarized in Table 5.2. The experimental errors of residual doses are derived from three aliquot analyses. Generally speaking, the present Hiroshima-roof tile shows more intense exposure of ionizing radiation in comparison with the present Nagasaki-roof tile from the atomic-bomb explosion. However, the dose-differences between two places will not furthermore be dealt with here because the accurate positions and distances from the hypocenters of each roof-tile could not be nowadays acquainted to us as mentioned above.

Although the residual doses evaluated consist of retrospective dose from atomic-bomb explosions plus naturally accumulating doses, the contribution of the latter constituents were found to be negligibly small from contents of radioactive nuclides within each roof tile.

In the quartz samples, the both highest doses, amounted to 47 and 11 Gy for Hiroshima and Nagasaki-samples, respectively, are evaluated when the RTL-measurements were applied. On the other hand, the BTL- and OSL-doses from the same quartz extracts were obtained less than the RTL-ones, giving 70-80 % of RTL-residual doses except for Hiroshima-BTL one. In principal, if there is no escaping of luminescence sources during storage period after the exposure, the residual doses from quartz should agree with each other.

In the case of the feldspar fractions, the highest dose was established in

far-RTL measurements such as 35 and 8.4 Gy for Hiroshima- and Nagasaki-samples, respectively. However, all of the residual TL-doses are usually smaller than the RTL-results. Since the almost all luminescence centers were formed simultaneously in quartz and feldspar minerals, the stability of the luminescence centers should reflect on the residual doses from respective luminescence-measurements. However, it should be mentioned here that the RTL of quartz was integrated in higher temperature regions (or 330-360 °C) than all TL-evaluations of feldspars (220-280 °C) because of no detectable TL-emission. In addition, the evaluated residual doses are apparently dependent on the detection wavelength regions, bringing on the larger residual doses according to the higher wavelengths, although the lower integrated luminescence intensities are correlated with the longer wavelengths. It is well-known that in the feldspar minerals the violet-visible TL- and IRSL-sources are significantly affected on the anomalous fading effects, whereas the far-RTL regions might be rarely suffered with such fading effects as described by Zink et al. (1995).

Particularly, the OSL- and IRSL-accumulated doses always show lower values than the RTL-ones from quartz and feldspar grains, respectively. These results mean that the OSL sources are liable to suffer some loss during storage period of 59 years, introducing .the underestimation of residual doses.

The residual doses from different luminescence measurements either in quartz or feldspar extracts should be in agreement with each other if luminescence sources were sufficiently stable during storage periods. The

present results are not the case, so that the RTL-sources showed most stable among various kinds of luminescence source even for the storage period of 59 years, in concordant with the preferable RTL-dosimetry and dating using burnt archaeological materials manufactured and utilized 3500-6000 years ago (Hashimoto et al., 2003b, 2005a).

5. 4. Conclusion

In the Hiroshima- and Nagasaki-roof tiles suffered with atomic-bomb explosion 59 years ago, the highest residual doses were estimated from RTL measurements of quartz grains. On the other hand, the results of feldspar grains, including the IRSL measurements, gave lower doses than that of quartz grains.

On the basis of the most stable luminescence sources, the RTL-measurements for quartz extracts are recommendable for either naturally accumulated radiation or retrospective dosimetry.

References

Aitken, M. J. (1985) Thermoluminescence Dating. Academic Press, London.

Aitken, M. J. (1998) An Introduction to Optical Dating. Oxford Science Pub., Oxford.

Azorin, J. (1986) Determination of thermoluminescence parameters from glow curves. Nucl. Tracks, **11**. 159-166.

Banerjee, D., Bøtter-Jensen, L., and Murray, A. S. (2000) Retrospective dosimetry: estimation of the dose to quartz using the single-aliquot regenerative-dose protocol. Appl. Radiat. Isotopes, **52**, 831-844.

Bøtter-Jensen, L. and Mckeever, S. W. S. (1996) Optically stimulated luminescence dosimetry using natural and synthetic materials. Radiat. Prot. Dosim. **65**, 273-280.

Bøtter-Jensen, L., Duller, G.A.T., Murray, A.S. and Banerjee, D. (1999a) Blue light emitting diodes for optical stimulation of quartz in retrospective dosimetry and dating. Radiat. Prot. Dosim. **84**, 335-340.

Bøtter-Jensen, L., Mejdahl, V. and Murray, A.S. (1999b) New light on OSL. Quat. Sci. Rev. **18**, 303-309.

Bøtter-Jensen, L., Solongo, S., Murray, A. S., Banerjee, D and Jungner, H. (2000) Using the OSL single-aliquot regenerative-dose protocol with quartz extracted from building materials in retrospective dosimetry. Radiat. Meas. **32**, 841-845.

Bøtter-Jensen, L., McKeever, S.W.S., and Wintle, A.G. (2003) Optically stimulated luminescence dosimetry. ELSEVIER, 141-143.

Campone, P., Magliocco, M., Spinolo, G. and Veeda, A. (1995) Ionic transport in crystalline SiO_2: The role of alkali-metal ions and hydrogen impurities. Phys. Rev. B, **52**, 15903-15908.

Chen, R. and Winer, A. A. (1970) Effects of various heating rates on glow curves. J. Appl. Phys. **41**, 5227-5232.

Chen, R. and Kirsh, Y. (1981) Analysis of thermally stimulated processes. Pergamon Press, London.

Chen, R. (1984) Thermoluminescence and thermoluminescent dosimetry Vol 1, ed Horowitz, Y. S. (Boca Raton, FL; CRC Press).

Chumak, V., Likhtarev, I., Sholom, S., Meckbach, R. and Krjuchkov, V. (1998) Chernobyl experience in field of retrospective dosimetry: reconstruction of doses to the population and liquidators involved in the accident. Radiat. Prot. Dosim. **77**, 91-95.

Cohen, A. J. (1960) Substitutional and interstitial aluminum impurity in quartz, structure and color center interrelationships. J. Phys. Chem. Solids, **13**, 321-325.

Edwards, A., Voisin, P., Sorokine-Durm, I., Maznik, N., Vinnikov, V., Mikhalevich, L., Moquet, J., Lloyd, D., Delbos, M. and Durand, V. (2004) Biological estimates of dose to inhabitants of Belarus and Ukraine following the Chernobyl accident. Radiat. Prot. Dosim. **111**, 211-219.

Endo, S., Tosaki, N., Hoshi, M. and Shimizu, K. (2000) Neutron dose equivalent estimation from the specific activity of ^{51}Cr. J. Environ. Radioact. **50**, 89-96.

Falgueres C., Yokoyama Y. and Miallier (1991) Stability of some centres in

quartz. Nucl. Tracks Radiat. Meas. **18** (1), 155-161.

Fatôme, M., Agay, D., Martin, S., Mestries, J. C. and Multon, E. (1997) Biological dosimetry after a criticality accident. Radit. Prot. Dosim. **70**, 455-459.

Edited by Fujimoto, K. (2001) Environmental measurements and dose assessment for the JCO accident. Proceedings of the 28th NIRS seminar.

Gartia, R. K., Singh, S. D., Singh, Th. S. C. and Mazumdar, P. S. (1992) Determination of the activation energy of a thermally stimulated luminescence peak for the case of a temperature-dependent frequency factor. J. Phys. D: Appl. Phys. **25**, 530-534.

Halliburton, L. E., Koumvakalis, N., Markes, M. E. and Martin, J. J. (1981) Radiation effects in crystalline SiO_2: the role of aluminum. J. Appl. Phys. **52** (5), 3565-3574.

Hammermaier, A., Reich, E. and Bögl, W. (1986) Chemiluminescence accident dosimetry with drugs and other solid materials. Radiat. Prot. Dosim. **17**, 171-174.

Hankins, D.E. (1980) Dosimetry of criticality accidents using activations of the blood and hair. Health Phys. **38**, 529-541.

Hase, H. (1985) Saturation studies of the electron spin resonance lines due to solvated electrons in organic glasses. Annual reports of the research reactor institute, Kyoto University. **18**, 113-132.

Hashimoto, T., Hayashi, Y., Koyanagi, A., Yokosaka, K. and Kimura, K. (1986) Red and blue colouration of thermoluminescence from Natural quartz sands. Nucl. Tracks Radiat. Meas. **11**, 229-235.

Hashimoto, T., Yokosaka, K. and Habuki, H. (1987) Emission properties of thermoluminescence from natural quartz-blue and red TL response to absorbed dose. Nucl. Tracks Radiat. Meas. **13**, 57-66.

Hashimotto, T., Yokosaka, K., Habuki, H. and Hayashi, Y. (1989) Provenance search of dune sands using thermoluminescence colour images (TLCIs) from quartz grains. Nucl. Tracks Radiat. Meas. **16**, 3-10.

Hashimoto, T., Sakai, T., Shirai, N., Sakaue, S. and Kojima, M. (1991) Thermoluminescent spectrum changes of natural quartzes dependent on annealing treatment and aluminium-contents. Anal. Sciences, **7**, 687-690.

Hashimoto, T., Kojima, M., Shirai, N. and Ichino, M. (1993) Activation energies from blue and red-thermoluminescence (TL) of quartz grains and means lives of trapped electrons related to natural red-TL. Nucl. Tracks Radiat. Meas. **21**, 217-223.

Hashimoto, T., Sakaue, S., Ichino, M. and Aoki, H. (1994) Dependence of TL-property changes of natural quartzes on aluminium contents accompanied by thermal annealing treatment. Nucl. Tracks Radiat. Meas. **23**, 293-299.

Hashimoto, T., Ojima, T., Takahashi, E., Konishi, M. and Kanemaki, M. (1995) Comparison of radiation-induced colouration images, thermoluminescence, and after-glow colour images with aluminium impurity distribution in Japanese twin quartzes. Radioisotopes, **44**, 379-388.

Hashimoto, T., Notoya, S., Komura, K. and Shirai, N. (1996a) Red-thermoluminescence dating of some volcanic-ash and pyroclastic-flow

layers related to Takamori pre-historical sites using quartz inclusion method. Archaeology and Natural Sciences. **33**, 1-15 (in Japanese).

Hashimoto, T., Notoya, S., Arimura, T. and Konishi, M. (1996b) Changes in luminescence colour images from quartz slices with thermal annealing treatments. Radiat. Meas. **26**, 233-242.

Hashimoto, T., Katayama, H., Sakue, H., Hase, H., Arimura, T. and Ojima, T. (1997a) Dependence of some radiation-induced phenomena from natural quartzes on hydroxyl-impurity contents. Radiat. Meas. **27**, 243-250.

Hashimoto, T., Sugai, N., Saakaue, H., Yasuda, K. and Shirai, N. (1997b) Thermoluminescence (TL) spectra from quartz grains using on-line TL-spectrometric system. Geochem. J. **31**, 189-201.

Hashimoto, T., Yasuda, K., Sato, K., Sakaue, H. and Katayama, H. (1998) Radiation-induced luminescence images and TL-property changes with thermal annealing treatment on Japanese twin quartz. Radiat. Meas. **29**, 493-502.

Hashimoto, T., Magara, M. and Nishiyama, E. (1999a) Observation of thermoluminescence colour images from some porcelain samples and their application to red-thermoluminescence (RTL) dating. Radioisotopes. **48**, 661-672 (in Japanese).

Hashimoto, T., Fujita, H. and Yasuda, K. (1999b) Mean-life evaluation of naturally trapped electrons associated with red- and blue thermoluminescent quartz-grains from dune sand. Radioisotopes. **48**. 673-682 (in Japanese).

Hashimoto, T., Saitou, Y., Satou, K. and Takano, M. (2000a) Red

thermoluminescence dating of some porcelain pieces using regeneration method with thin disc samples and ICP-MS (inductively coupled plasma-mass spectrometry) analysis. Radioisotopes. **49**, 523-531 (in Japanese).

Hashimoto, T., Hase, H., Hong, D. G., Fujita, H. and Katayama, H. (2000b) Correlation of aluminum hole centers with hydrogen radicals from gamma-irradiated quartzes of different origins. J. Nucl. Radiochem. Sci. **1**, 47-50.

Hashimoto, T., Takano, M., Yanagawa, Y and Tsuboi, T. (2000c) Radiation dosimetry using thermoluminescence from ceramic and glass samples at the JCO critical accident site. J. Environ. Radioact. **50**, 97-105.

Hashimoto, T., Yamazaki, K., Morimoto, T. and Sakue, H. (2001) Radiation-induced luminescence color images from some feldspars. Anal. Sci. **17**, 825-831.

Hashimoto, T., Hong, D. G. and Takano, M. (2002a) Retrospective dosimetry at JCO using luminescence from ceramics pieces and quartz grains. Adv. in ESR Appl. **18**, 197-202.

Hashimoto, T., Nakagawa, T., D. G. Hong, and Takano, M. (2002b) An automated system for both red/blue thermoluminescence (TL) and optically stimulated luminescence (OSL) measurement. J. Nucl. Sci. Technol. **39**, 108-109.

Hashimoto, T., Nakagawa, T., Usuda, H. and Yawata, T. (2002c) Development of an automated system equipped with a small X-ray irradiator for red/blue thermoluminescence and optically stimulated

luminescence measurement from natural minerals. BUNSEKI KAGAKU, **51**, 625-632 (in Japanese).

Hashimoto, T., Yamaguchi, T., Fujita, H. and Yanagawa, Y. (2003a) Comparison of infrared spectrometric characteristics of Al-OH impurities and thermoluminescence patterns in natural quartz slices at temperature below 0 ^{o}C. Radiat. Meas. **37**, 479-485.

Hashimoto, T., Yawata, T. and Takano, M. (2003b) Preferable use of red-thermoluminescence (RTL) dating for quartz extracts from archaeological burnt pottery – comparison of RTL and BTL (blue-TL) measurements using single-aliquot regenerative-dose (SAR) method. Ancient TL. **21**, 85-92.

Hashimoto, T., Yawata, T. and Takano, M. (2005a) Comparison of naturally accumulated radiation-doses between RTL, BTL, OSL, and IRSL using white minerals from burnt archaeological materials and usefulness of RTL-dating from quartz extracts. Geochem. J. **39**, 201-212.

Hashimoto, T., Nakata, Y. and Yawata, T. (2005b) Naturally accumulated radiation doses and dating of archaeologically burntmaterials using luminescence from white minerals. Proceeding of the 5HLNRRA, International congress Series. **1276**, 231-232.

Heide, L. and Bögl, W. (1987) Chemiluminescence dosimetry of accidental gamma and X ray exposures with solid substances. Radiat. Prot. Dosim. **19**, 35-41.

Hoogenstraaten, W. (1958) Electron traps in zinc sulphide phosphors. Philips. Res. Reps. **13**. 515-562.

Horowitz, Y. S. and Yossian, D. (1995) Computerised glow curve deconvolution: application to thermoluminescence dosimetry. Radiat. Prot. Dosim. **60**, (1), 1-114.

Huntley, D.J., Godfrey-Smith, D.I. and Thewalt, M.L.W. (1985) Optical dating of sediments. Nature, **313**, 105-107.

Igarashi, Y., Aoyama, M., Miyao, T., Hirose, K., Komura, K. and Yamamoto, M. (1999) Air concentration of radiocaesium in Tsukuba, Japan following the release from the Tokai waste treatment plant: comparisons of observations with predictions. Appl. Radiat. Isot. **50**, 1063-1073.

Ikeya, M., Miyajima, J. and Okajima, S. (1984) ESR dosimetry for atomic bomb survivors using shell buttons and tooth enamel. J. J. Appl. Phys. **23**, L697-L699.

Isoya, T. and Weil, J.A. (1988) EPR of the TiO_4 / Li center in crystalline quartz. J. Magn. Reson. 79, 90-98.

Iwasaki, F. and Iwasaki, H. (1993) Impurity species in synthetic and Brazilian natural quartz. Jpn. J. Appl. Phys. **32**, 893-901.

Kai, A., Ikeya, M. and Miki, T. (1990) ESR accident dosimetry using medicine tablets coated with sugar. Radiat. Prot. Dosim. **34**, 307-310.

Kamenopoulou, V., Barthe, J., Hickman, C. and Portal, G. (1986) Accidental gamma irradiation dosimetry using clothing. Radiat. Prot. Dosim. **17**, 185-188.

Kats, A. (1962) Hydrogen in alpha-quartz. Philips Res. Rep. **17**, 133-195, 201-293.

Komura, K., Hashimoto, T., Takano, M., Yanagawa, Y., Tsuboi, T. et al.

(2000) The JCO criticality accident at Tokai-mura, Japan: an overview of the sampling campaign and preliminary results. J. Environ. Radioact. **50**, 3-14.

Krbetschek, M.R., and Trautmann, T. (2000) A spectral radioluminescence study for dating and dosimetry. Radiat. Meas. **32**, 853-857.

Kryshev, I. I., Romanov, G. N., Isaeva, L. N. and Kholina, Yu. B. (1997) Radioecological state of lakes in the southern Ural impacted by radioactivity release of the 1957 radiation accident. J. Environ. Radioact. **34**, 223-235.

Marazuev, Yu.A., Brik, A.B., and Degoda, V.Ya. (1995) Radioluminescent dosimetry of α-quartz. Radiat. Meas. **24**, 565-569.

Marfunin, A. S. (1979) Spectroscopy, luminescence and radiation centers in minerals. Springer, Heidelberg, 236-237.

Martini, M., Paleari, A., Spinolo, G. and Vedda, A. (1995) Role of $[AlO_4]^0$ centers in the 380 nm thermoluminescence of quartz. Phys. Rev. B, **52**, 138-142.

May, C. E. and Patridge, J. A. (1964) Thermoluminescent kinetics of alpha-irradiated alkali halides, J. Chem. Phys. **40**, 1401.

McKeever, S. W. S. (1985) Thermolumiescence of solids. Cambridge University Press, Cambridge, 103-105.

McKeever, S. W. S. (1991) Minerals of thermoluminescence production: some problems and a few answer? Nucl. Tracks Radiat. Meas. **18**, 5-12.

McMorris, D. W. (1971) Impurity Color Centers in Quartz and Trapped Electron Dating: Electron Spin Resonance, Thermoluminescence Studies. J.

Geophys. Res. **76**, 7875-7887.

Murray, A. S. and Mejdahl, V. (1999) Comparison of regenerative-dose single-aliquot and multi-aliquot (SARA) protocols using heated quartz from archaeological sites. Quat. Geochron. **18**, 223-229.

Nakagawa, T. and Hashimoto, T. (2003) Sensitivity change of OSL and RTL signal from natural RTL quartz with annealing treatment. Radiat. Meas. **37**, 397-400.

Nickel, Th., Pitt, E. and Scharmann, A. (1991) Lyoluminescence dosimetry with sugar after accidental gamma ray exposures. Radiat. Prot. Dosim. **35**, 173-177.

Person, B. D. and Weil, J. A. (1974) Atomic hydrogen in a-quartz. J. Magn. Res. **15**, 594.

Pető, A., and Kelemen, A. (1996) Radioluminescence properties of alpha-Al_2O_3 TL-dosimeters. Radiat. Prot. Dosim. **65**, 139-142.

Petrov, S. A. and Bailiff, K. (1997) Determination of trap depth associated with TL peaks in synthetic quartz (350-550 K). Radiat. Meas. **27**, 185-191.

Polf, J. C., Yukihara, E. G., Akselrod, M. S. and McKeever, S. W. S. (2004) Real-time luminescence from Al_2O_3 fiber dosimeters. Radiat. Meas. **38**, 227-240.

Prokein, J. and Wagner, G. A. (1993) Analysis of thermoluminescence glow peaks in quartz derived from the KTB drill hole. Radiat. Meas. **23**, No.1, 85-94.

Rinneberg, H. and Weil, J.A. (1972) EPR studies of Ti^{3+}-H^{+} centers in X-irradiated α-quartz. J. Chem. Phys. **56**, No. 5, 2019-2028.

Science and Technology Agency, Japan. (1997) On the investigation into the caused of a fire and explosion accident at bituminization facility, Power Reactor and Nuclear Fuel Development, Tokai-Works.

Schilles, T., Poolton, N. R., Bulur, E., Bøtter-Jensen, L., Murray, A. S., Smith, G. M., Riedi, P. C., and Wagner, G. A. (2001) A multi-spectroscopic study of luminescence sensitivity changes in natural quartz induced by high-temperature annealing. J. Phys. D: Appl. Phys. **34**, 722-731.

Singh, T. S. C., Mazumdar, P. S. and Gartia, R. K. (1990) A critical appraisal of methods of various heating rates for the determination of the activation energy of a thermoluminescence peak. J. Phys. D: Appl. Phys. **23**, 562-566.

Spooner, N. A. (1994) On the optical dating signal from quartz. Radiat. Meas. **23**, 593-600.

Takano, M., Yawata, T. Hashimoto, T. (2003) Luminescence dosimetry of archaeological and ceramic samples using a single-aliquot regenerative-dose method. J. Nucl. Radioanal. Nucl. Chem. **255**, 365-368.

Toyoda, S. (1998) Studies on thermal stabilities of paramagnetic lattice defects in quartz: Basis for the ESR dating method. Chikyuukagaku, **32**, 127-137.

United Nations Scientific Committee on the Effects of Atomic Radiation. (2000) UNSCEAR 2000 Report to the general assembly with Scientific Annexes, United Nations, New York.

Weeks, R. A. and Abraham, M. (1965) Electron spin resonance of irradiated quartz: atomic hydrogen. J. Chem. Phys. **42**, 68.

Weil, J.A. (1984) A Review of Electron Spin Spectroscopy and Its Application to the Study of Paramagnetic Defects in Crystalline Quartz. Phys. Chem. Minerals. **10**, 149-165.

Wintle, A. G. (1975) Thermal quenching of thermoluminescence in quartz. Geochem. J. Royal Astronomical Society. **41**. 107-113.

Wintle, A. G. (1977) Detailed study of a thermoluminescent mineral exhibiting anomalous fading. J. Lumin. **15**, 385-393.

Wintle, A. G. and Murray, A.S. (1999) Luminescence sensitivity changes in quartz. Radiat. Meas. **30**, 107-118.

Wintle, A. G. and Murray, A. S. (2000) Quartz OSL: Effects of thermal treatment and their relevance to laboratory dating procedures. Radiat. Meas., **32**, 387-400.

Wu, K., Guo, L., Cong, J. B., Sun, C. P., Hu, J. M., Zhou, Z. S. and Wang, S. (1998) Researches and applications of ESR dosimetry for radiation accident dose assessment. Radiat. Prot. Dosim. **77**, 65-67.

Zink, A., Visocekas, R., Bos, A. J. j. (1995) Comparison of 'Blue' and 'Infrared' emission bands in thermoluminescence of alkali feldspars. Radiat. Meas. **24**, 513-518.

Tables

Figures

Table 2.1
Some values for trapping parameters of RTL peak from Medeshima quartz

Annealing temperatures / ^{o}C	Activation energy E / eV	Frequency factor s / s^{-1}	Method*	Kinetic order b	Mean life τ / years
Unannealed (as-received)	2.1	5.6×10^{18}	ITD	1.1	3.3×10^{10}
Unannealed (as-received)	1.6	3.8×10^{11}	VHR	1.0	1.4×10^{7}
600	1.7	4.7×10^{14}	ITD	1.2	3.1×10^{7}
600	1.8	4.3×10^{13}	VHR	1.0	2.8×10^{9}
700	1.6	1.1×10^{13}	ITD	1.3	8.9×10^{6}
800	1.0	1.6×10^{7}	ITD	1.5	2.0×10^{2}
800	1.5	2.8×10^{11}	VHR	1.0	1.9×10^{7}
900	0.92	2.3×10^{6}	ITD	1.7	5.9×10
900	1.8	4.5×10^{14}	VHR	1.0	5.4×10^{8}
1000	0.92	2.8×10^{6}	ITD	1.7	4.3×10

* ITD, isothermal decay method; VHR, various heating rates method.

Table 4.1

Detection limit of VTL dose evaluation method at each peak

Range No.	Detection limit (mGy)
Range 1 (110 °C peak)	9
Range 2 (130 °C peak)	2 x 10
Range 3 (200 °C peak)	7 x 10
Range 4 (270 °C peak)	2×10^2

Table 4. 2
Some values for trapping parameters of VTL peak from quartz extracted from surface soil around JAEA.

Range No.	Activation energy E / eV	Mean life τ / years
Range 2 (130 °C peak)	2.1	5.9×10^{-4}
Range 3 (200 °C peak)	1.6	3.8
Range 4 (270 °C peak)	1.7	2.5×10^{4}

Table 5.1
TL/SAR measuring protocol.

Step	Treatment	Signal
1	Give X-ray dose, D_i	-
2	Preheat	-
3	Heat up 40℃ to 390 ℃	L_i
4	Heat up 40℃ to 390 ℃	B
5	Give test dose, D_t	-
6	Preheat	-
7	Heat up 40℃ to 390 ℃	T_i
8	Heat up 40℃ to 390 ℃	B
9	Return to step 1	-

For as-recieved sample, $i = 0$, and $D_0 = 0$ Gy.
Heating rate is 1.0 ℃/ sec.
All X-ray irradiations, including test dose of 5 Gy, were done with a constant dose-rate of 5.5 Gy / min.
TL values were derived from L_i minus a background B.

Preheating conditions in both TL and OSL (IRSL) were 210 ℃ and 150 ℃ for 3 min for quartz and feldspar aliquot, respectively.

OSL (and IRSL) / SAR protocols are also similar to this sequence except for stimulation for 100 sec at 125 ℃ and application of cutheat at 160 ℃ after test dosing stage.

Table 5.2

Comparison of residual doses from TL and OSL (IRSL) measurements of quartz and feldspar extracts from atomic bomb-suffered roof-tiles.

(a) Quartz grains

Sample	RTL / Gy (330-360 ℃)	BTL / Gy (310-330 ℃)	OSL / Gy (1 sec of initial decay)
Hiroshima	47 ± 4	42 ± 3	28 ± 3
Nagasaki	11 ± 2	6.7 ±1.5	8.2 ± 1.1

(b) Feldspar grains

Sample	far-RTL / Gy (220-280 ℃)	RTL / Gy (240-270 ℃)	GreenTL / Gy (290-320 ℃)	BTL / Gy (250-290 ℃)	VTL / Gy (290-330 ℃)	IRSL / Gy (1 sec of initial decay)
Hiroshima	35 ± 3	29 ± 2	23 ± 3	24 ± 3	22 ± 5	17 ± 2
Nagasaki	8.4 ±1.3	8.0 ±0.9	6.7 ±0.9	6.3 ±1.5	5.7 ±1.7	6.0 ±0.7

Parenthesis shows integrated temperature regions or period.
Final dose and its error are mean value and standard deviation of every three determinations, respectively.

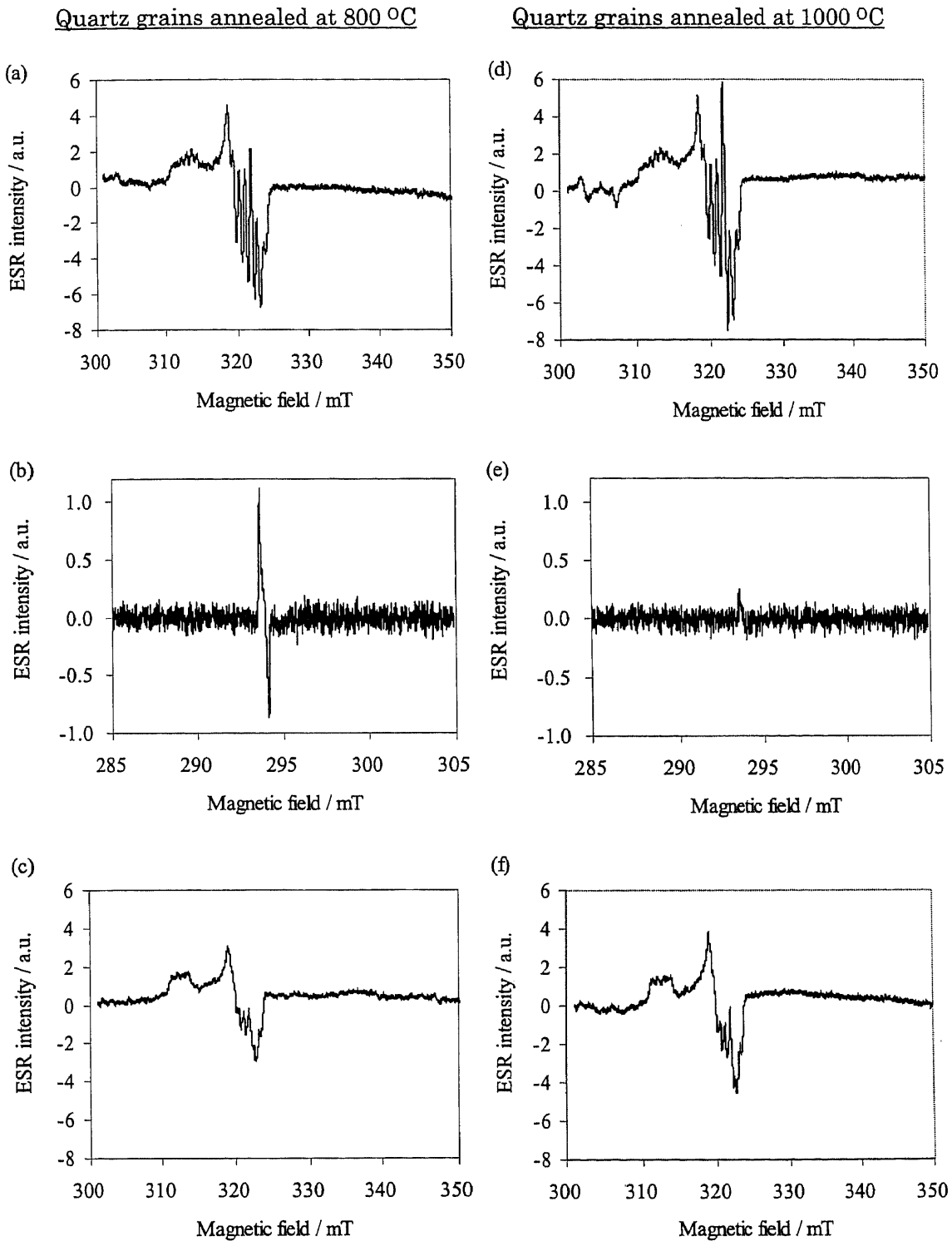

Figure 2.1

ESR spectra of Al-hole center and atomic hydrogen regions in quartz grains.

Initial Al-hole centers (a, d) and atomic hydrogens (c, e) were measured at -196 °C. Second Al-hole centers (c, f) were measured at -196 °C after warming up to room temperature.

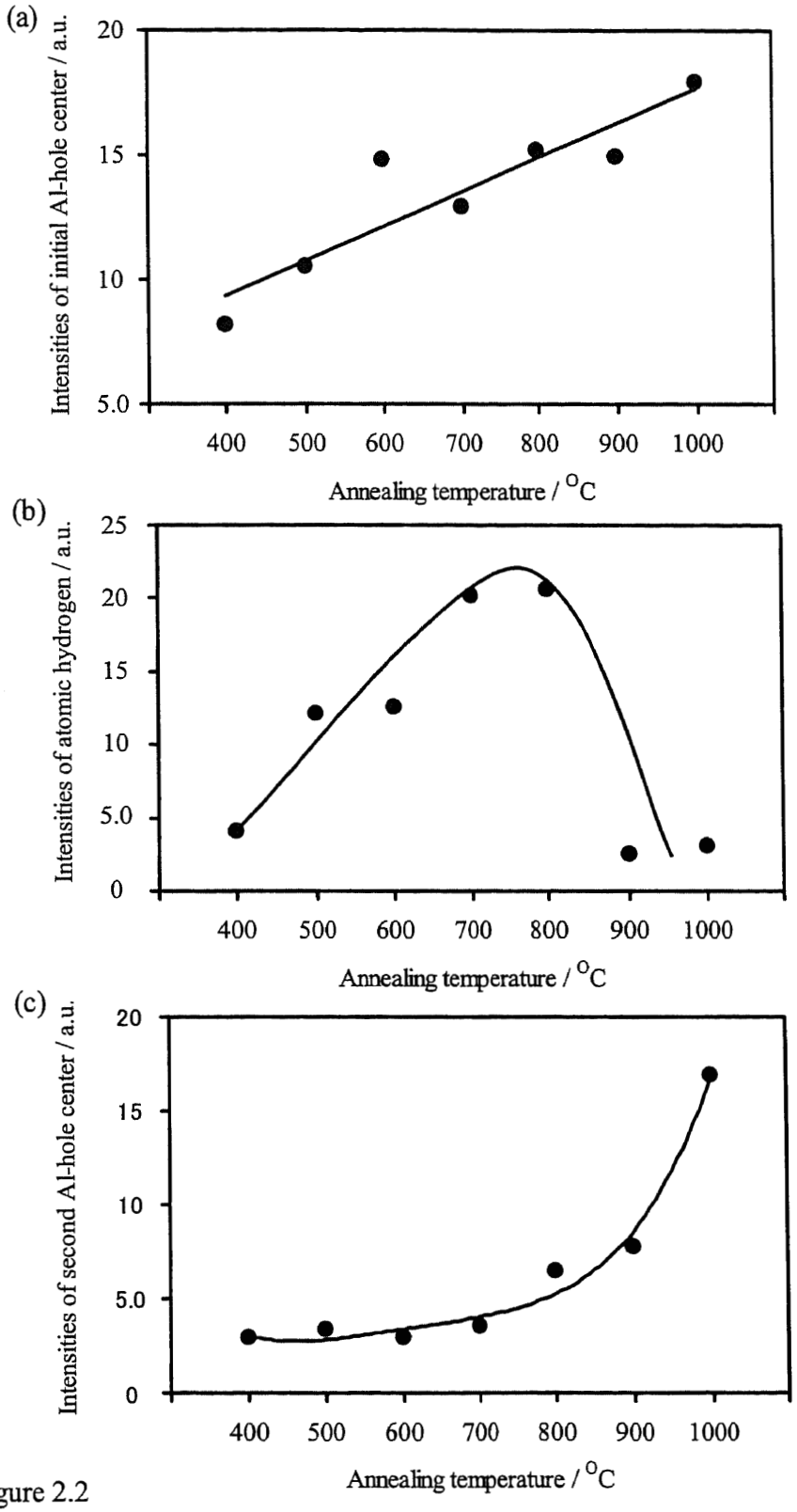

Figure 2.2

Intensities of ESR signal from annealed quartz irradiated at -196 °C.
(a) initial Al-hole center, (b) atomic hydrogen, (c) second Al-hole center

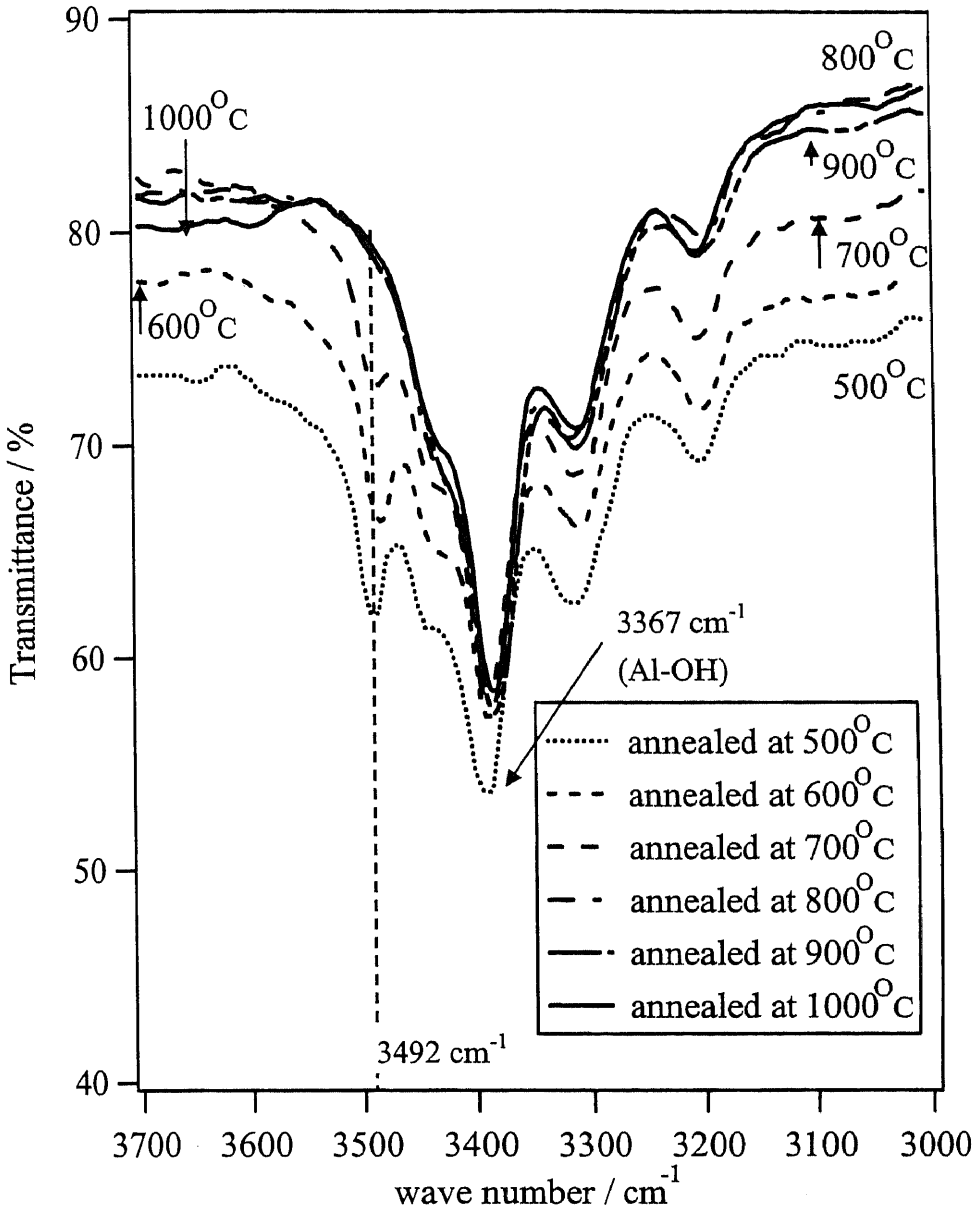

Figure 2.3

IR transmittances on Madagascar quartz slices annealed at several temperatures.

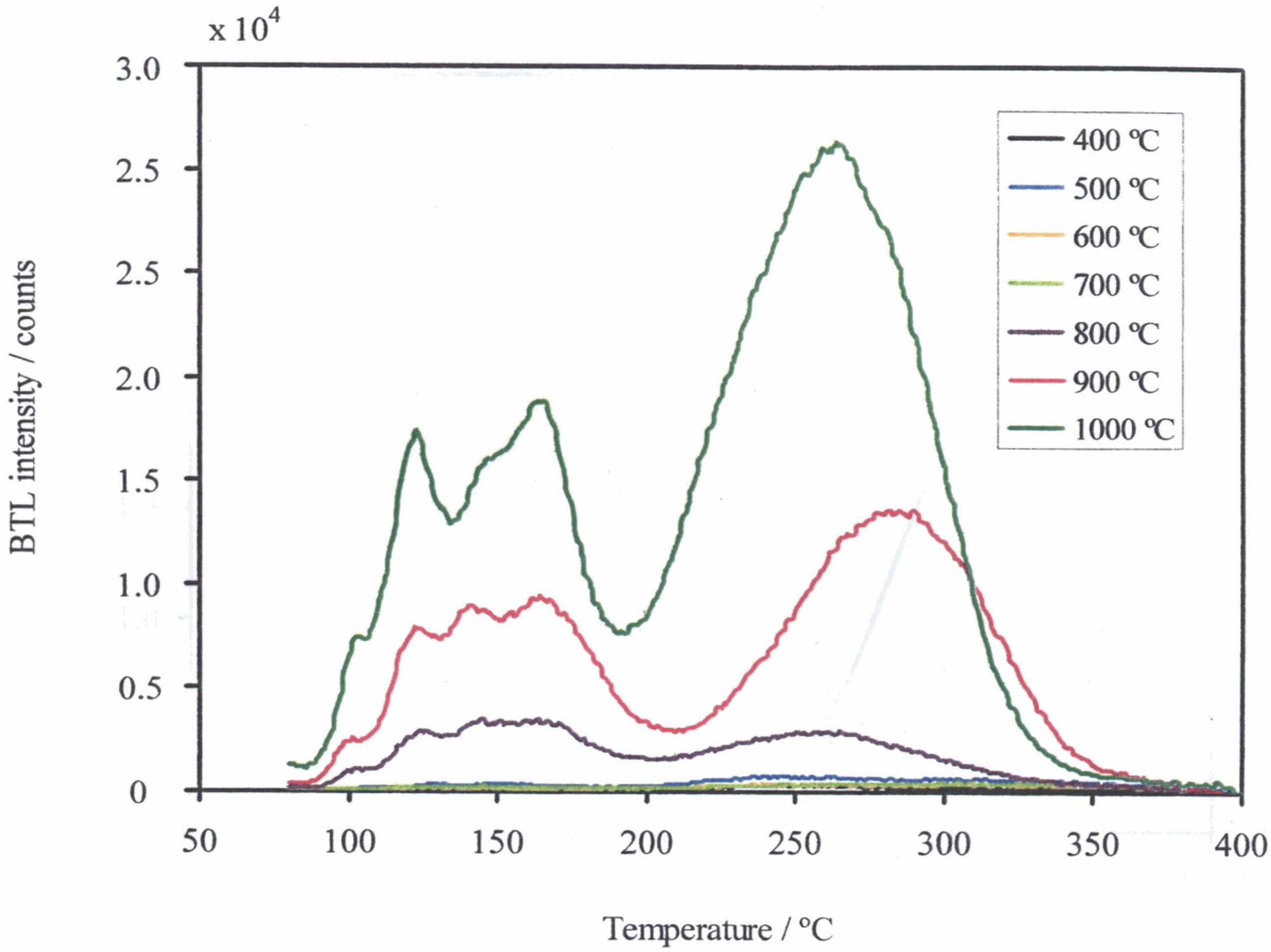

Figure 2.4

Dependence on several annealing temperatures of BTL glowcurves.

Samples were originated from Madagascar quartz.

Quartz samples were annealed for 1 day at an interval of 100 °C from 400 °C to 1000 °C.

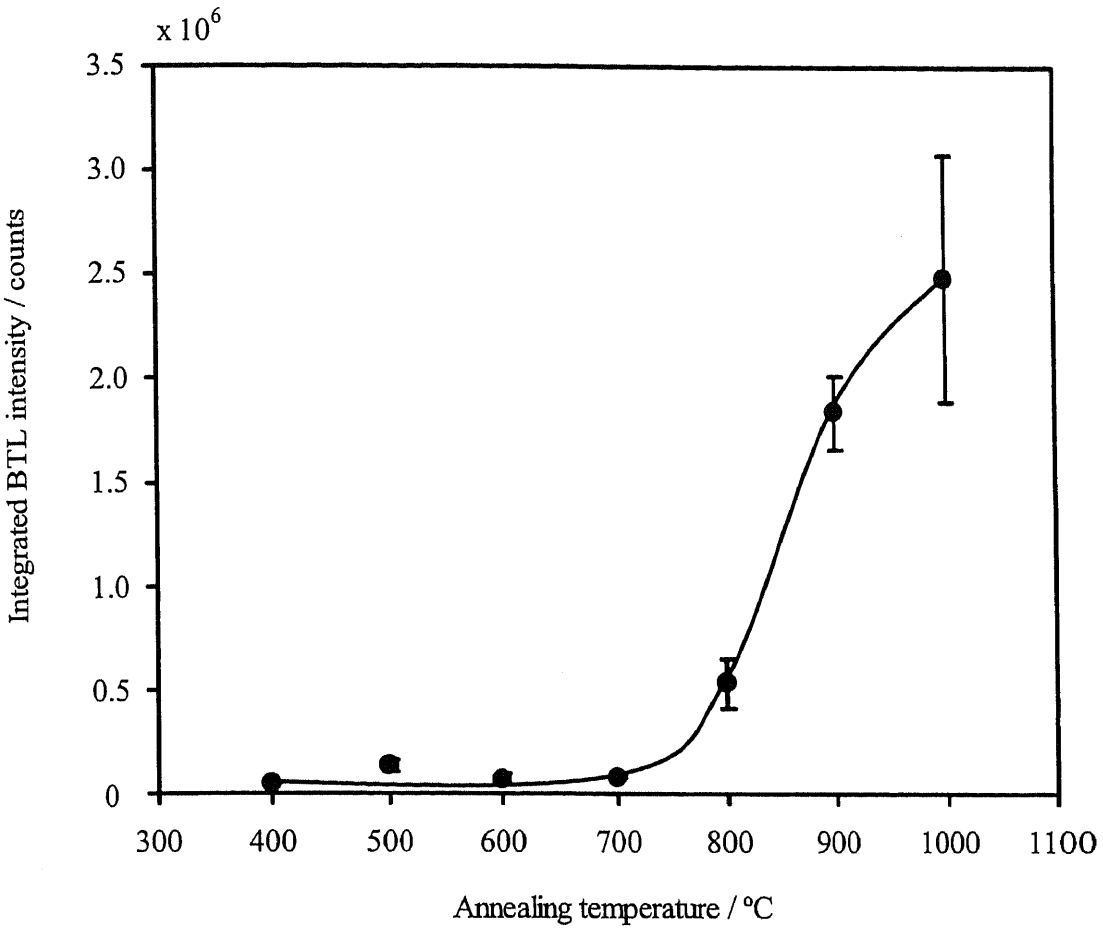

Figure 2.5

Tendency of integrated BTL intensities with several annealing temperatures.

The integrated BTL intensity is total photon counts in the whole region of glowcurve.

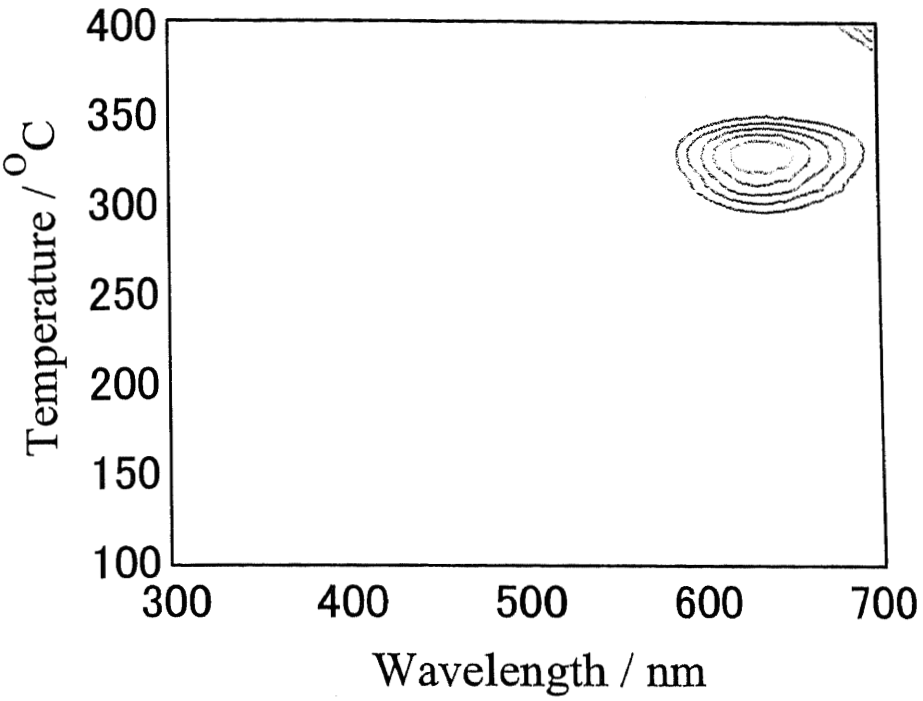

Figure 2.6

TL emission spectrum from Medeshima quartz.

Contour interval was fixed at 100000 cps and maximum of contour line was 900000 cps.

The sample temperature was controlled to be heated at a linear heating rate of 1 °C sec^{-1}.

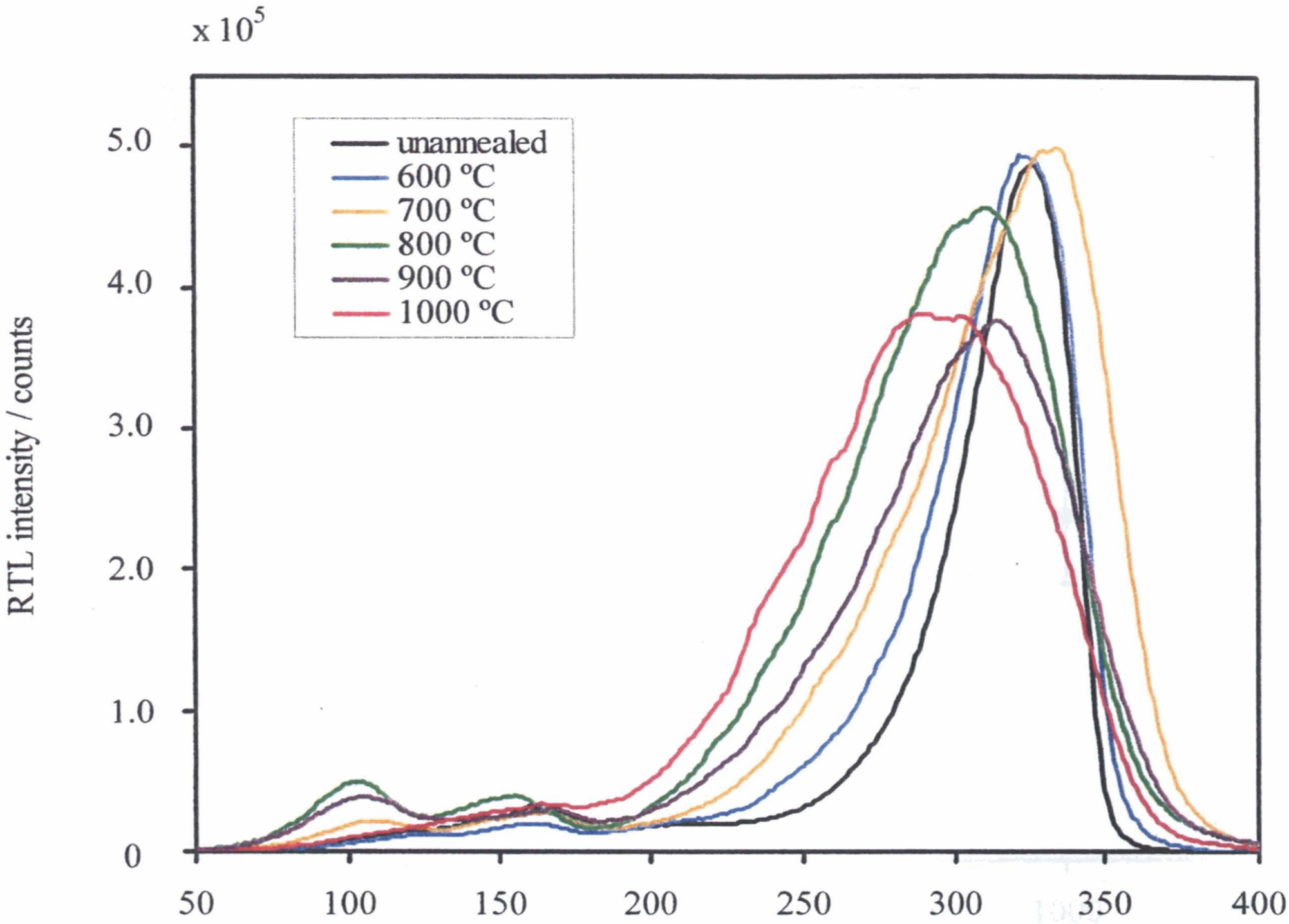

Figure 2.7
Dependence on various annealing temperatures of RTL glowcurves.
Quartz grains were extracted from Medeshima tephra layer.
Quartz samples were annealed for 1 day at an interval of 100 ºC from 400 ºC to 1000 ºC.

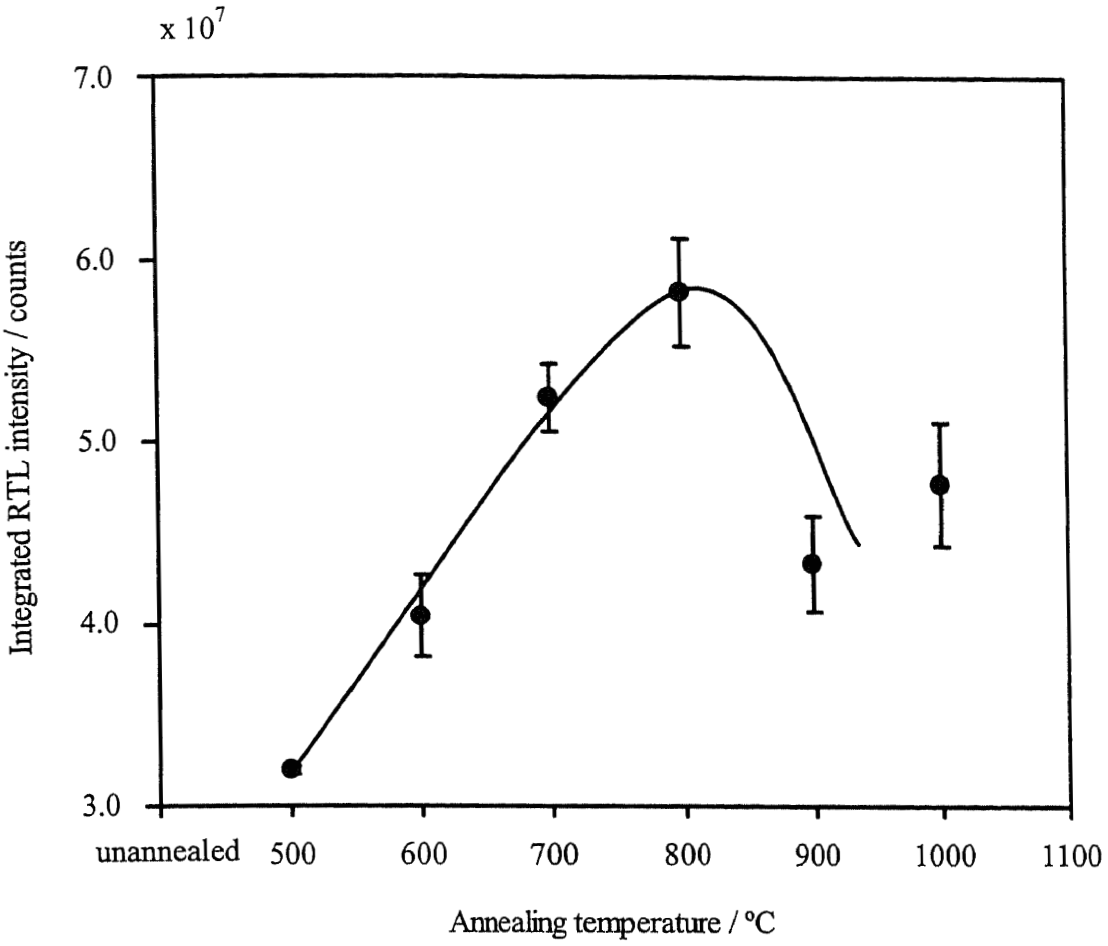

Figure 2.8
Tendency of RTL intensities with various annealing temperatures.
The integrated RTL intensity is total photon counts in the whole region.

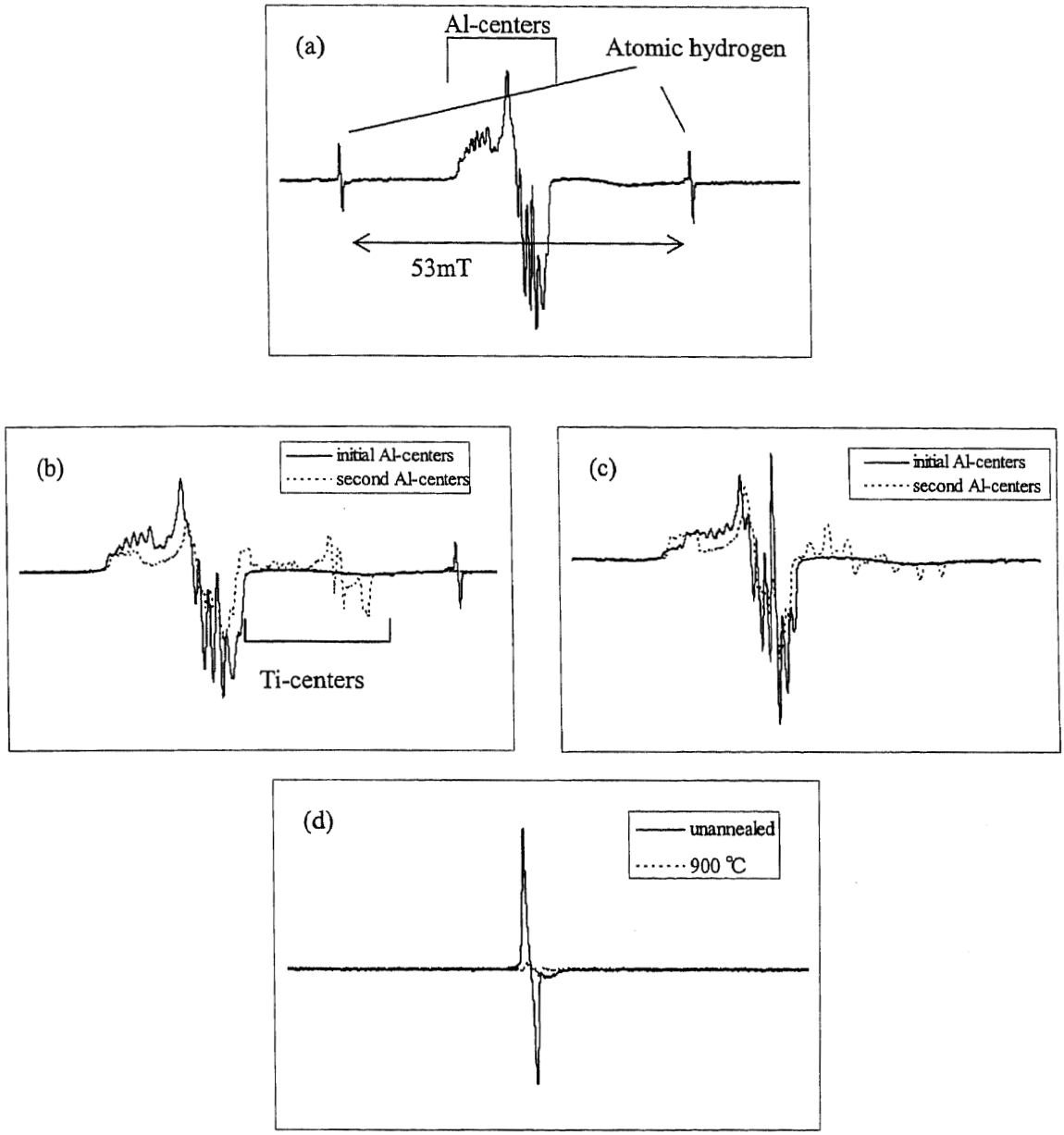

Figure 2.9

ESR spectra at -196 °C in quartz grains from Medeshima.

The spectra of (a) and (b) were obtained from unannealed grains; that of (c) was from annealed grains.

(d) was enlarged for the atomic hydrogen signal at lower magnetic field.

The microwave powers were 1mW for (a), (b) and (c); 0.64μW for (d).

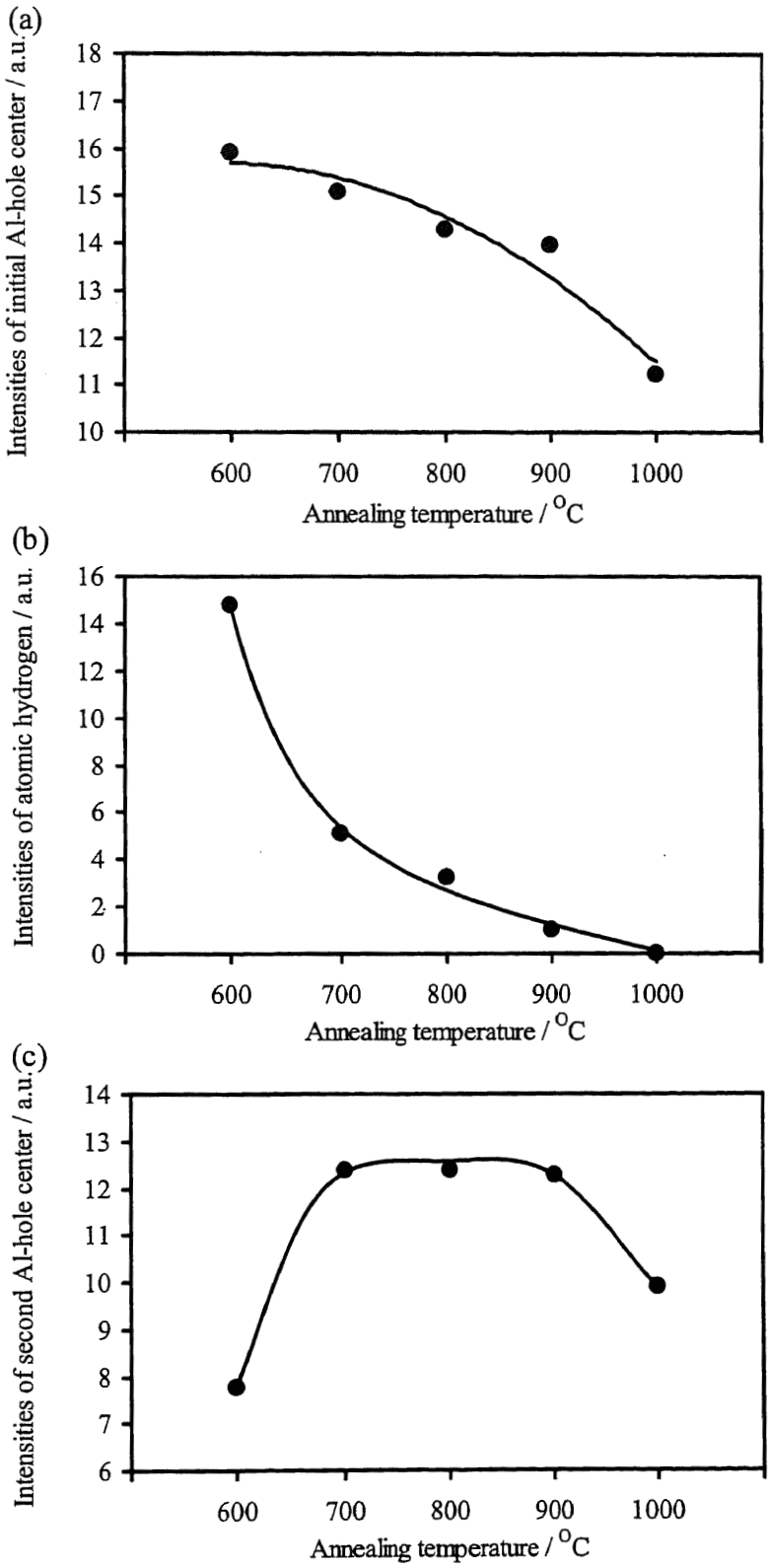

Figure 2.10

Intensities of ESR signal from annealed Medeshima quartz irradiated at -196 °C.
(a) initial Al-hole center, (b) atomic hydrogen, (c) second Al-hole center

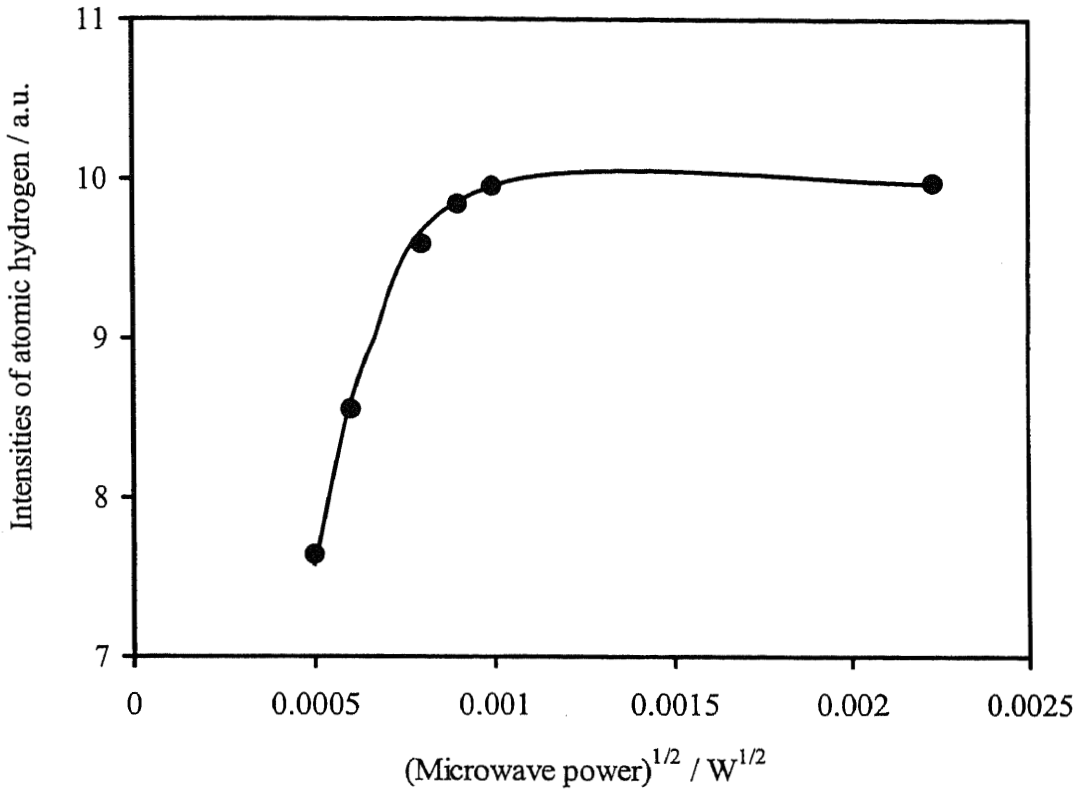

Figure 2.11
Saturation curve of atomic hydrogen intensities measured at -196 ^{o}C.

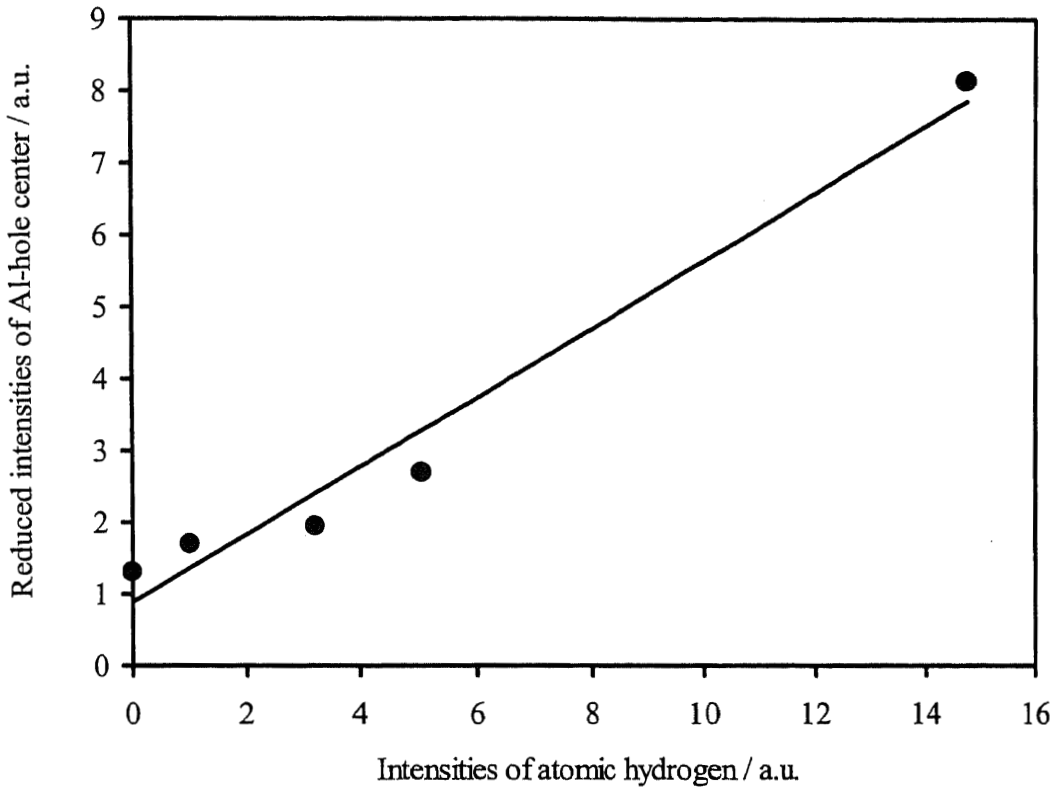

Figure 2.12

Correlation of the reduced intensities of Al-hole centers and atomic hydrogens from Medeshima quartz grains with several annealing treatments.

The difference between initial and second Al-hole center intensities after warming up to room temperature is corresponding to the reduced intensities of Al-hole centers.

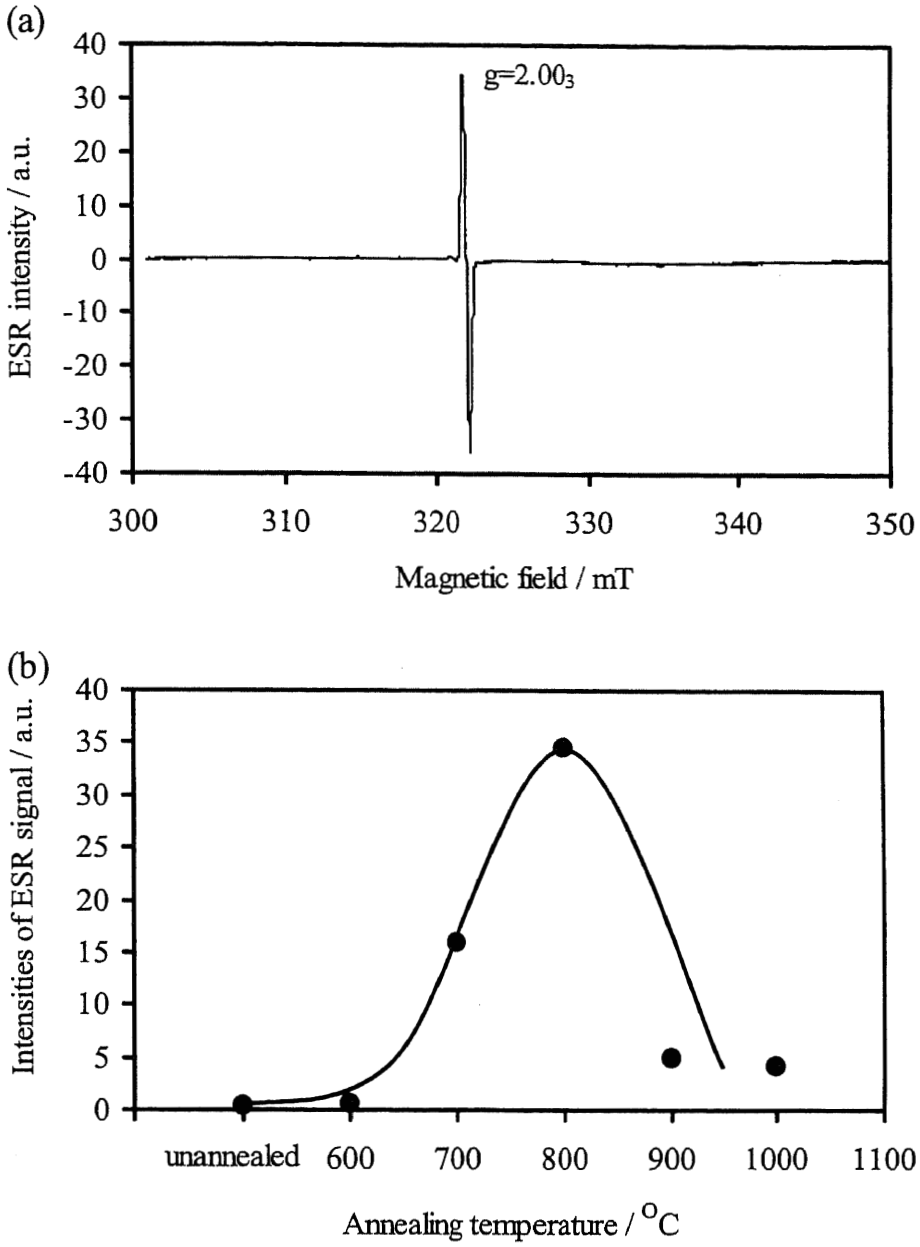

Figure 2.13

ESR signal of unidentified centers related to RTL.

(a) ESR spectra in unidentified centers region measured at room temperature. Annealing temperature: 900 ^{o}C, irradiation: 5 kGy at -196 ^{o}C

(b) Intensities of ESR signals, unidentified centers of quartz, with various annealing treatments.

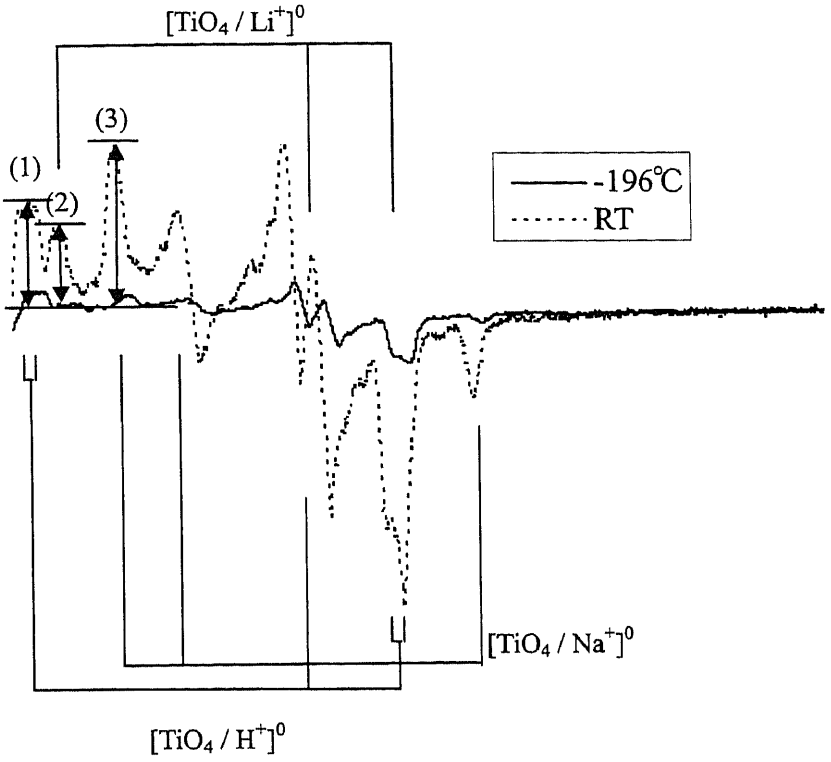

Figure 2.14

ESR signals for Medeshima quartz at -196 ^{O}C.

In -196 ^{O}C – irradiated quartz, three kinds of Ti-centers were observed after warming once up to the room temperature as seen in Figure 2.9 (b) and (c).

Samples were irradiated at -196 ^{O}C and at room temperature.

ESR intensities are the height of (1) for $[TiO_4 / H^+]^0$, that of (2) for $[TiO_4 / Li^+]^0$ and that of (3) for $[TiO_4 / Na^+]^0$ in the spectra.

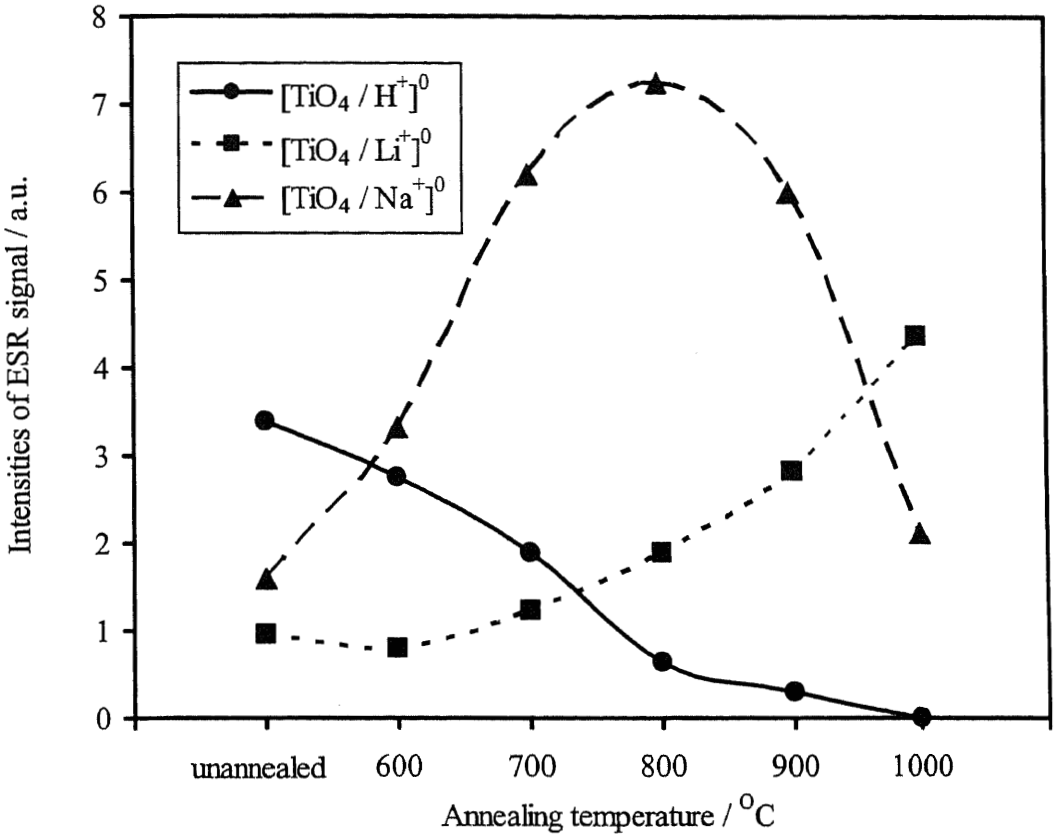

Figure 2.15

Intensity changes of Ti-centers in quartz samples without and with annealing treatments at different temperatures.

All quartz samples were irradiated and measured at -196 °C after warming up to the room temperature.

$[TiO_4 / H^+]^0$, $[TiO_4 / Li^+]^0$ and $[TiO_4 / Na^+]^0$ center intensities were measured from most left side signals in each identified spectrum as indicated in Figure 2.14.

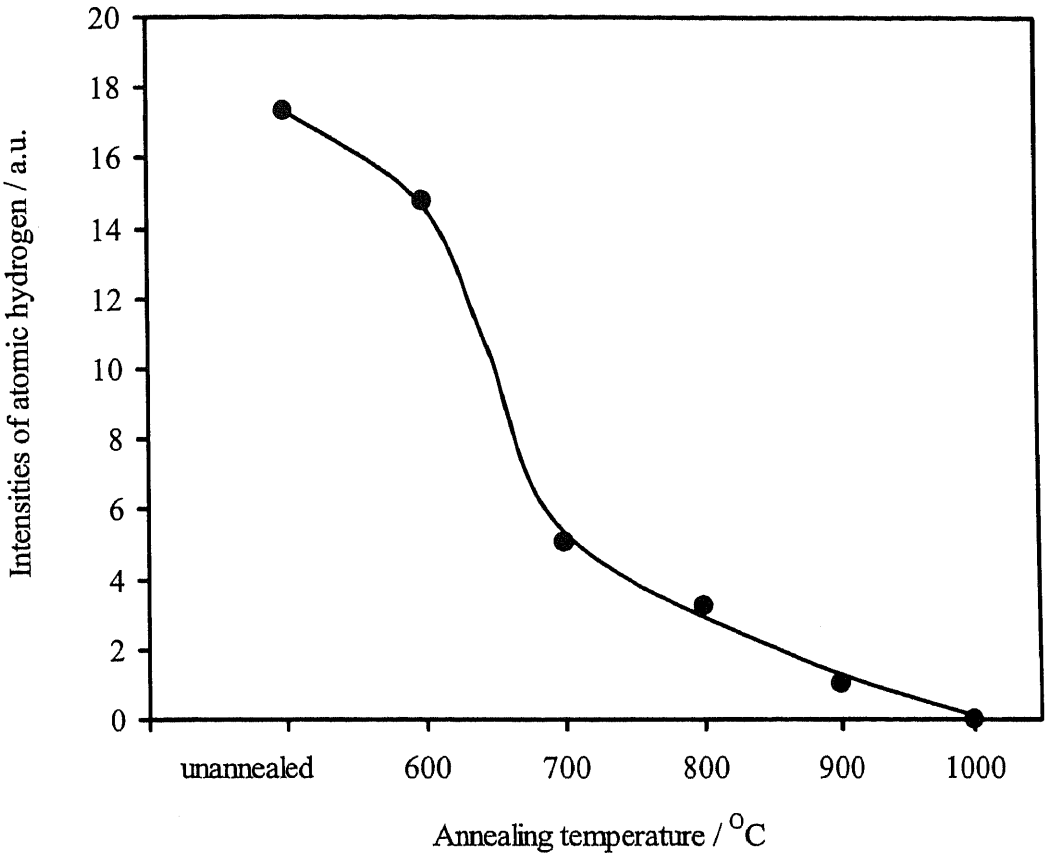

Figure 2.16

Intensity changes of atomic hydrogen from quartz samples without annealing and with annealing treatments at different temperatures.

The intensities of atomic hydrogen were measured at -196 °C.

Each quartz sample was annealed for 24 hr at different temperatures.

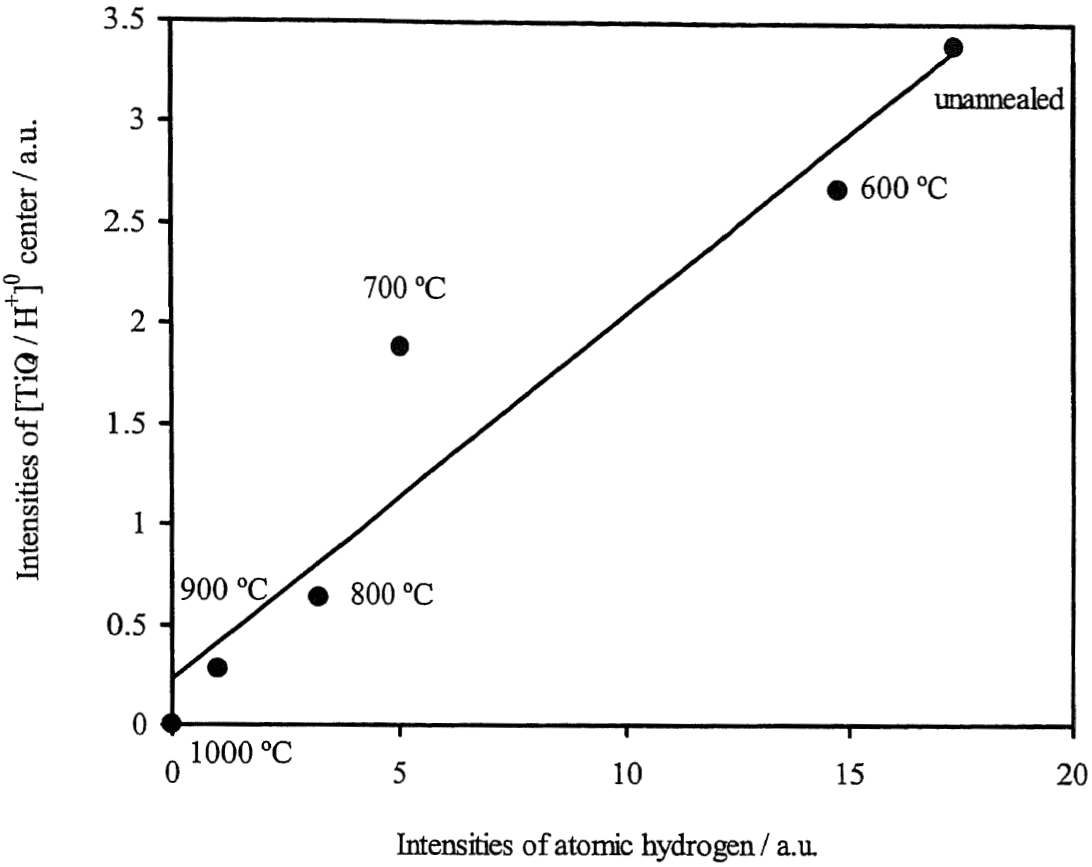

Figure 2.17

Correlation between the intensities of atomic hydrogen and $[TiO_4 / H^+]^0$ center from Medeshima quartz.

Both irradiation and H^0 measurements were carried out of -196 ^oC.

$[TiO_4 / H^+]^0$ centers were measured in the same way as described in Figures 2.15.

Quartz samples were unannealed or annealed at different temperatures.

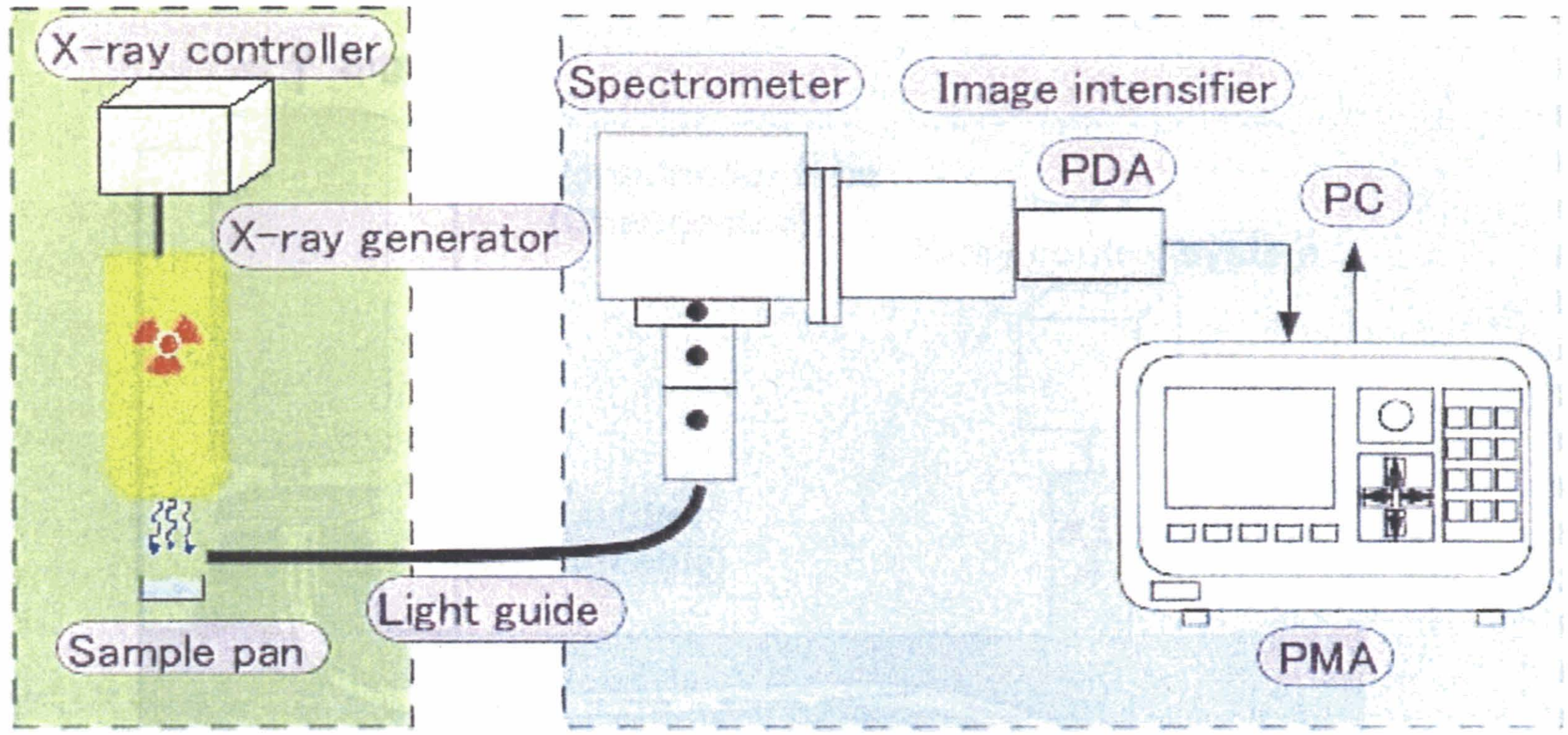

Figure 3.1
Schematic diagram of an on-line RL-spectrometric system.

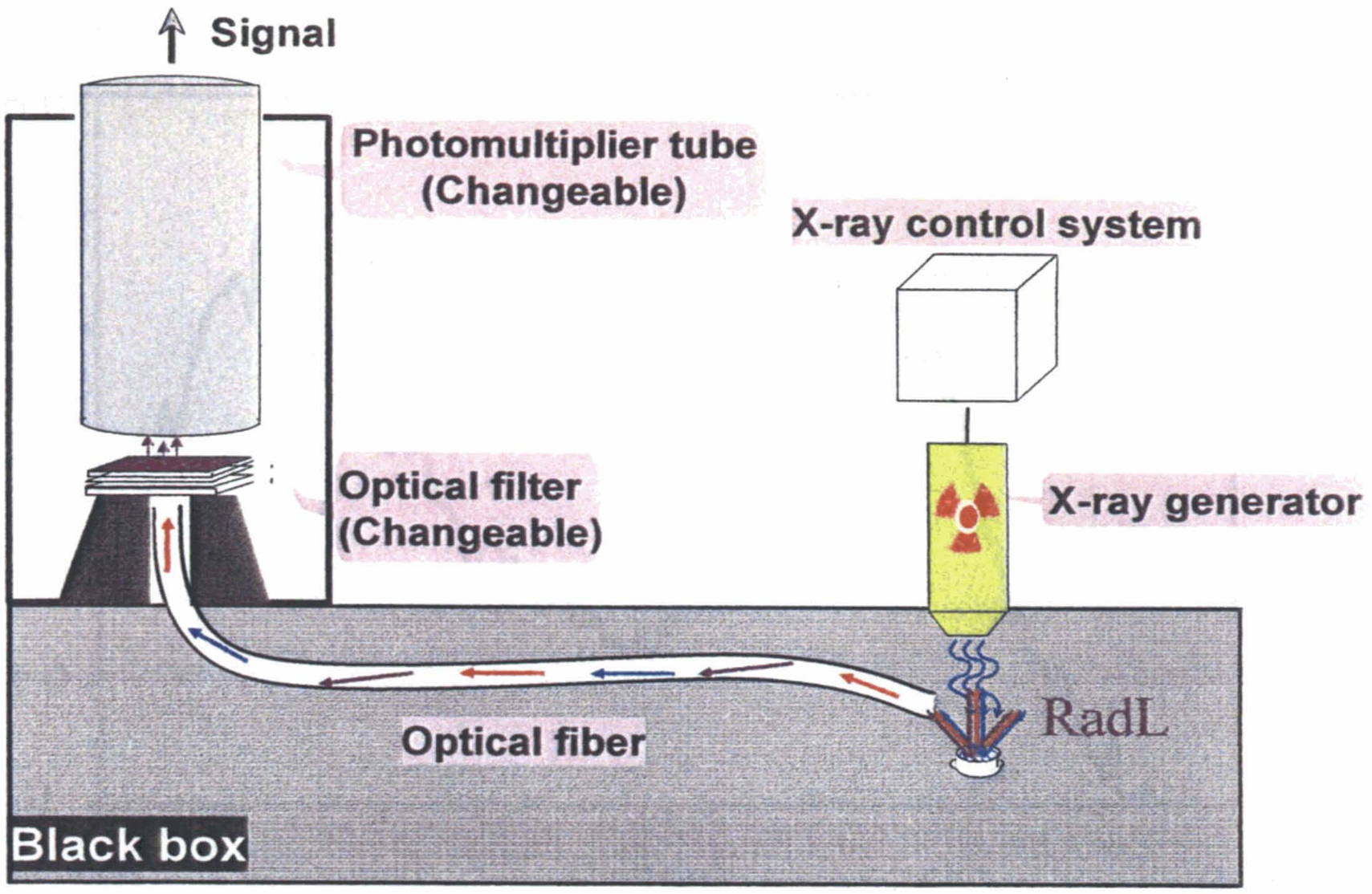

Figure 3.2
Conceptual view of an RL measuring system.
For the RL-measurements, this available to both V-RL and R-RL by changing PMT and optical filters.

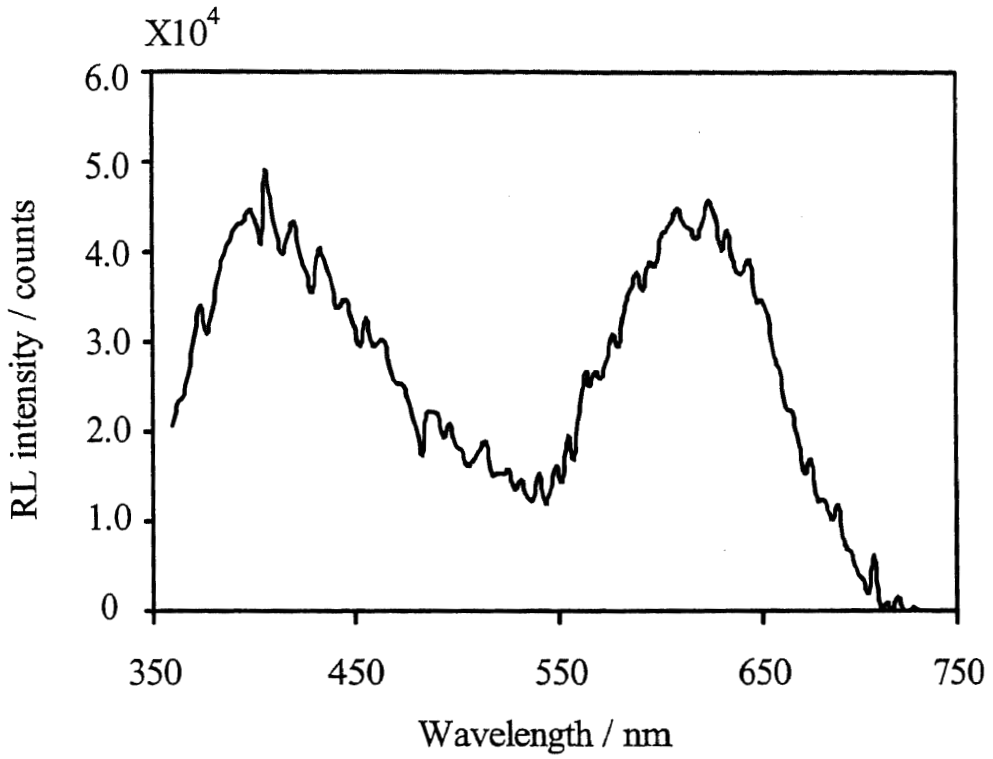

Figure 3.3

RL emission spectrum from an aliquot of natural quartz at room temperature. A quartz grain aliquot was collected around JAEA and irradiated with X-ray at about 30 Gy.

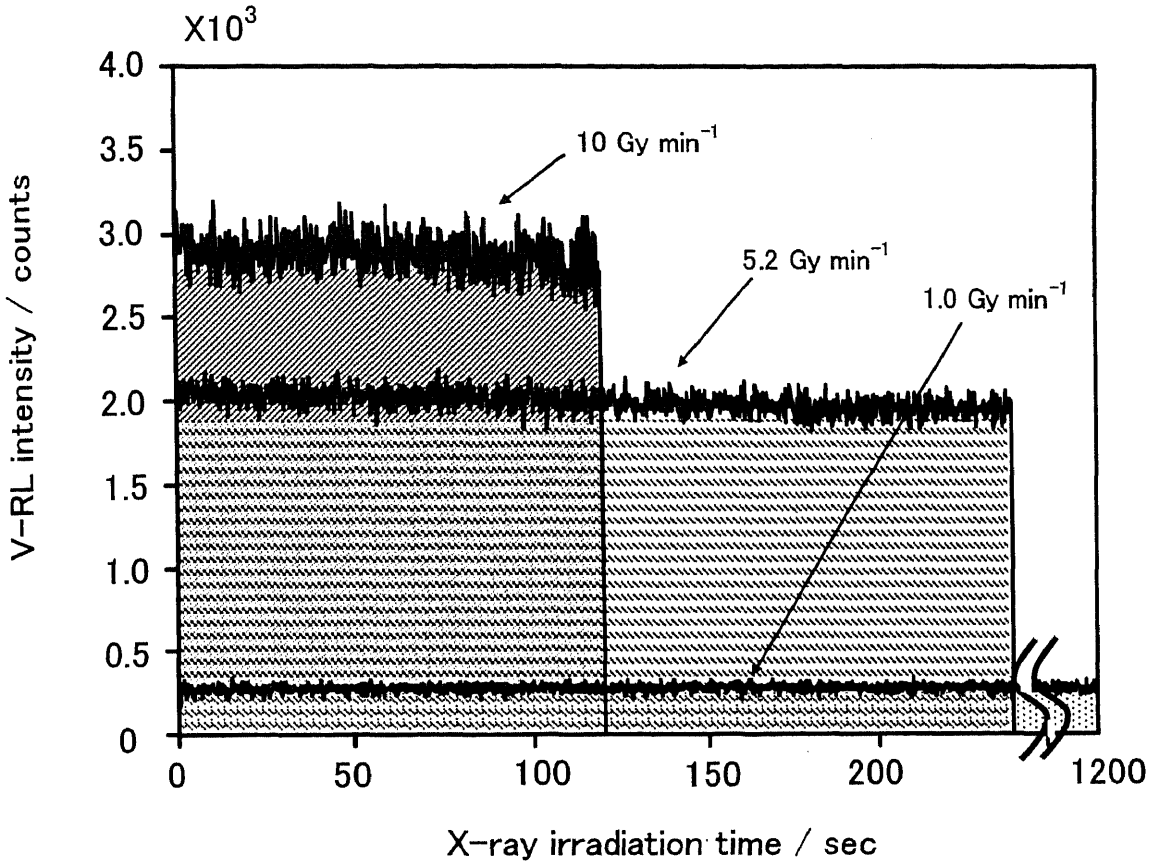

Figure 3.4

Changes of V-RL intensities as a function of the X-ray exposure period at three kinds of dose rates.

A quartz grain aliquot was collected from surface soil around JAEA.

Each shadow area is equivalent to the total V-RL during irradiation of 20 Gy.

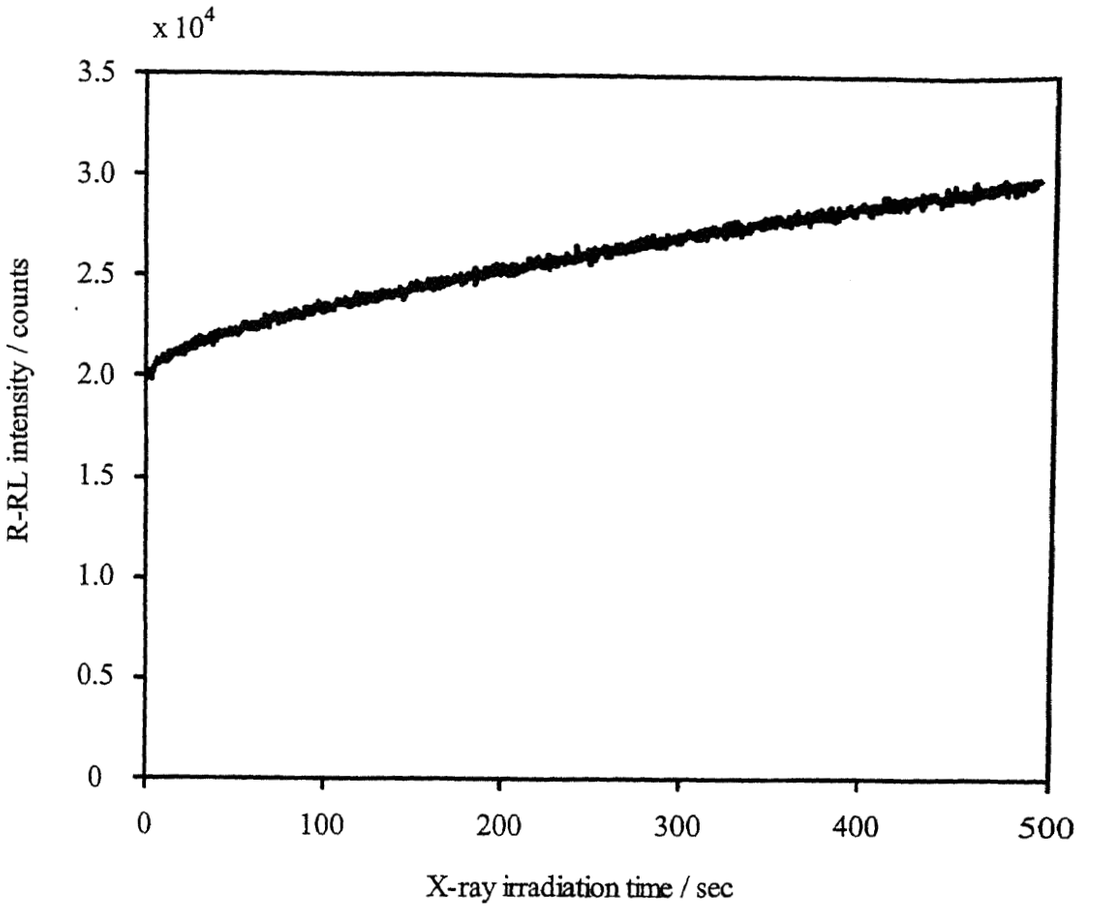

Figure 3.5
Changes of R-RL intensities as a function of X-ray exposure period.
A quartz grain aliquot was collected from surface soil around JAEA
Dose rate is 5.2 Gy min^{-1}.

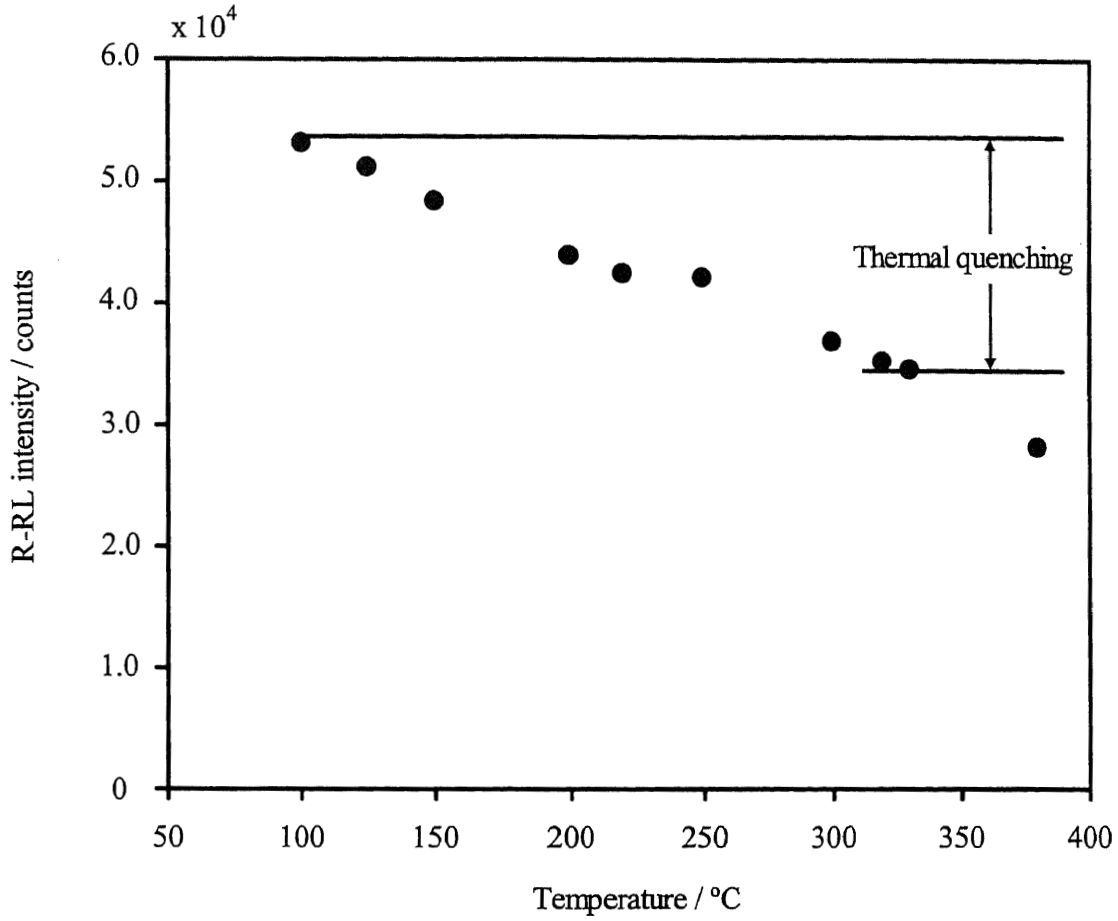

Figure 3.6
Relationship between R-RL and sample heating temperature.
Sample: Quartz grains from surface soil around JAEA.

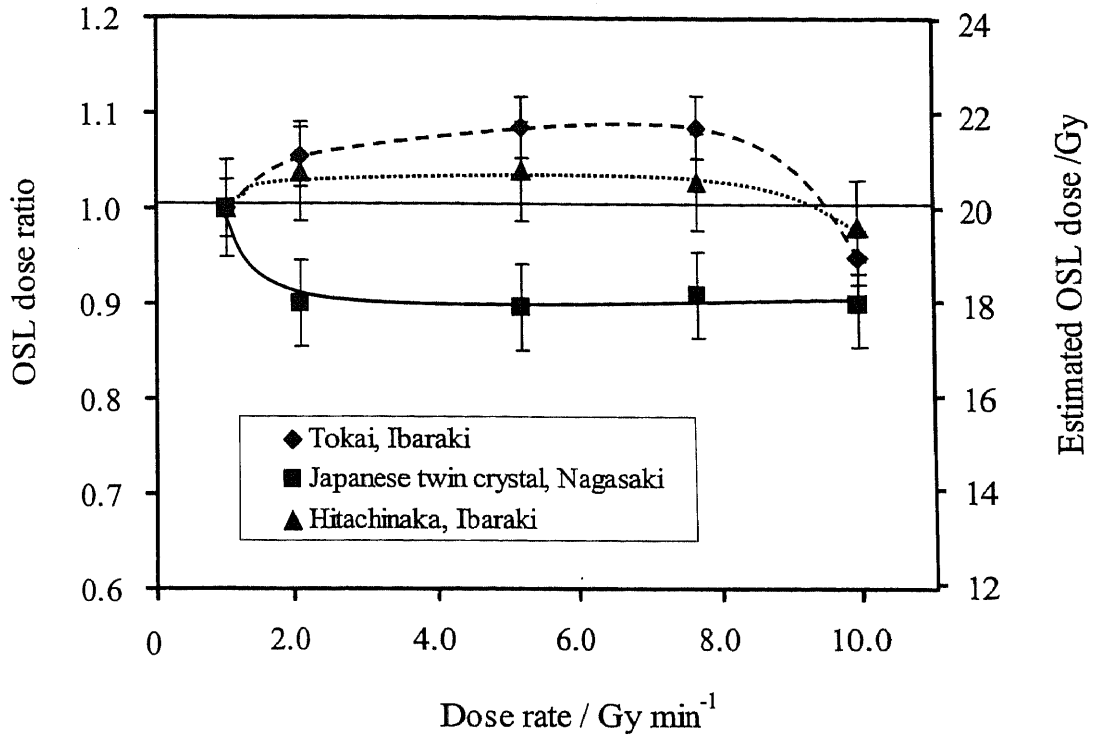

Figure 3.7

Dose-rate dependences of estimated OSL-doses.

OSL doses are normalized to unity for OSL doses evaluated at 1.0 Gy min^{-1}.

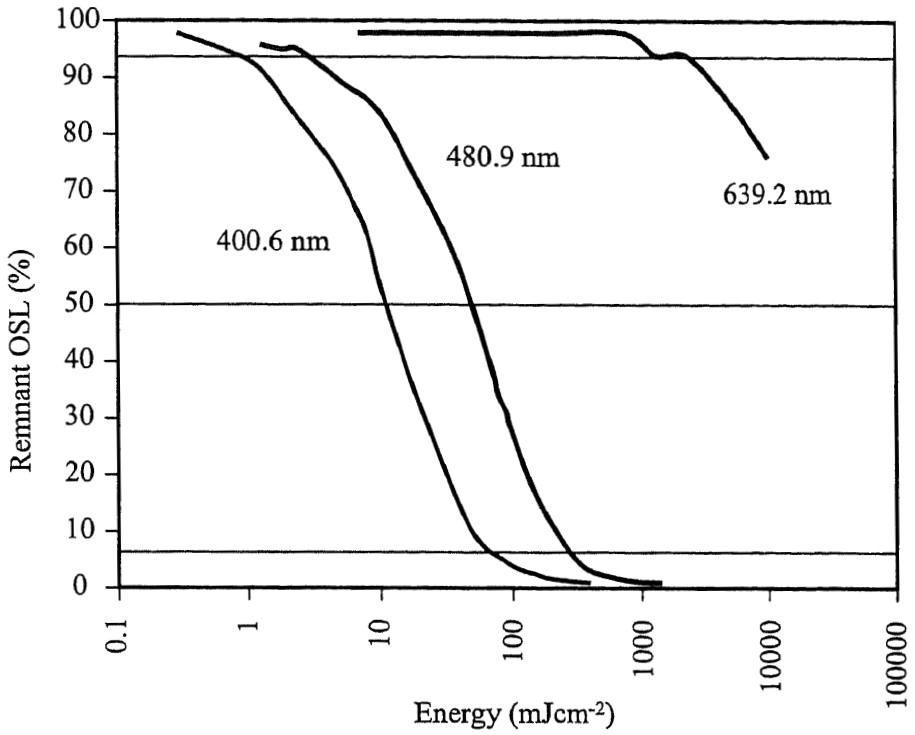

Figure 3.8

Bleaching of the 514.5 nm-stimulated OSL by various narrow wavebands (~10 nm FWHM) of visible light.

Individual aliquots were used for each bleaching waveband and all are normalized by short exposures (514.5 nm) given before commencement of bleaching. Data have had their background count rate subtracted and are corrected for depletion due to the cumulative monitoring exposures (514.5 nm). The bleaching curves are plotted against every deposited in that waveband. The transects allow determination of the total energies required for 5, 50 and 95 % reduction of the OSL for any given waveband (referred to Spooner, 1994).

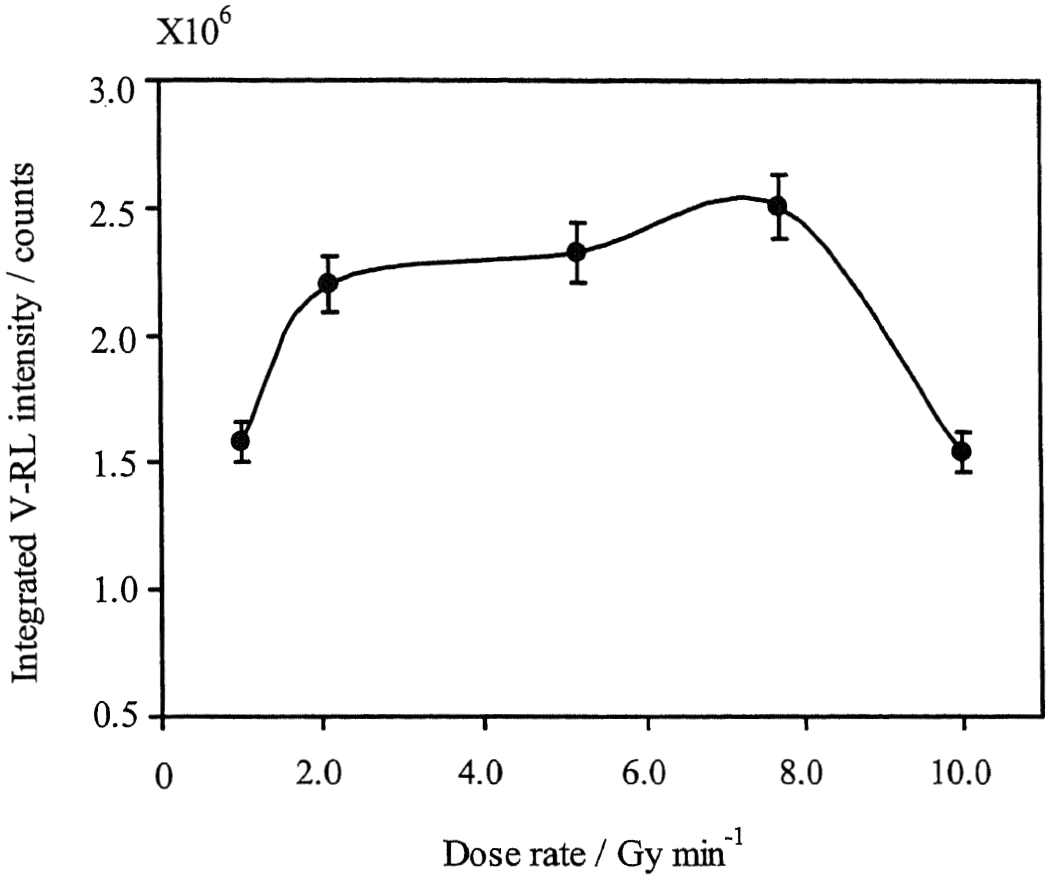

Figure 3.9

Variation of integrated V-RL intensities by the dose rates of X-ray generator when the exposure dose was fixed to 20 Gy.

The natural quartz grains were collected around JAEA (Tokai, Ibaraki).

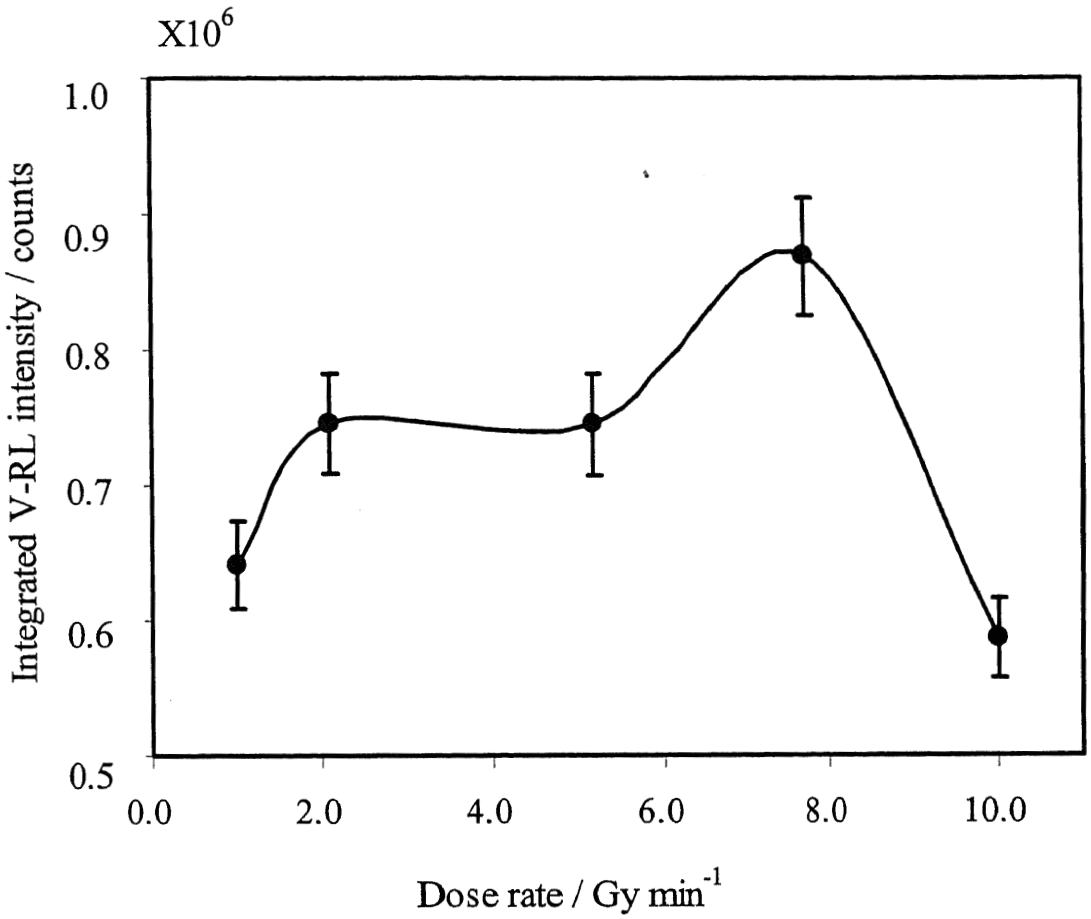

Figure 3.10

Variation of integrated V-RL intensities by the dose rates of X-ray generator when the exposure dose was fixed to 20 Gy.

The natural quartz grains were collected around JAEA (Hitachinaka, Ibaraki).

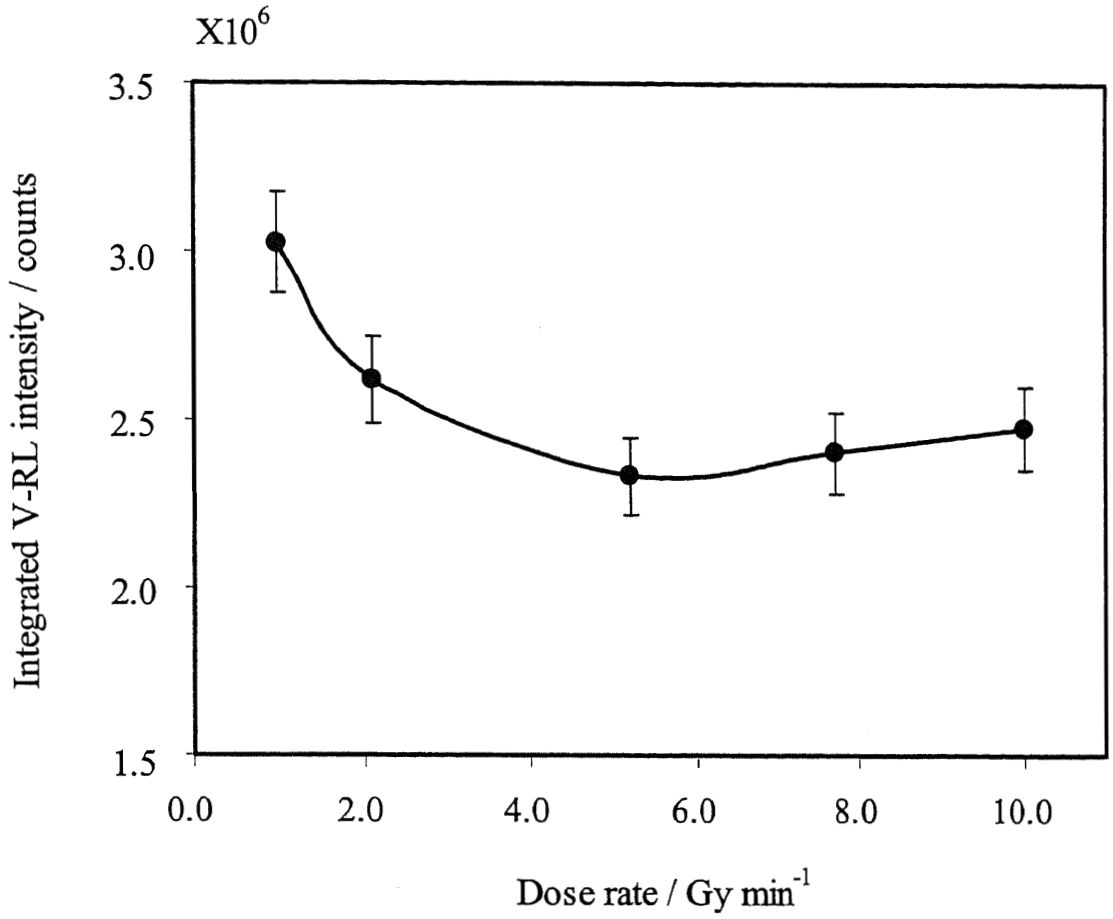

Figure 3.11

Variation of integrated V-RL intensities by the dose rates of X-ray generator when the exposure dose was fixed to 20 Gy.

The natural quartz grains were Japanese twin crystal.

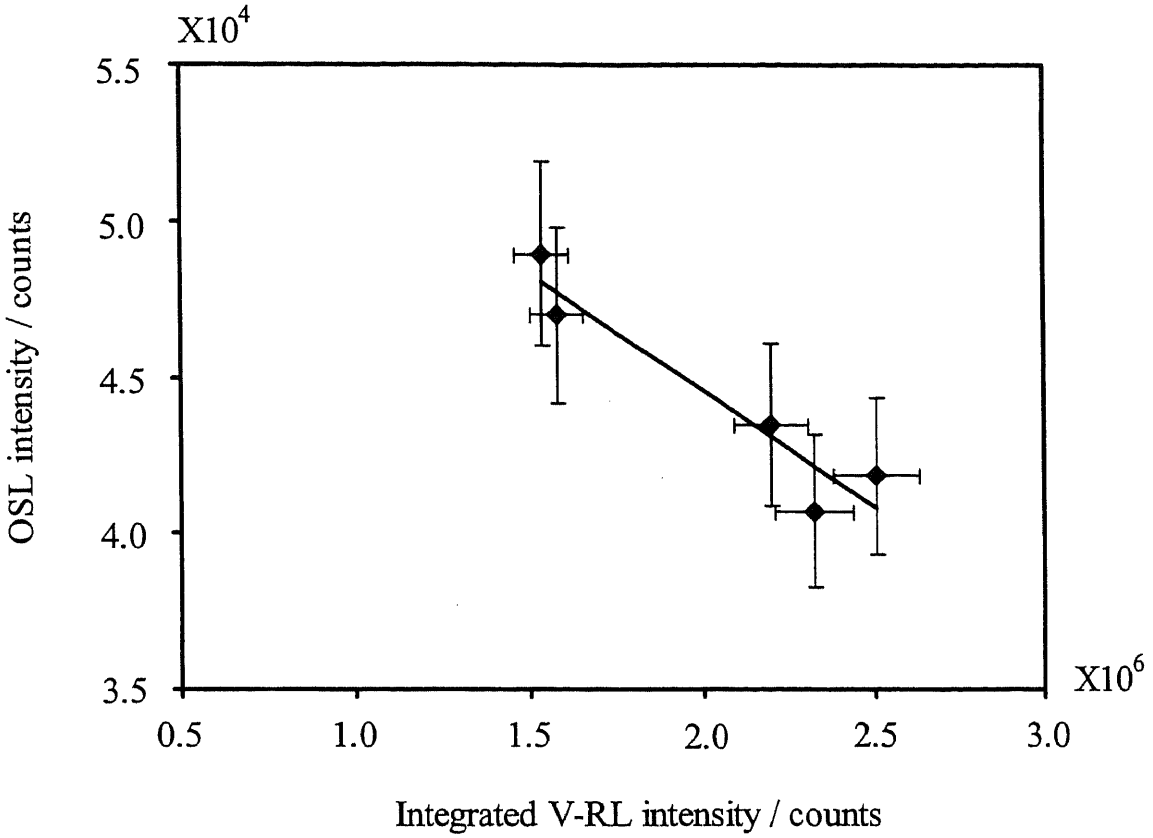

Figure 3.12
Relationship between integrated V-RL intensity and OSL one when different dose rates were applied.
A quartz grain aliquot was collected around JAEA (Tokai, Ibaraki). The total dose was fixed to be 20 Gy.

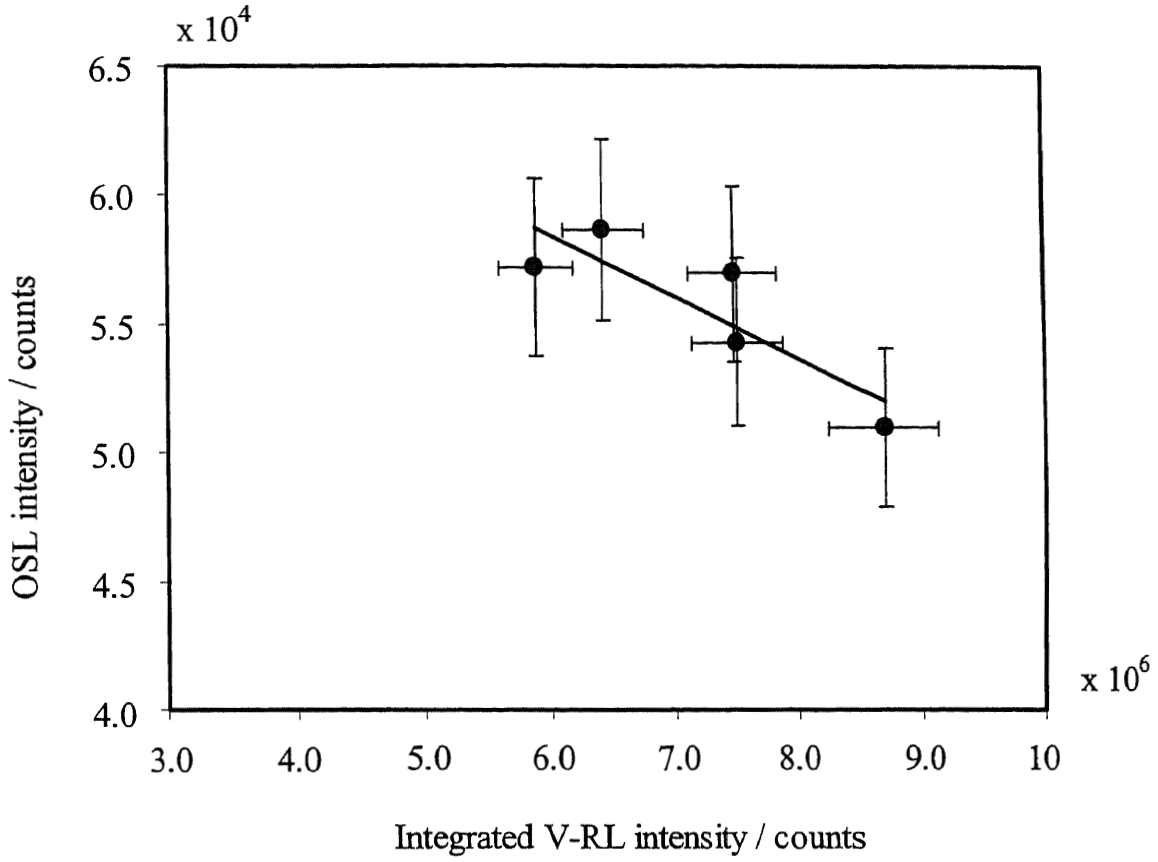

Figure 3.13

Relationship between integrated V-RL intensity and OSL one when different dose rates were applied.

A quartz grain aliquot was collected around JAEA (Hitachinaka, Ibaraki). The total dose was fixed to be 20 Gy.

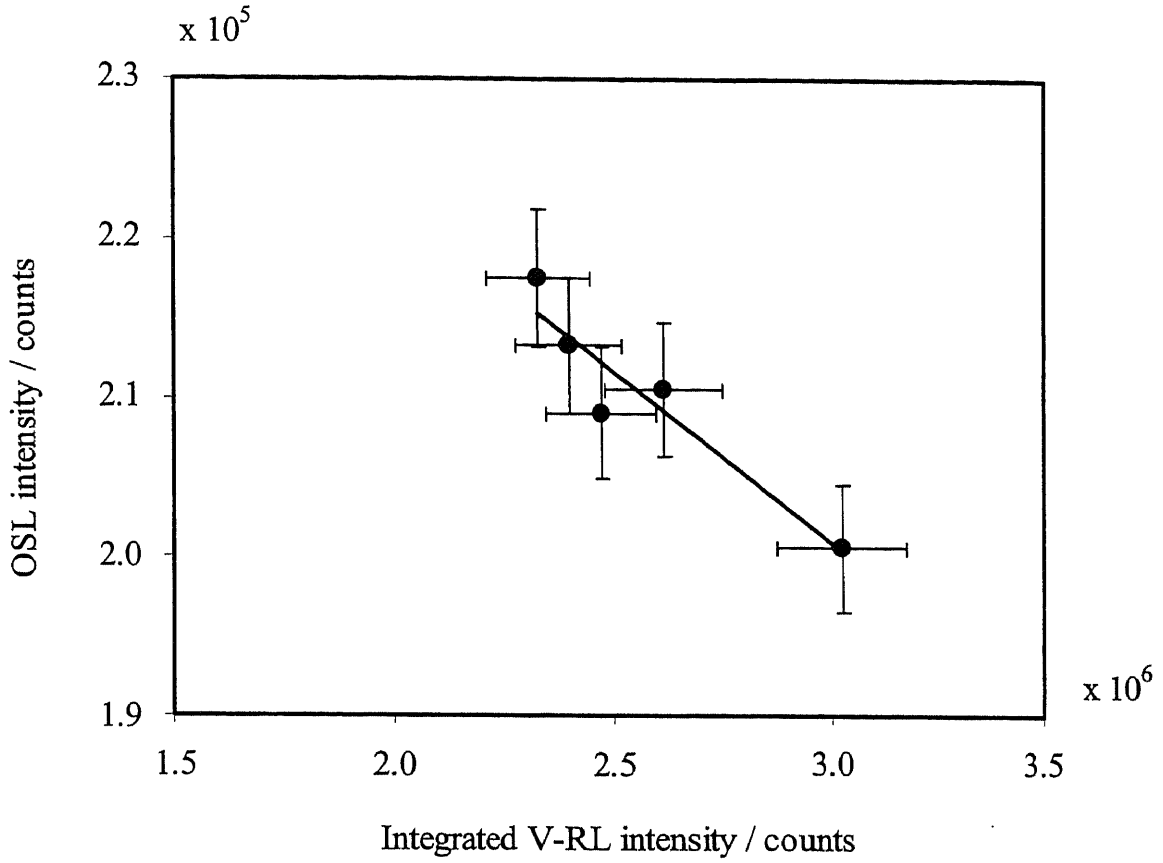

Figure 3.14

Relationship between integrated V-RL intensity and OSL one when different dose rates were applied.

A quartz grain aliquot was collected around JAEA (Japanese twin crystal). The total dose was fixed to be 20 Gy.

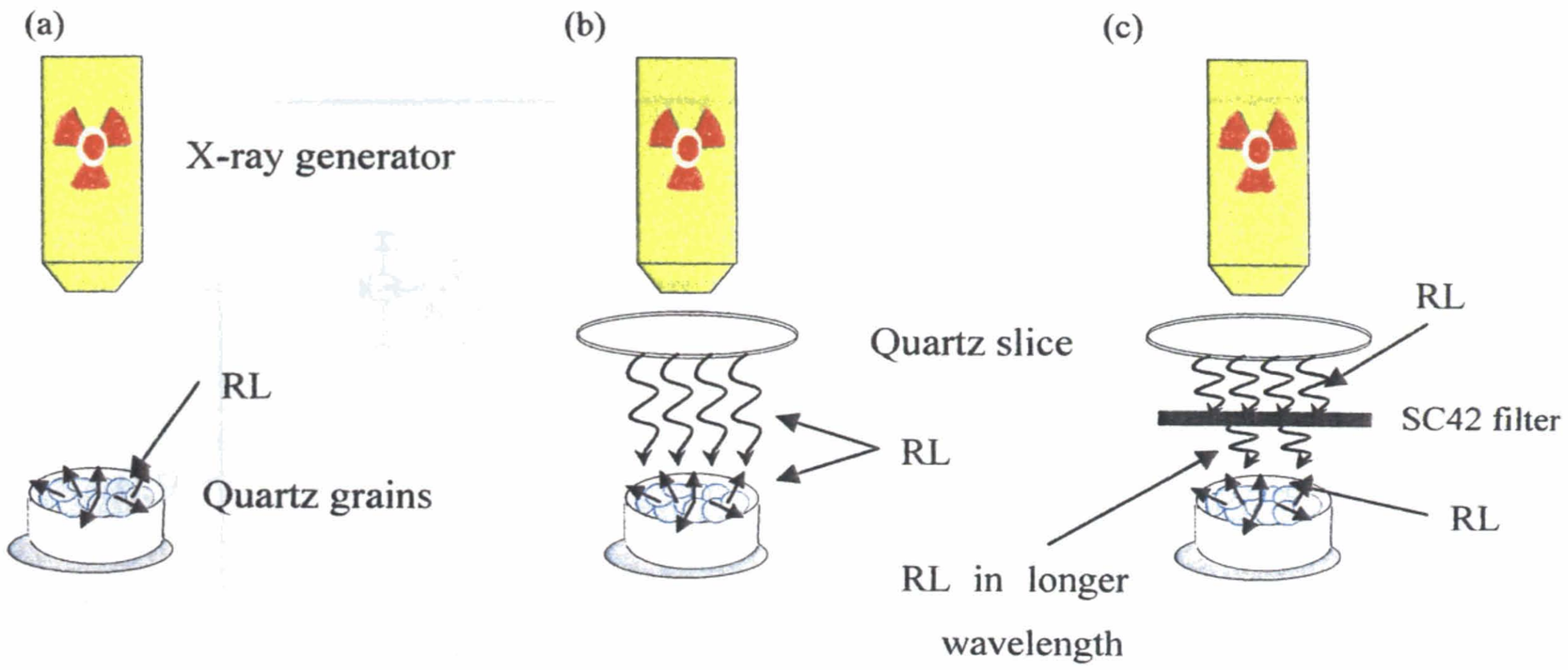

Figure 3.15
Schematic X-ray irradiation arrangements for determining the influence of RL on OSL.
(a) a standard arrangement
(b) insertion of quartz slice
(c) insertion of quartz slice and SC42 filter
In (b) and (c) arrangements, quartz grains were covered with different slices of V-RL intensities during X-ray irradiation.

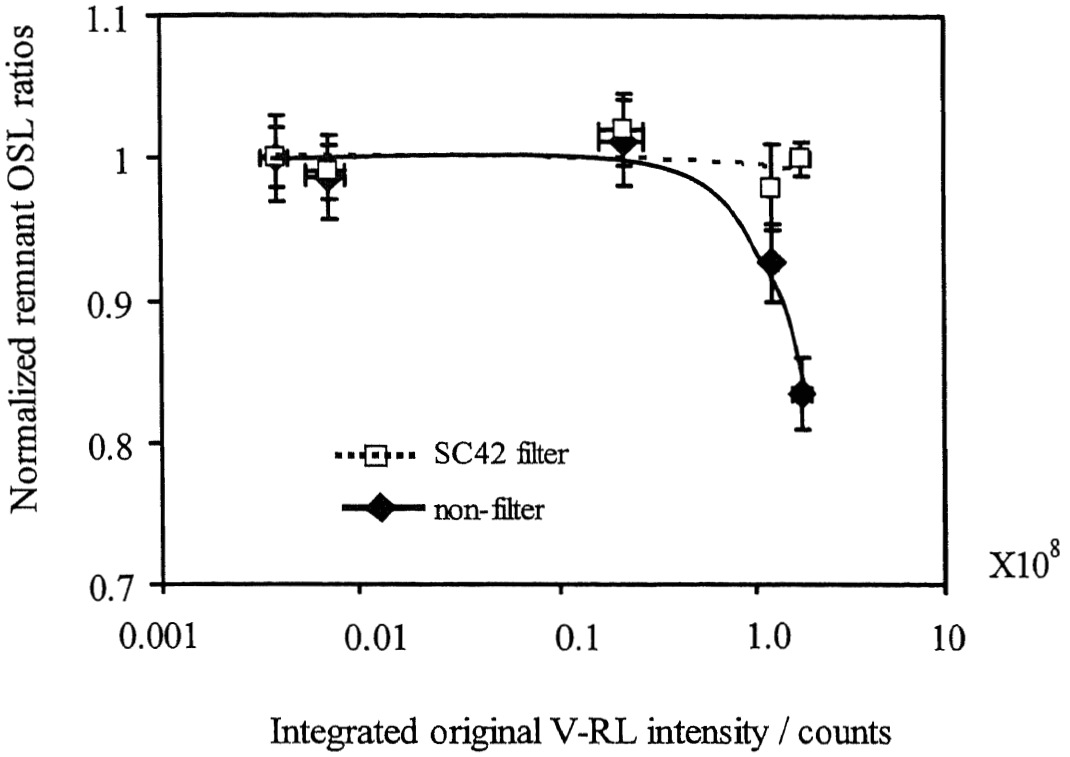

Figure 3.16
Relationships between the normalized remnant OSL ratios and V-RL intensities of quartz slices.
Each sample was irradiated to 20 Gy.
Remnant OSLs were normalized to unity from the lowest V-RL intensity quartz slice
A SC42 filter made from gelatin cuts enough the light shorter than 420 nm, but passes completely the light longer than 420 nm light as seen in the irradiation arrangement (c). The non-filter experiment was carried by the arrangement (b) in Figure 3.16.

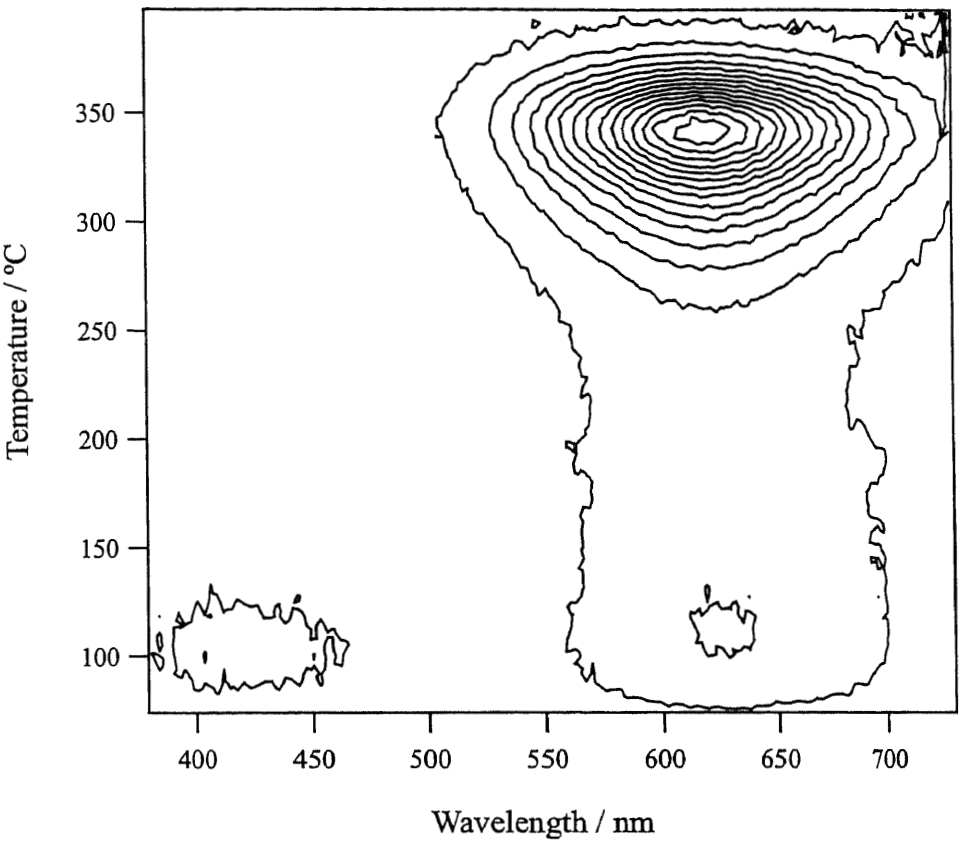

Figure 4.1

TL emission spectrum for quartz extracted from surface soil around JAEA.

The sample temperature was controlled to be heated at a linear heating rate of 1 °C sec^{-1}.

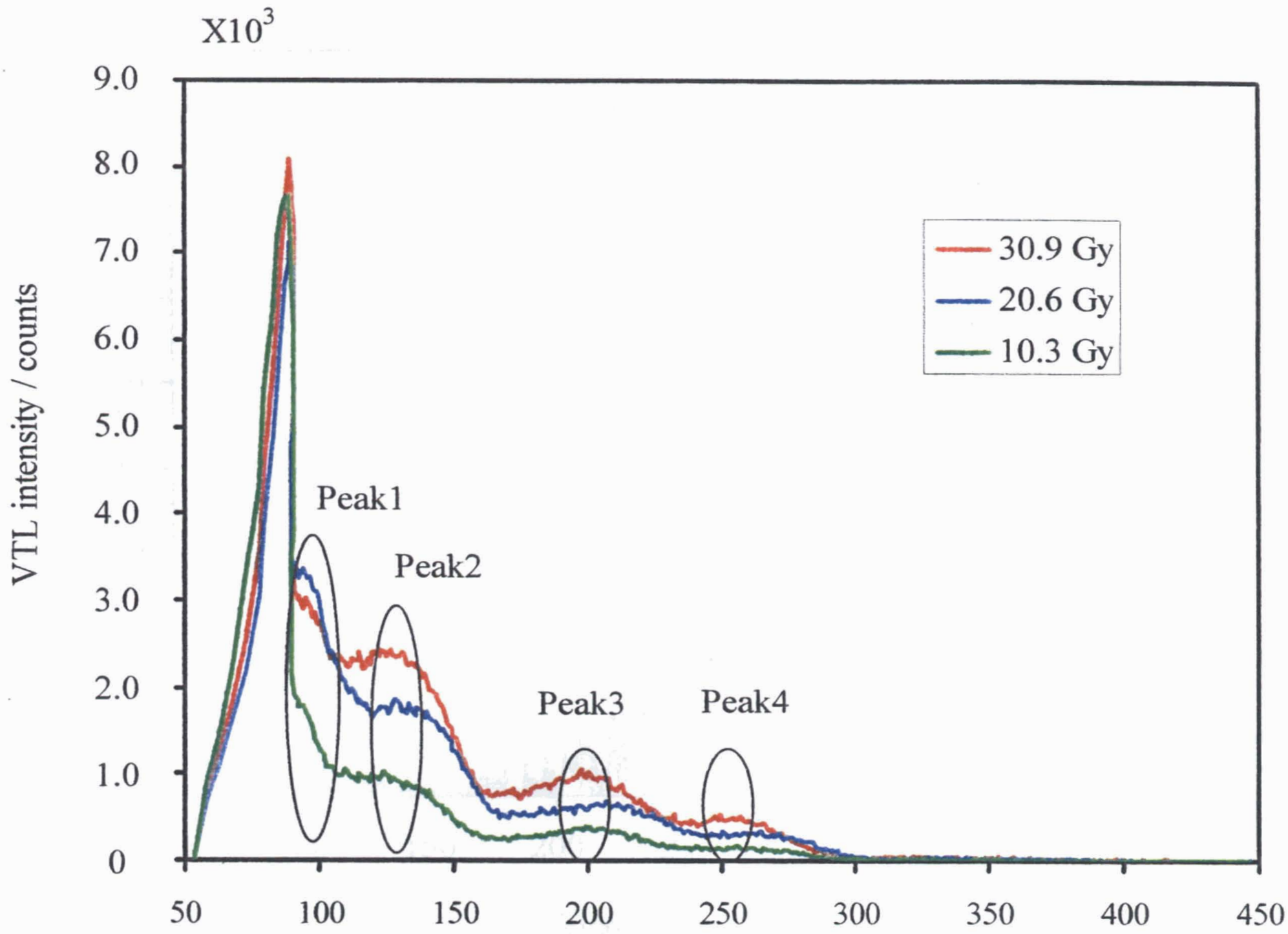

Figure 4.2

Changes of VTL glowcurves associated with artificial irradiation doses by X-ray.

Quartz extracts are obtained from surface soil around JAEA.

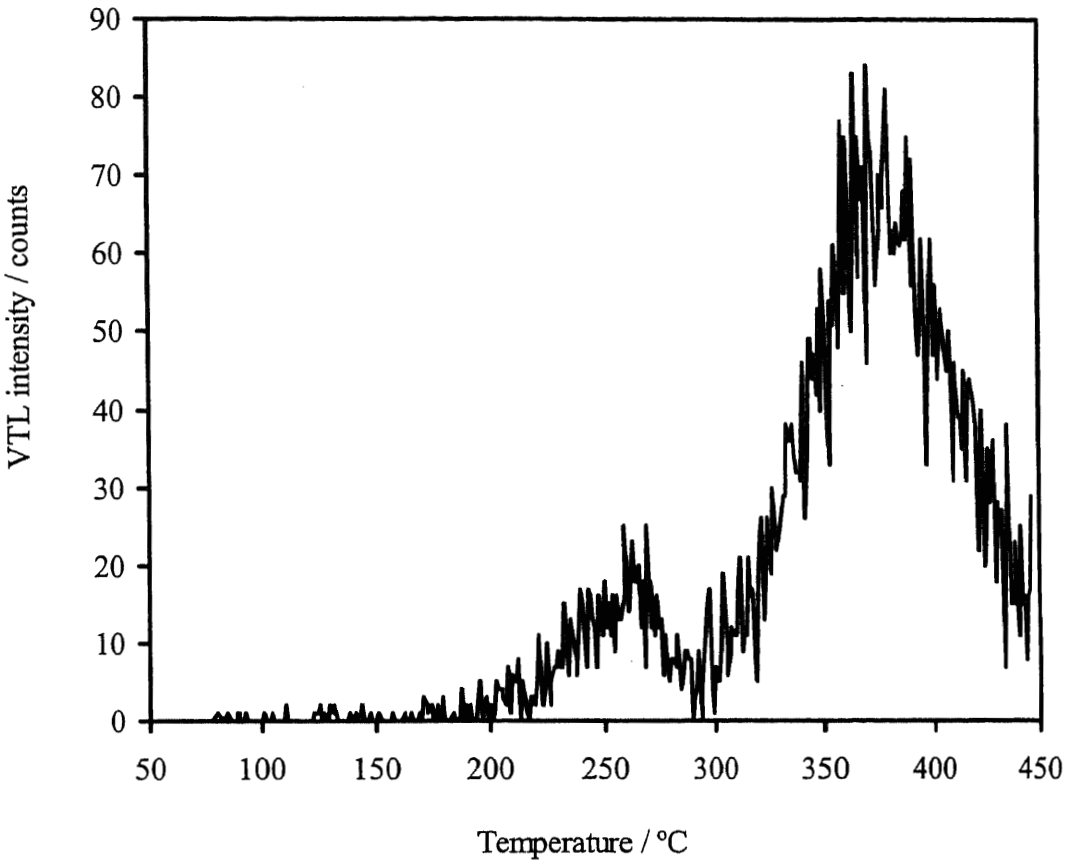

Figure 4.3
VTL glowcurve of quartz grains from surface soil collected around JAEA.
The glowcurve was accumulated in environmental irradiation.

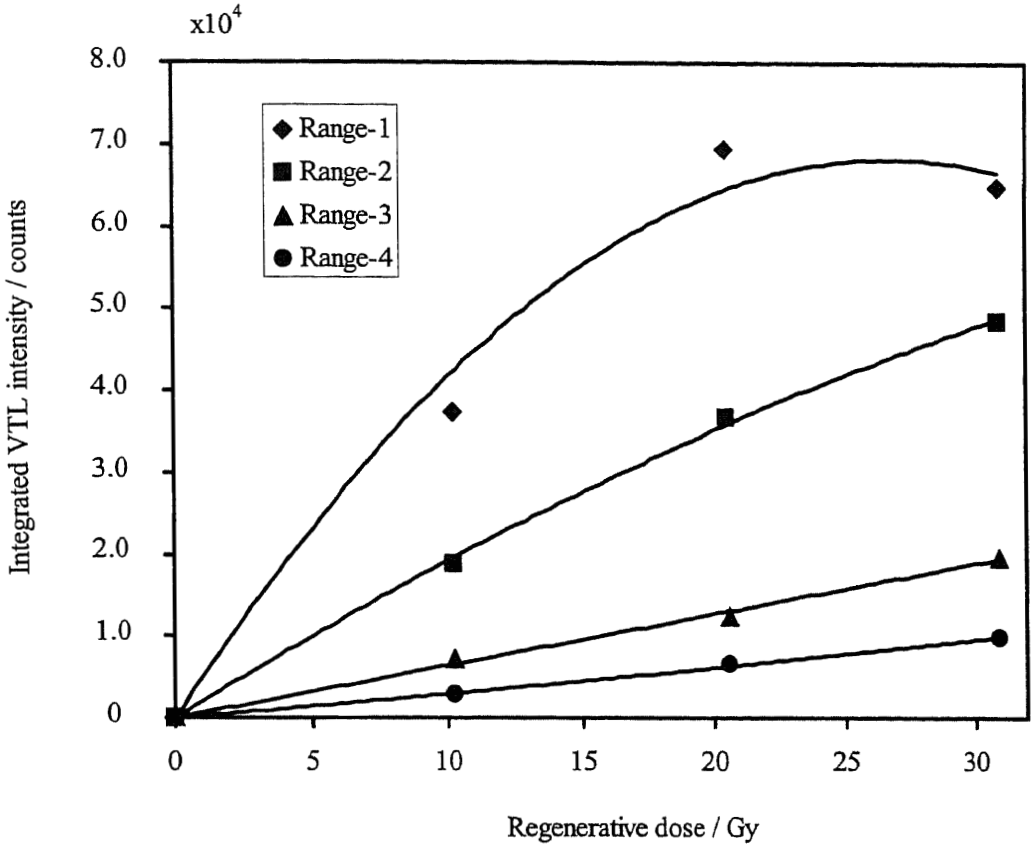

Figure 4.4

VTL response curves as a function of regenerative doses.

Each response curves were the VTL intensity integrated between 20 ^{o}C intervals across each peak.

Range 1: Peak at 110 ^{o}C, Range 2: Peak at 130 ^{o}C

Range 3: Peak at 200 ^{o}C, Range 4: Peak at 270 ^{o}C

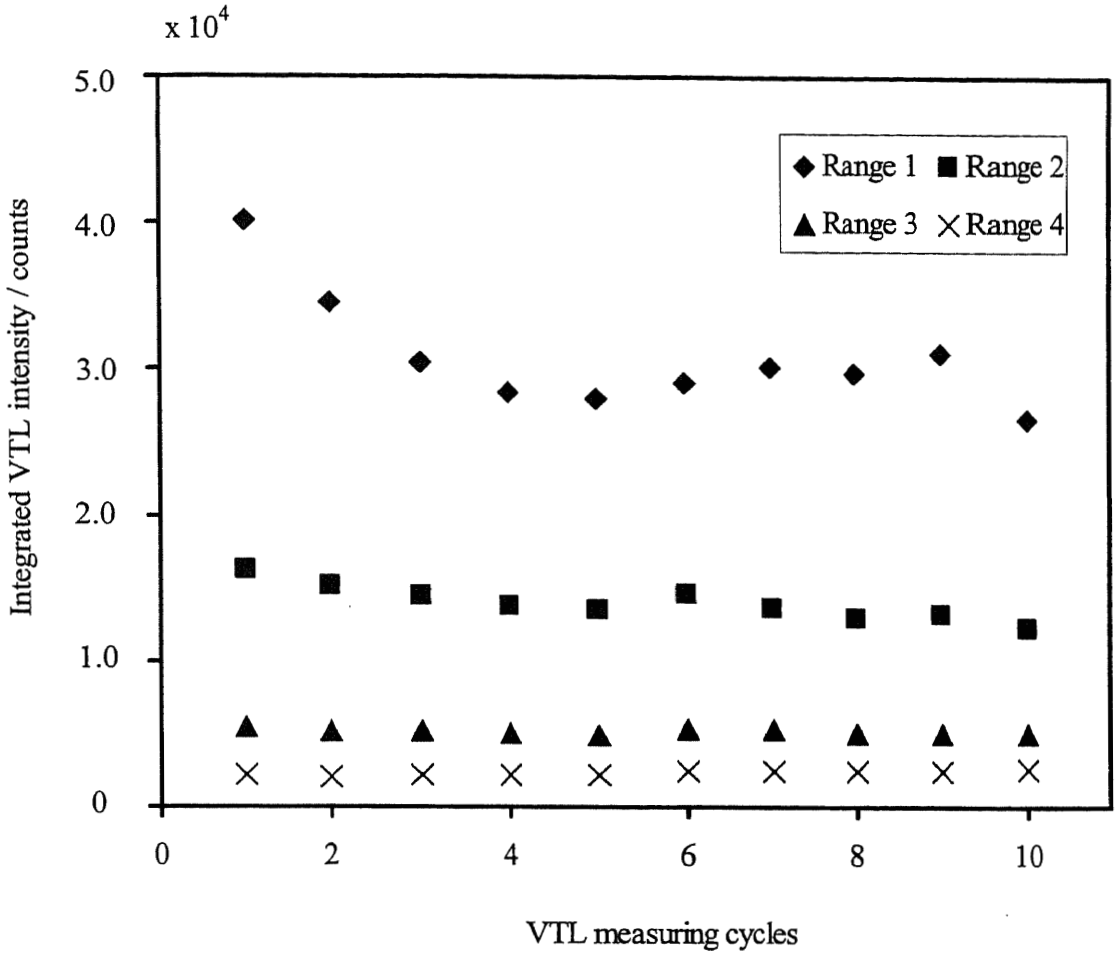

Figure 4.5

Sensitivity changes of the quartz grains when applying VTL-measurements cycles.

The quartz grains were irradiated with X-ray of 20 Gy.

Range 1: Peak at 110 °C, Range 2: Peak at 130 °C

Range 3: Peak at 200 °C, Range 4: Peak at 270 °C

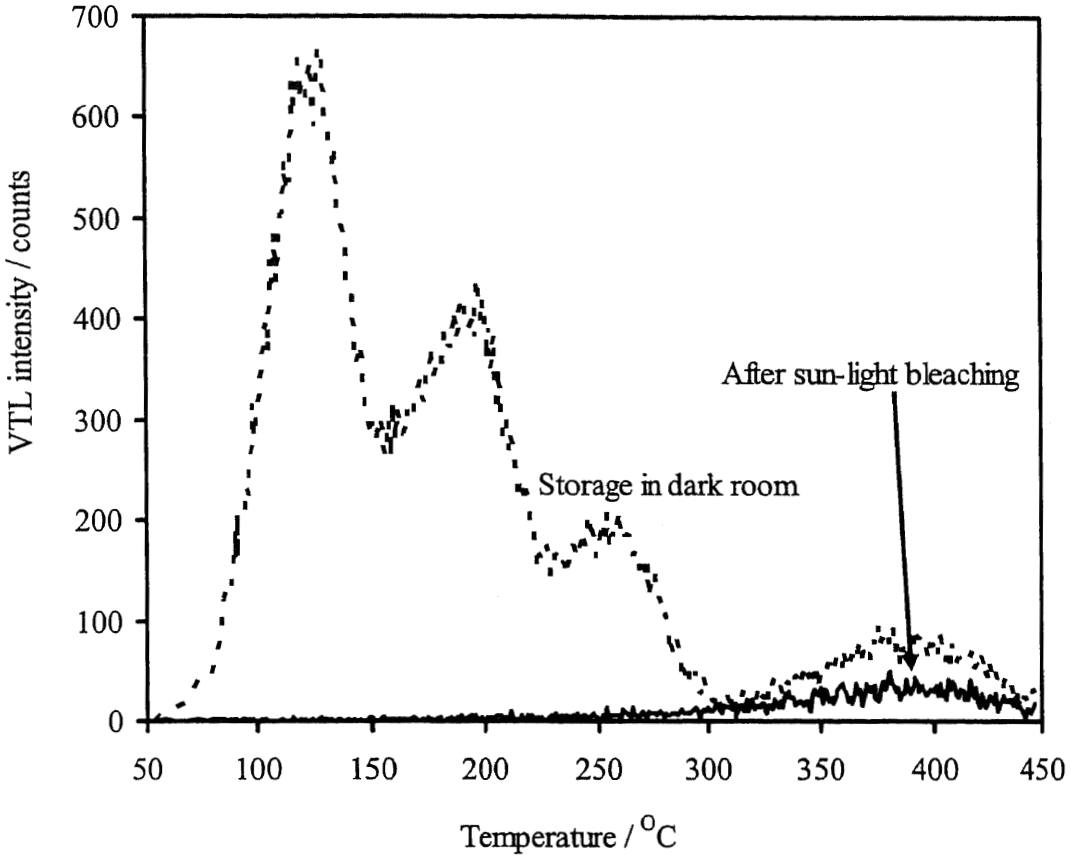

Figure 4.6

Comparison of VTL glowcurves between with and without sun-light bleaching (max. 28000 lux) for 8 hr.

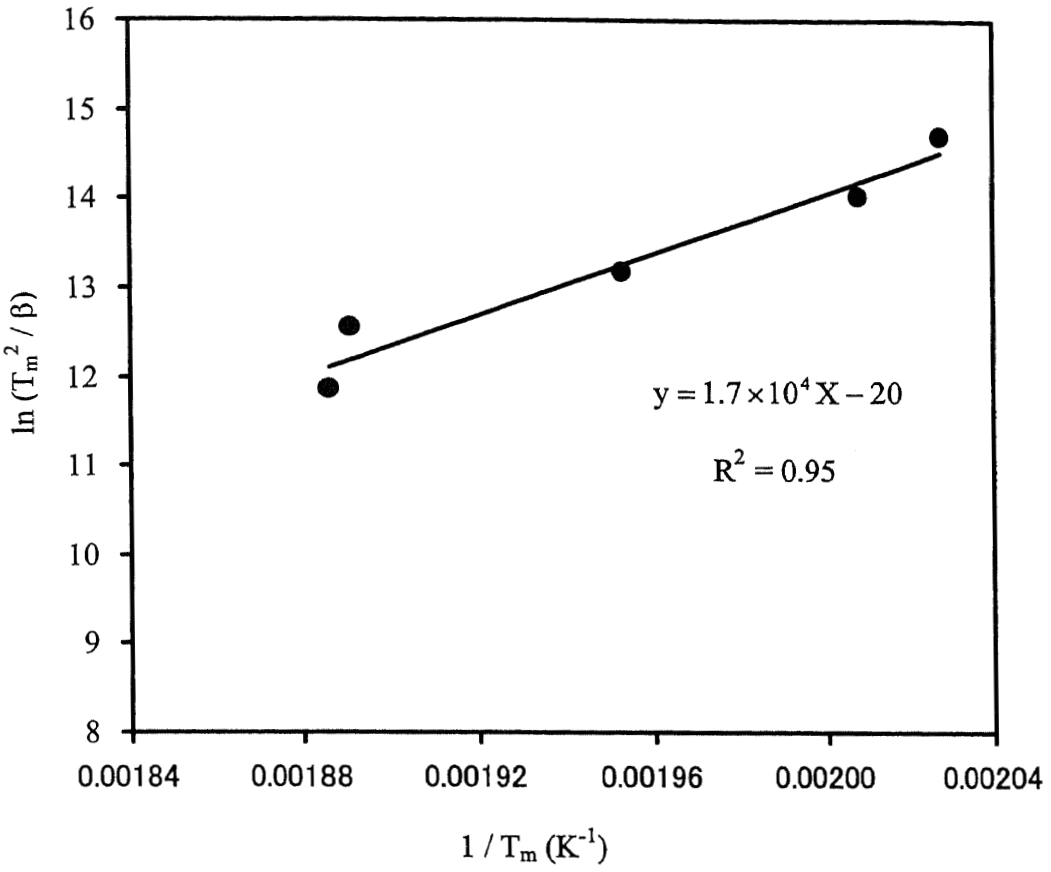

Figure 4.7

Arrhenius plot of artificially accumulated VTL from quartz grains extracted surface soil around JAEA in the case of 250 ^{o}C peak.

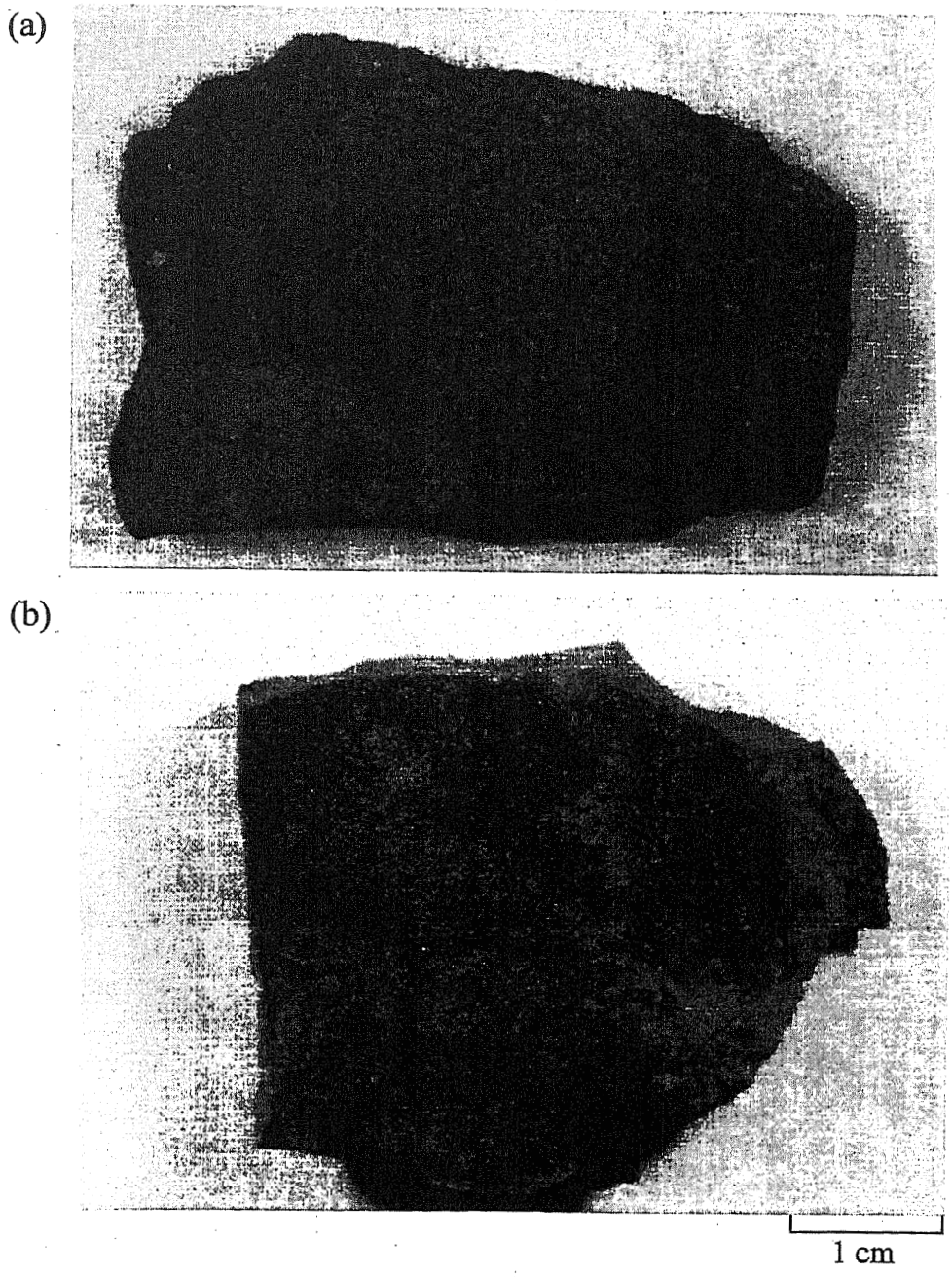

Figure5.1

Two pieces of roof tiles suffered by atomic-bomb explosion.

These were collected from (a) Hiroshima Pease Memorial Park and (b) Nagasaki Peace

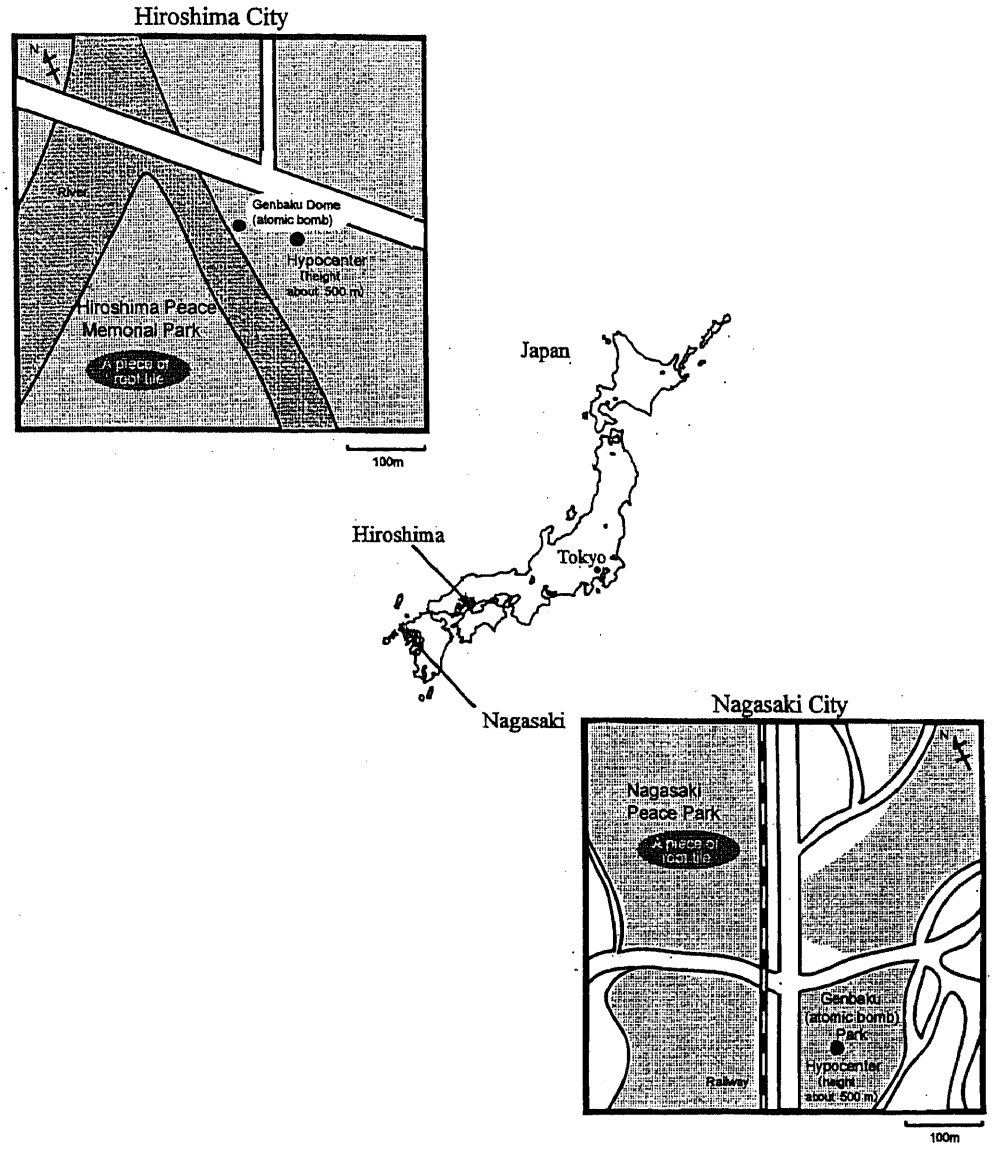

Figure 5.2
Sample collecting sites.

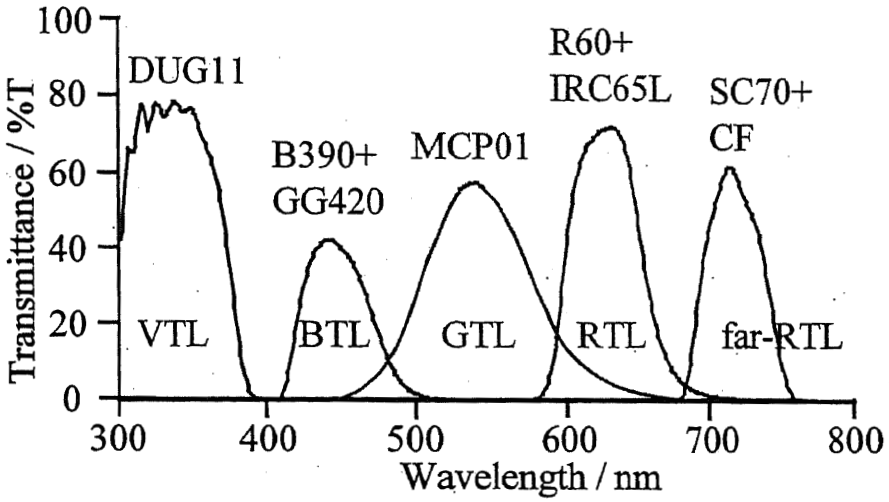

Figure 5.3

Optical transmission properties of filter combinations for five kinds of TL- measurements.

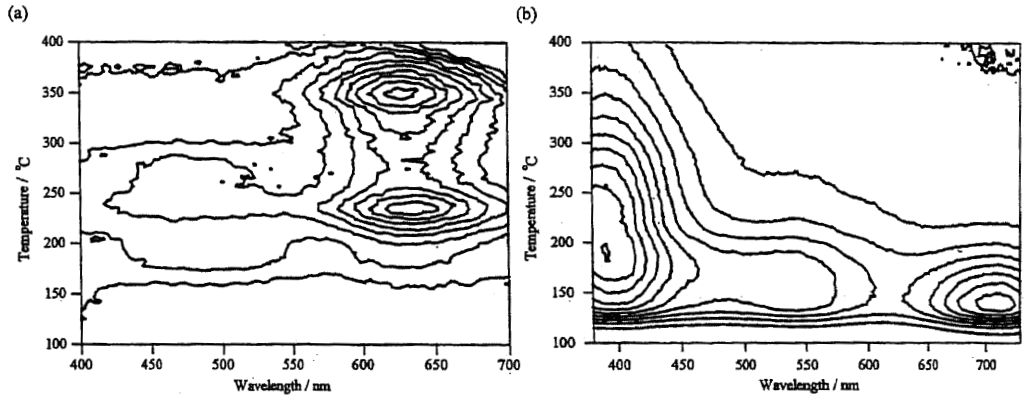

Figure 5.4

Contour expressions of TL-emission from (a) quartz and (b) feldspar extracts from Nagasaki roof tile.

Each 10 mg-grain samples was irradiated with X-rays of 1.2 kGy

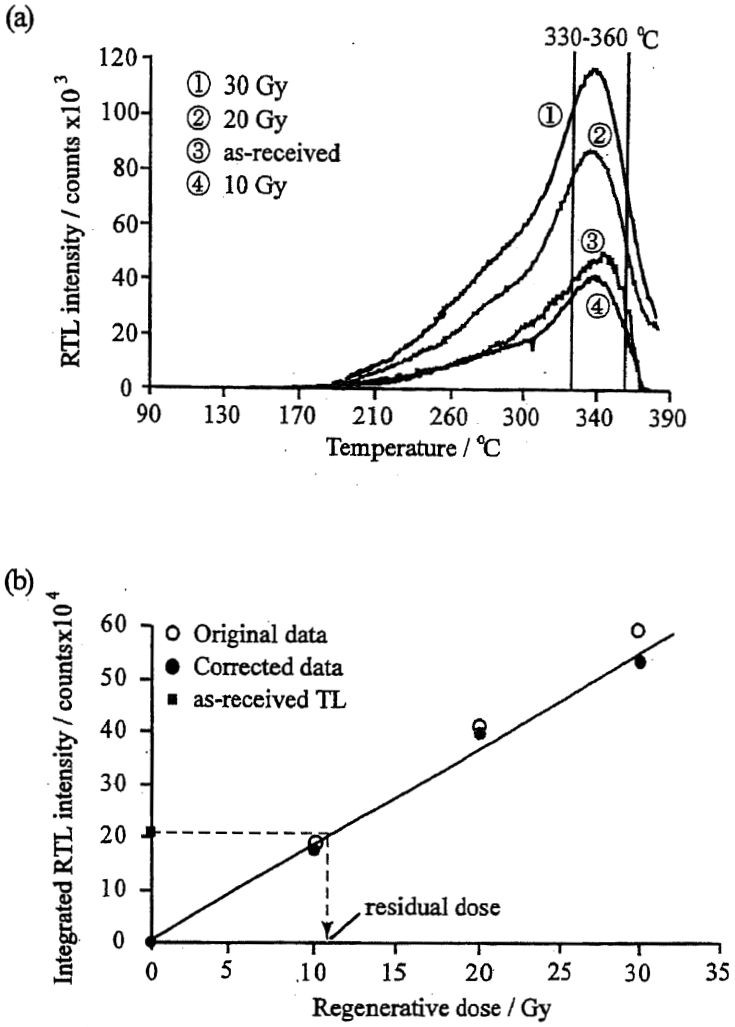

Figure 5.5

(a) Growth of RTL glow-curves and (b) their dose-response of quartz extracts from Nagasaki roof-tile.

The RTL was integrated in 330-360 °C regions of each glowcurve on the basis of plateau test.

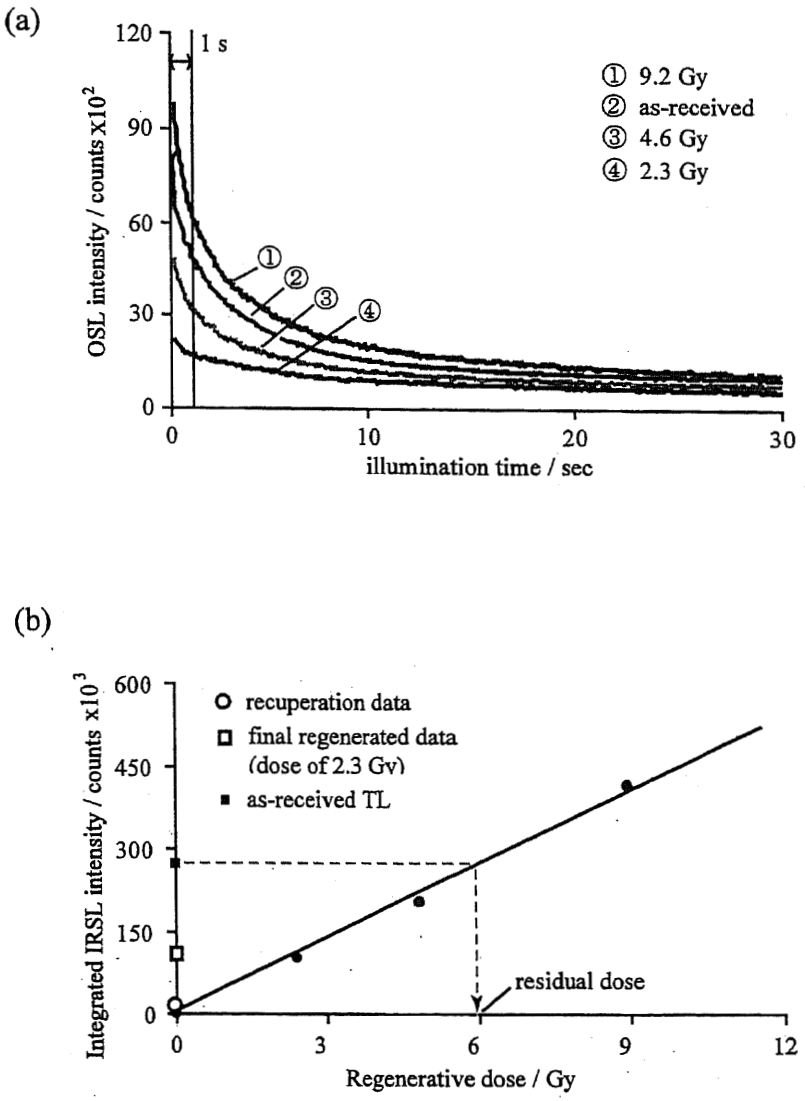

Figure 5.6

(a) Variations of IRSL-decay curves according to regenerative doses and (b) their dose response curve.

Sample was feldspar extract from Nagasaki roof tile.

IRSL-values integrated for initial 1 sec of decay curves were employed for the formation of dose-response curve.

ACKNOWLEDGEMENTS

The author wishes to grateful acknowledge Professor Tetsuo Hashimoto of Niigata University for giving him a splendid chance to challenge a doctoral degree with detailed directions, and Professors Hiroshi Imaizumi, Kiyoshi Sawada, Takaaki Horaguchi, Hisaaki Kudo and Shinichi Goto of Niigata University.

The author is very grateful to the Japan Atomic Energy Agency (JAEA), which permitted him to enter the doctoral course of Niigata University, and particularly to Dr. Kunihiko Shinohara, Mr. Kenjiro Miyabe, Dr. Sadaaki Furuta, Mr. Minoru Takeishi, Mr. Naoto Miyagawa, Mr. Hitoshi Watanabe, Mr. Kenji Imaizumi, Dr. Yasuhiro Uezu and Mr. Masanao Nakano of JAEA for their warm encouragement throughout this study.

The author also would like to thank Dr. Jun Koarashi, Mr. Yukihisa sanada, Mr. Masato Morisawa, Mr. Masanori Takeyasu, Mr. Chiaki Kato, Mr. Yuji Kokubun and Ms. Tomoko Mizutani for suggesting and helping him.

The author also would like to thank Dr. Akihiro Takeuchi of Niigata University and Dr. D.G. Hong of Kangwon national university for suggesting him to refine English of the thesis.

Finally, the author has to appreciate deeply his wife for her understanding and support.

参考論文等

1. Fujita, H. and Hashimoto, T. Influence of radioluminescence on optically stimulated luminescence from natural quartz grains. Radioisotopes. (in press)

2. Fujita, H. and Hashimoto, T. Effects of annealing temperatures on some radiation-induced phenomena in natural quartz. Radiat. Meas. (Submitted)

3. Hashimoto, T., Fujita, H., Sakaue, H. and Nomura, S. Comparison of residual doses for quartz and feldspar extracts from atomic bomb-suffered roof tiles using several luminescence-dosimeters. Radiat. Meas. (Submitted)

4. Hashimoto, T., Hase, H., D.G. Hong, Fujita, H. and Katayama H. (2000) Correlation of aluminum hole centers with hydrogen radicals form γ-irradiated quartzes of different origins. J. Nucl. Radiochem. Sci. **1**, 47-50.

5. Hashimoto, T., Fujita, H. and Hase, H. (2001) Effects of hydrogen radicals and annealing temperature on some radiation-induced phenomena in differently originated quartzes. Radiat. Meas. **33**, 431-437

6. Hashimoto, T., Yamaguchi, T., Fujita, H. and Yanagawa, Y. (2003) Comparison of infrared spectrometric characteristics of Al-OH impurities and thermoluminescence patterns in natural quartz slices at temperature below 0^{O}C. Radiat. Meas. **37**, 489-485.

その他論文等

１．橋本哲夫、藤田博喜、安田賢哉 (1999) 天然石英粒子からの赤色と青色熱ルミネッセンス(TL)に関連した捕捉電子の寿命評価, Radioisotopes, **48**, 673-682.

２．橋本哲夫、藤田博喜 (1999) 赤色 TL による年代測定, 地球, **26**, 119-124.